A Study on Seismic Design for Infrastructures in a Low Seismicity Region

A Dissertation Submitted to
the Department of Urban Management
Graduate School of Engineering of Kyoto University

In partial Fulfillment
of the Requirements for the Degree of
Doctor of Engineering

by

Sherliza Zaini Sooria

2012

ABSTRACT

An effective approach to mitigate the destructive effects of an earthquake is by implementation and enforcement of seismic resistant design. Evidence of seismic hazard from distant seismic sources and ground motions recorded within the country is enough proof to warrant a serious consideration for seismic resistant design for structures, particularly bridges, in Malaysia. This is because bridges are critical lifelines, which support the everyday life of the public and must be operational at all times including in the event of an earthquake.

Despite being located in the stable Sunda shelf, Malaysia is exposed to low seismic hazard. Felt earthquakes have psychologically affected the public in several occasions and the questions on how the structures fare when subjected to earthquake excitations have been debated publicly and in the Parliament of Malaysia a few times. Consequently, several government agencies, including the Public Works Department, have been assigned to address these issues since 2003.

This research is an attempt to act in line with Malaysia's spirit to improve the nation's preparedness against unpredictable earthquake events. Malaysia has a moral obligation and responsibility to start considering seismic resistant design to secure the public safety and address the issues related to seismic risk due to the lack of seismic resistance in structures. Thus, the main objective of this research is to evaluate a suitable seismic design motion for the design of bridges by surpassing the challenges posed by insufficient ground motion data.

Four main tasks were conducted to complete the research. These include examining suitable attenuation relationships, which best represent the seismic condition of Malaysia. Four attenuation models were selected to predict peak ground acceleration (PGA) and velocity (PGV) values, which were then used to compare with observed PGA and PGV values recorded at seismic stations. It was deduced that attenuation models established by Dahle *et al.* (1990) and that by Atkinson and Boore (1995) may appropriately reflect the seismic conditions of Malaysia.

The maximum magnitude earthquake for Peninsular Malaysia has been predicted as magnitude 6.5, based on historical data of Malaysia. Peak ground velocity is estimated at 60 cm/s, while peak ground displacement is estimated as 150 mm. For this reason and considering near-fault earthquakes, the Kobe ground motion has been selected for dynamic

i

analysis. It is also of interest to adopt the peak ground displacement of 150 mm as the maximum displacement allowed in bridges, in the event of moderate to large earthquakes.

The major bulk of the research involves selecting the Samudera Bridge as a subject for seismic assessment. A multiple-degree-of-freedom (MDOF), three-dimensional, model was developed in OpenSees and later subjected to seismic simulation using three input ground motions, namely the 1995 Kobe, 1940 El Centro and 2005 Sumatera earthquakes. Structural responses demonstrate nonlinear behavior of piers and the bridge would suffer considerable damage under the large Kobe earthquake. However, small damages are anticipated in the bridge following excitation under the El Centro and the 2005 Sumatera time-histories. In general, the Samudera Bridge is expected to survive without collapse when subjected to all chosen ground motions, if transverse reinforcements are sufficiently provided in the piers. The most important deduction from this task is that the displacement capacity is a more significant factor, than the seismic coefficient, in ensuring bridge survival during an earthquake excitation.

Many people perceive that seismic resistant design is an expensive 'solution' to mitigating the destructive effects of earthquakes. A supporting sub-research was carried out to examine the impact of implementing seismic resistant design on the construction cost. This is a study carried out to observe the relationship between reducing the displacement response and the construction cost. The price difference was based on the contractual price of the steel reinforcement and concrete materials as listed in the bill of quantities for the Samudera Bridge project. The increase in construction cost has been determined to not exceed one percent of the bridge structure cost only.

ACKNOWLEDGEMENTS

TABLE OF CONTENTS

4 Bridge Modeling and Procedures of Seismic Performance Investigation in OpenSees — 73

5 Nonlinear Static Pushover (NSP) Analysis as a Tool to Estimate Seismic Capacity and the Seismic Coefficient Value — 97

LIST OF FIGURES

LIST OF TABLES

Chapter 1

Introduction

1.1   Background of Research

1.1.1   Rationale for Seismic Resistant Design of Bridges in Low Seismicity Region

The world can be categorized into the high, low to moderate and stable seismicity regions. Despite of having different levels of seismic hazard, countries belonging to each region collectively share a common aim: safeguarding the public safety and welfare. Theoretically, the public safety may be improved if the seismic risk is mitigated. One of the effective strategies, which may be employed to mitigate the destructive effects of earthquakes, is by implementing seismic resistant design (Paz, 1994).

Essentially, a bridge goes beyond connecting one location to the other. It serves as a dynamic connectivity in our daily lives. It plays an important role in boosting the nation's economy, and effectively connects the social path of humans. Therefore, due attention should be given to reinforced concrete bridges, mainly bridge piers, as they are important civil structures (Nguyen, 2008). Observations of past earthquakes have shown how severe damages and failure of bridge structures have caused highways closure and disrupted traffic flow, such as that caused by the 1995 Hyogoken-Nanbu (or Kobe) earthquake (Scawthorn, 2003). Bridges are vital lifelines, which when severely damaged may hamper rescue attempts, disrupt social activities and community functioning (Elnashai and Di Sarno, 2008). Thus, essentially, a bridge must remain operational at all times, including during an earthquake event.

It has been recognized in some megacities, of the world, that population growth is so rapid that human security is of great concern. Urbanization and economy boost in big cities within a country have also attracted larger population to these cities, and as such, the authorities have to play a major role to provide and maintain acceptable safety levels for the

1

public. In the context of earthquake engineering, lost of lives and economy devastation in these cities cannot be tolerated.

In recent years, various researchers have shown great interests in improving the seismic performance of bridges following extensive damage and disruption of these lifelines during large-scale earthquakes, for instance during the 1994 Northridge and the 1995 Hyogoken-Nanbu earthquakes. Although the majority of these researches have generally concentrated on the impacts of large earthquakes in seismically active regions, with increased awareness, considerable attention has also been directed, recently, to possible earthquake disasters in the low to moderate seismicity areas. As such, researchers have managed to convey a message that seismic resistant design of bridges is indispensible in seismically affected regions including that in the low to moderate seismicity region.

Malaysia acknowledges the effects of distant earthquakes, from its neighboring countries, which include vibrations in tall dwellings, public and office buildings; infrastructure damages on roads; and non-structural damages, such as cracks of wall plastering in affected houses. Several experiences with motions in tall buildings have prompted the authorities to categorize bridges as important structures, alongside buildings, which require due attention in seismic design. The main reason for this is that bridge structures are equally affected by ground motions as tall buildings are.

Earthquakes cannot be prevented nor can it be accurately predicted. Even in the low seismicity regions, seismic hazard is real and apparent. Regardless of their level of seismic hazard, low seismicity regions must prepare themselves for the unpredictable nature, frequency, or magnitude of earthquakes. This is because injuries and death are known to have been caused by the collapse or destruction of 'unsatisfactorily' designed structures, and not due to the ground shaking.

In view of the above discussion, seismic resistant design is seen as an effective approach to address all of these concerns because it improves the seismic performance of bridges, and as a result may effectively minimize injuries and death during a devastating earthquake event.

1.2   Significance of Research

The motivation for implementation of seismic resistant design in the low seismicity regions lies in the fact that there is clear evidence of seismic activities within the region, indicating the presence of seismic hazard. A country such as Malaysia, although situated on the stable

seismicity zone of the Sunda plate, has been reported to record small to medium size locally generated ground motions, and has been affected by distant earthquakes from the active seismic sources of Indonesia and the Philippines (MOSTI, 2009). Thailand and Singapore experience similar situation with recorded ground motions within their countries, as well as from neighboring countries.

Seismic risk is perceived as considerable when there is a lack of seismic resistance in bridge structures. Such situation is common in low seismicity countries because the design of bridges in these countries continues to follow the traditional method of accounting for vertical loads and a small percentage of horizontal loads, such as that calculated to resist wind loading. Therefore, exposure of these bridge structures to seismic loads may be devastating. In line with human security engineering, there is enough warrant to begin seismic resistant design of bridges, as well as to investigate the vulnerability of existing bridges to seismic forces in countries belonging to the low seismicity region.

Following reports of felt ground motion in building structures, in several occasions; the government of Malaysia has embarked on seismic hazard research for Malaysia since 2003. In parallel with the government's intention, the Public Works Department of Malaysia (PWD) has conducted various studies including the investigation on the vulnerability of public buildings to seismic loads. The ultimate goal is to revamp the design codes used in current practice, by designers, to include seismic loadings in the design of new structures as a strategy to mitigate seismic risk. This research is performed as a support to the continuous effort by a group of researchers, practitioners, and implementers, in Malaysia, towards preparing Malaysia for the impacts of larger ground motions.

1.3   Objectives of Research

In view of the above scenario, the main objective of this research is to clarify an advanced concept of seismic design for bridges in a low seismicity region such as in Malaysia. The ultimate aim of this research is to derive an acceptable seismic design coefficient and allowable ultimate displacement to incorporate in the current bridge design code as a measure to secure the public safety against the potential destruction brought about by an earthquake motion.

In order to achieve the main objective of the research, the following tasks are proposed:

i. evaluate existing attenuation models, previously developed by various researchers, and select suitable attenuation relationships to reflect the seismicity and hazard for Malaysia,

ii. examine the seismic performance of an existing reinforced concrete bridge using finite element modeling, as in OpenSees (Mc Kenna *et al.*, 2001), to observe its dynamic response to selected input ground motions,

iii. estimate base shear capacity and ultimate displacement of selected bridge structure by conducting nonlinear static pushover analysis. The resulting pushover curve shall then be used to evaluate the damage state of the bridge in a dynamic analysis,

iv. examine the implication on the economy following implementation of seismic resistant design in Malaysia, and

v. justify the requirement for fail-safe mechanism to prepare for unexpected ground motions in Malaysia.

The investigation on the impact of seismic resistant design on construction cost is particularly important for economically challenging countries, such as Malaysia, because higher construction cost, than normal, may become a hindrance to practicing seismic resistant design.

The objective of this research is limited to understanding of the seismic behavior in a typical bridge in Malaysia, whereby the behavior shall be discussed in reference to the ultimate displacement, and anticipated damages in the longitudinal reinforcements and crushing of concrete.

1.4   Methodology

To accomplish the objectives mentioned in section 1.3, the research is divided into two main tasks. The first task is dedicated to determining a reasonable seismic design motion, which reflects the seismicity of Malaysia. An important tool, which may be used to estimate design motion is by examining existing attenuation models. Existing attenuation relationships are selected and estimated values of peak ground acceleration (PGA) and peak ground velocities (PGV) calculated from these models are compared with PGA and PGV values recorded at the Malaysian network of seismic stations. Details of this study are as discussed in chapter 3.

The second task emphasizes on modeling of a bridge structure near Kuala Lumpur prior to performing the pushover and dynamic analyses. The bridge model is then used to perform pushover analysis to determine its seismic capacity, ultimate displacement, and seismic coefficient. Next, the model is simulated under selected ground motions; its seismic response is observed and evaluated for adequacy against seismic forces. The dynamic analysis is an essential method of analysis in that it helps to determine an appropriate design of a bridge structure, which can satisfactorily withstand the effects of frequent small earthquakes, as well as perform with sufficient ductility in the event of a large earthquake. As a result, a flexible design of a bridge structure is possible, in place of a strong and stiff structure, which is uneconomical for developing countries.

Although design motions are generally presented as peak ground accelerations (PGA) in attenuation models or pseudo-acceleration response spectrums, this research has to divert away from this 'usual' procedure developed for seismically active regions due to scarcity of ground motion data. While this poses a challenge in the course of the research, an alternative approach to address this matter is considered through the application of the static nonlinear pushover analysis. After all, pushover analysis has been widely used in the seismic design codes across the globe to propose seismic forces for use in seismic resistant design of structures. Moreover, seismically active countries, for instance Japan, are still using the seismic coefficient method, together with the dynamic analysis, in the design of highway bridges. The flow and mapping of this research is as illustrated in Figure 1.1.
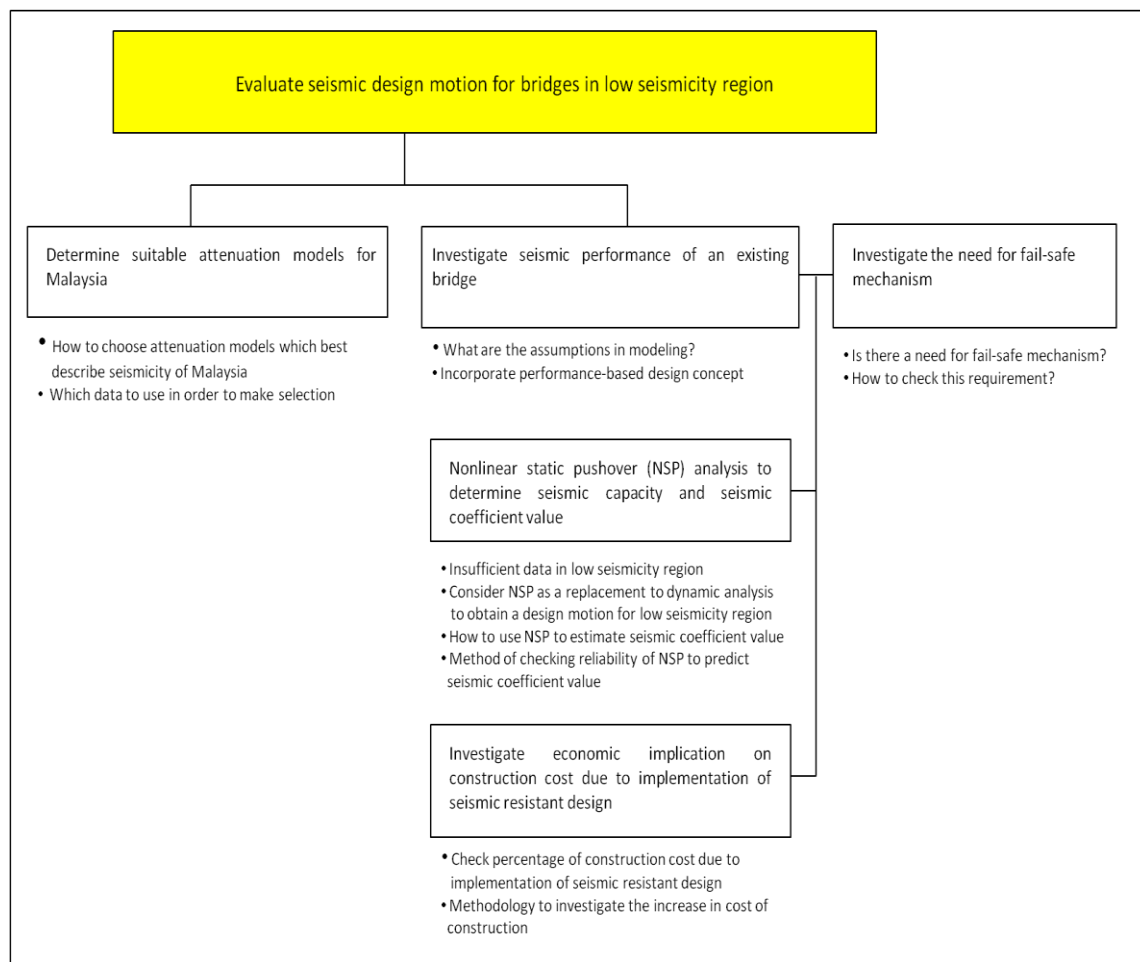
Figure 1.1   Study flow diagram.

1.5   Outline of the Thesis

The thesis consists of eight chapters. Following this introductory chapter, Chapter 2 reviews and discusses a list of available literatures on:

i.   attenuation models considered in the research before concluding the best model to represent the seismicity and seismic hazard for Malaysia,

ii.   the benefits and capability of the open source software, OpenSees used in the seismic simulation of the selected bridge structure,

iii.   modeling assumptions in finite element modeling of the bridge structure in OpenSees,

iv.   the mechanical behavior and application of constitutive models of material for analyzing nonlinear behavior of pier structures,

v.   application of moment-curvature analysis to develop the backbone curve of pier hysteresis, represented as dashed line in the pier hysteresis diagrams, and

vi.   nonlinear static pushover analysis as the means to estimate base shear and seismic coefficient value, C, as a result of ground motion excitation on the bridge structure.

Chapter 3 presents a sub-research on identifying the most suitable attenuation model to represent the seismic hazard of Malaysia. This is a step in the research deemed necessary to understand the characteristics of locally recorded earthquakes in Malaysia. Furthermore, an estimate of a design motion is meaningless without information on the seismic hazard.

The description and development of the Samudera Bridge model and the selection of input ground motions to use in the investigation are explained in detail in Chapter 4. The main features of the bridge elements and materials; modeling assumptions; selection of loading patterns; constitutive law of materials employed in the analysis; and selected ground motions used in simulating the expected dynamic behavior of the bridge are presented here.

The major bulk of the research work involves selecting the Samudera Bridge as a subject of seismic assessment by employing the nonlinear static pushover analysis (NSP) and the dynamic analysis. The pushover analysis is performed to determine the seismic capacity, the ultimate displacement, and seismic coefficient of the bridge. This is discussed in detail in Chapter 5.

The multiple-degree-of-freedom (MDOF), three dimensional model developed in Chapter 4 is excited to three input ground motions, namely the 1995 Kobe, 1940 El Centro and 2005 Sumatera earthquakes. Chapter 6 illustrates the results of this dynamic analysis in terms of the moment-curvature relationship of pier sections, displacement response, stress-strain response, and pier hysteresis. The discussion of results is limited to observation of damages based on the comparison of the seismic demand obtained from dynamic analysis with the seismic capacity obtained from Chapter 5, pier hysteresis, and yielding of longitudinal reinforcement and concrete crushing.

Chapter 7 addresses the typical issue surrounding the perception, on the stakeholders' side, that implementation of seismic resistant design is an expensive 'solution' to mitigating the destructive effects of earthquakes. Many believe that enforcement of seismic requirements would escalate construction cost beyond their means. A supporting sub-research is conducted to examine the impact of reducing displacement response on

construction cost. The price difference is calculated based on the contractual price of the steel reinforcement and concrete materials listed in the bill of quantities for the Samudera Bridge project. This chapter also briefly discusses about the need for fail-safe mechanism. Introduction of the 'flexible' pier section as a seismic resistant option, in low seismicity regions, may risk increasing the displacement response during an earthquake excitation. Thus, fail-safe mechanism is an important element to be considered, even in a low seismicity region, to prepare for the unexpected earthquake events.

The overall conclusions of the research activities performed in chapters 3 through 7 are summarized in chapter 8.

1.6   Conclusions

Recently, Malaysia has accepted the fact that seismic effects may pose threats to structures, including bridges, which lack aseismic provisions. Thus, Malaysia is moving towards implementing seismic resistant design as a measure to mitigate potential destructive effects of earthquakes. The primary aim of this research is to propose a seismic design coefficient and allowable ultimate displacement for consideration in the design of new bridges.

Due to a lack of ground motion data, this research has to divert away from the 'usual' trend of defining seismic loading as attenuation model or response spectrum. Rather, representation of seismic design motion is proposed as acceleration coefficient or seismic coefficient value.

References

Elnashai, A. and L. Di Sarno (2008). *Fundamentals of Earthquake Engineering*, John Wiley & Sons, Ltd., West Sussex, United Kingdom.

Ministry of Science, Technology and Innovation of Malaysia (2009). *Seismic and Tsunami Hazards and Risks Study in Malaysia: Final Report*, prepared by the Academy of Science Malaysia, Kuala Lumpur for the Inter Agency Committee and Tsunami Risk Management, Kuala Lumpur, Malaysia.

Nguyen, V.B., (2006). *Numerical Modeling of Reinforced Concrete Bridge Pier Under Artificially Generated Earthquake Time-Series* (Thesis). The University of Birmingham.

Paz, M (1994). *International Handbook of Earthquake Engineering, Codes, Programs, and Examples*, Chapman & Hall, New York.

Scawthorn, C., Chapter 1 (2003). Earthquakes: A historical perspective. *Earthquake Engineering Handbook*, ed. Chen, W.F., and C. Scawthorn, CRC Press, Boca Raton, Florida.

Chapter 2

Literature Review

2.1 Introduction

Historical data of felt earthquakes collected by the Malaysian Meteorological Department since more than a century ago, of local and distant origins, shows apparent seismic hazard in Malaysia. The following discussion provides justification for an improvement of the bridge design code in Malaysia.

Seismic resistant design of bridges is one of the answers to ensure public welfare and safety in the event of an earthquake. As such, it is indispensible to include seismic design provisions, which is currently absent, in existing the design codes as a tool for seismic risk mitigation.

Inclusion of the seismic design provisions in design codes may well begin with the evaluation of a seismic design motion. A seismic design motion is generally represented by a design spectrum, capacity spectrum, seismic hazard map, attenuation model, or seismic coefficient. However, in some cases locally recorded data for such evaluation is insufficient for the development of a design motion. The question now arises: how best to evaluate seismic design motions for countries with a lack of ground motion records? Reference to seismic design guidelines in Japan and the United States of America indicate that representation of the seismic design motion is feasible in terms of seismic coefficients. This method is also largely used internationally in seismic design codes across the globe.

This chapter provides a brief review of the seismic hazard and seismicity conditions in Malaysia to understand the seismicity of Malaysia, as well as to justify the need for evaluation of a seismic design motion for the country. A larger remaining portion of this chapter is attributed to giving an overview of the performance-based design, displacement-based design, and nonlinear static pushover analysis employed in the course of evaluating a seismic design motion for Malaysia. A brief mention of the OpenSees software is presented

in this chapter to highlight the features, and advantages of using an open source software framework in the analysis of a bridge.

2.2   Seismic Hazard and Seismic Studies in Malaysia

Many believe that an earthquake, large enough to cause life-threatening crisis, will never affect Malaysia. Such is mainly because Malaysia is situated on the stable Sunda shelf. However, previous reports of felt ground motions in the country, and the fact that existing structures lack seismic resistance, have initiated efforts, by the government, to prepare the country for potential danger from a larger earthquake impact. The following paragraphs illustrate the reasons for concern and the need to develop a suitable seismic design motion for the design of new bridges and assessment of existing bridge structures.

2.2.1   Bridge Design Code for Loading in Malaysia

The design of bridges in Malaysia follows the British Standards BS 5400 (British Standards Institution, 1978). BS 5400 consists of ten main parts, and has been accepted as the code of practice (CP) for the design and construction of bridges on motorways and highways. For the design of reinforced concrete bridges, bridge designers in Malaysia are familiar with the specification for loading, denoted by BS 5400:Part 2:1978 (hereinafter called BS 5400:Part 2). The main specification for the design of concrete bridges is BS 5400:Part 4:1990 (hereinafter called BS 5400:Part 4). It is worth to note that the code of practices in the BS 5400 group do not require consideration of seismic loading or detailing in a bridge design. Designers are also familiar with the Design Manual for Roads and Bridges, BD37/01 (The Highway Agency, 2001), which specifies the loadings to be used for the design of highway bridges through the attached revision of BS 5400:Part 2. According to BS 5400:Part 2, and BD 37/01, the design of bridges should consider dead, superimposed dead, highway live, horizontal and temporary loads. Design practice in Malaysia also requests that designers account for horizontal loads as a function of basic wind speed applied to the entire bridge height. Evidently, the absence of seismic design provisions, in the existing design codes, resulted in the lack of seismic resistance in almost all existing bridges in Malaysia. Consequently, existing bridges are exposed to seismic risk.

In 2006, the Bridge Section of the Public Works Department of Malaysia (PWD) incorporated the seismic design requirement in its Terms of Reference (TOR) for Bridges

and Viaduct Structures (Public Works Department, 2006). In clause 1.4(b) of the TOR, PWD calls for the application of earthquake loading to complex and long-span lifeline bridges equivalent to 1.0 in the ultimate limit state considering load combination 4 only i.e. combination of permanent load, primary and secondary live loads. Application of the horizontal seismic load is required in any direction at the superstructure level and has the following pattern:

$$\text{Horizontal seismic loading} = \frac{10\% \text{ (permanent DL+superimposed DL)}}{+} \quad (2.1)$$
$$20\% \text{ longitudinal HA traffic load}$$

where DL and HA denote the dead load and normal vehicle loading, respectively.

The seismic loading requirement in the TOR was derived from the value recommended by the consultant for the Penang Bridge when the structure was designed in the 1980s (Ismail Mohamed Taib, 2009, personal communication). It should be noted that until 2008 PWD has only instructed, in a few occasions, for seismic design of bridges in earthquake prone areas, for instance in the Federal Territory of Kuala Lumpur and Selangor.

2.2.2   The Seismicity of Malaysia

A seismotectonic study conducted by the Minerals and Geoscience Department of Malaysia (MGDM) confirms that Malaysia is tectonically situated within the relatively stable Sundaland. Thus, Malaysia belongs to the low seismicity group, except for the state of Sabah, which shows clear rate of crustal deformation (MGDM, 2006). Sabah owes its moderate seismicity condition to the active Mensaban, and Lobou-Loubo fault zones, which have brought about earthquakes that caused light damages to infrastructures, such as roads.

Most people perceive that Malaysia is free from life-threatening seismic crisis. In reality, seismic hazard in Malaysia is irrefutable, with seismic hazard originating from seismically active neighboring countries of Indonesia and the Philippines. Distant ground motions have been recorded by the Malaysian network of seismic stations, from two most active plate tectonic margins in the world, the Sumatran subduction zone, and the 1650 km long Sumatran fault; and the Philippines plate alike. In general, the impacts of these distant earthquakes, as reported, include panick-attack among inhabitants of tall buildings, and felt

ground motion in high-rise dwelling and office buildings (Pan and Sun, 1996; Pan, 1997; Pan *et al.,* 2001).

Records of felt earthquakes in Malaysia are available for events that began since 1815; however, they are "scanty and poorly correlated" (MOSTI, 2009). The information obtained from the Malaysian Meteorological Department (MMD) indicated that within a period of more than a century, beginning 1909, Peninsular Malaysia has experienced tremors of maximum intensity equivalent to VI, on the Modified Mercalli Intensity (MMI) scale. Between 1984 and 2007, Peninsular Malaysia recorded 35 distant ground motions, resulting from seismic events in Sumatera. In addition, it has also recorded 32 weak earthquakes, of local origin, with magnitudes ranging from 0.3 to 4.2 M_b (Chai *et al.*, 2011). These weak earthquakes occurred between November 2007 and December 2009 in the Bukit Tinggi area, which is approximately 50 km from Kuala Lumpur. Mustaffa Kamal Shuib (2009) suggests that the earthquake occurrences in the Bukit Tinggi area were the result of "fault reactivation due to stress buildup as a result of the present-day tectonics in the Sundaland". He further discussed that the weak earthquakes detected at the Bukit Tinggi area indicates that, following the December 26, 2004 Sumatera earthquake, the Sundaland core is deforming.

While Peninsular Malaysia has only experienced weak local earthquakes and been jolted by distant earthquakes from Sumatera, East Malaysia has recorded moderate scale tremors of magnitudes between 3.6 and 6.5 between 1984 and 2007. Since 1897, the state of Sabah has recorded the highest number of ground motions in the country i.e. 77 earthquake events, most of which are of local origin believed to be contributed by several active faults. The maximum intensity reported was VII on the MMI scale. It is worth noting that an earthquake of scale VII can cause human injuries and property damages. Records of felt earthquake in the state of Sarawak may be traced back from 1874 and until recently, 21 events with magnitude between 3.5 and 5.8 have been observed. Table 2-1 shows the list of felt earthquakes and their frequency of occurrences by state, recorded during the period of observation between 1874 and 2010. Earthquakes originating from the Philippines and Indonesia have also affected East Malaysia. Figure 2.1 illustrates the seismic activities, within Malaysia and around its region for the past 35 years, recorded between 1973 and 2008. The epicenters of the Bukit Tinggi earthquakes are as depicted in Figure 2.2. A magnified pictorial of the seismicity of Sabah is as shown in Figure 2.3. A study conducted by the Minerals and Geoscience Department of Malaysia (MGDM) has confirmed the

presence of the Mensaban and Loubo-Loubo active faults, in the Ranau-Kinabalu area, which have contributed to the non-structural damages in the Kundasang High School and the teacher's quarters. Some of these damages are as captured and shown in Figure 2.4.

Table 2-1   Frequency and intensity of felt earthquakes recorded from 1874 to 2010

State	Frequency of Occurrence	Maximum Intensity (MMI)
Peninsular Malaysia (1909 – July 2010)		
Perlis	3	V
Kedah	18	V
Penang	41	VI
Perak	24	VI
Selangor	50	VI
Negeri Sembilan	14	V
Malacca	19	V
Johor	32	VI
Pahang	35	III
Terengganu	2	IV
Kelantan	3	IV
Kuala Lumpur/Putrajaya	38	VI
East Malaysia		
Sabah (1897- July 2010)	40 (77)*	VII
Sarawak (1874 – July 2010)	17 (21)**	VI

Frequency of occurrence recorded as 40 by MMD, but reported as 77 by MOSTI (2009)

**Frequency of occurrence recorded as 17 by MMD, but reported as 21 by MOSTI (2009)
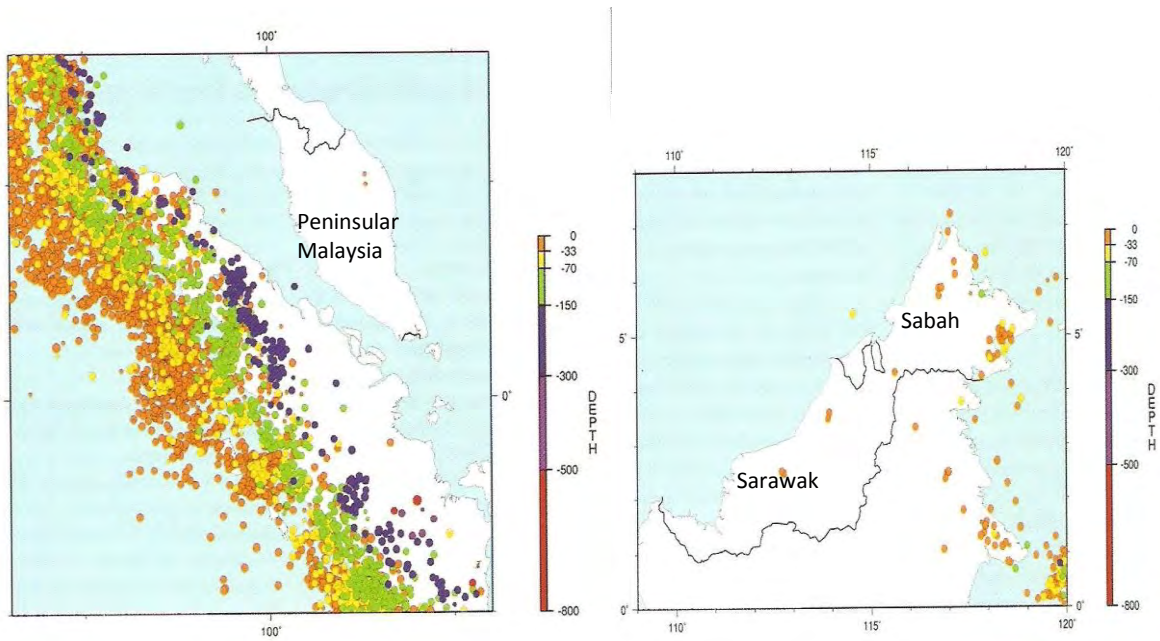
Figure 2.1   Records of earthquake epicenter in Malaysia and neighboring
countries between 1973 and 2008, excluding the Bukit Tinggi events
(adopted from the USGS website).
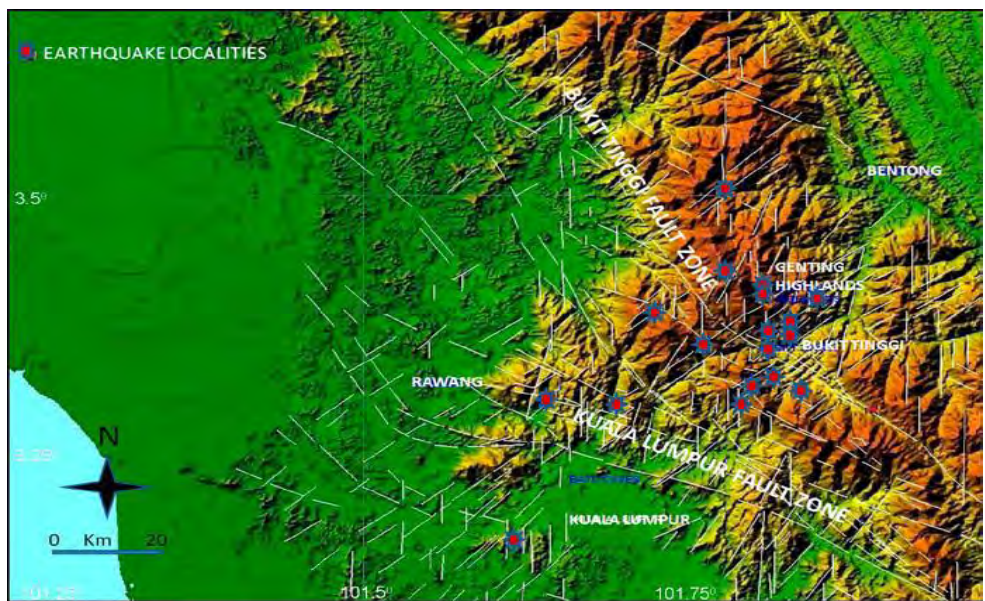
Figure 2.2   Epicenters of the Bukit Tinggi earthquakes recorded
between 2007 and 2008 (Shuib, 2009).

16
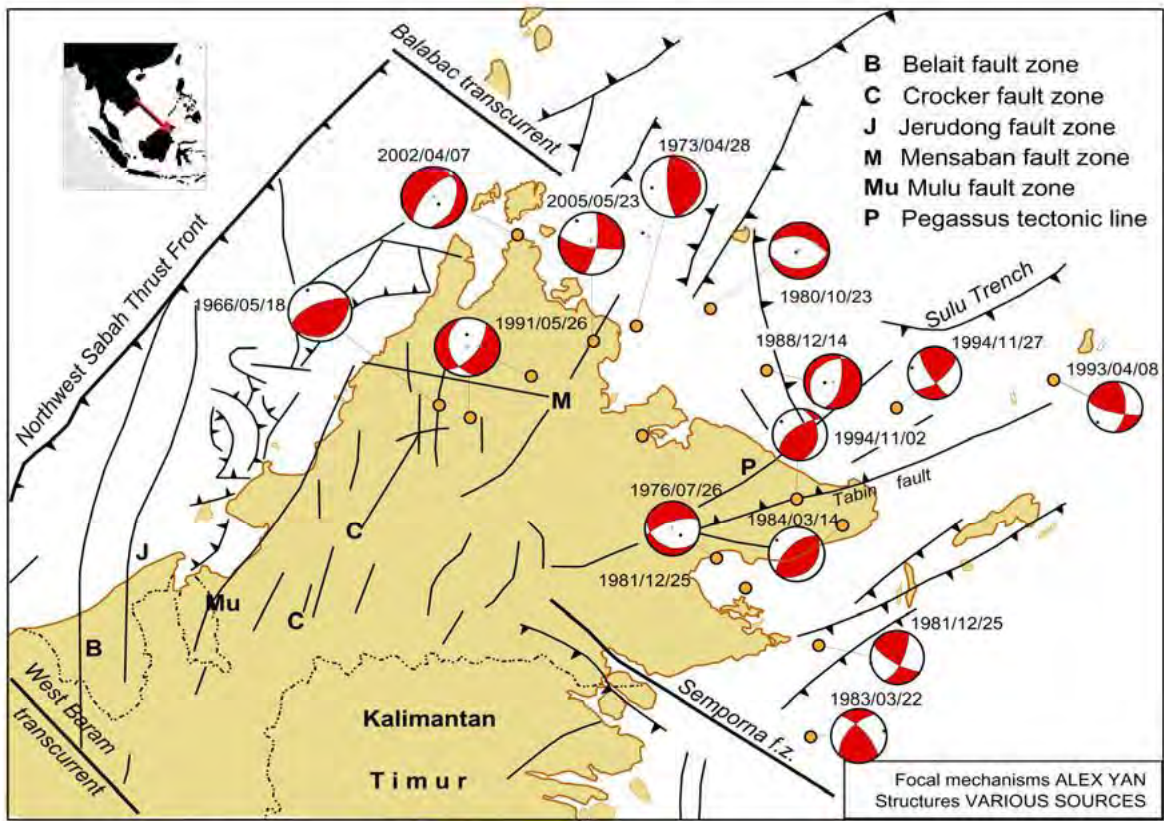
FOCAL MECHANISMS OF SABAH EARTHQUAKES 1976-2006

Figure 2.3   Focal mechanisms of earthquakes in Sabah for the period of 1976 to 2006 (MOSTI, 2009).
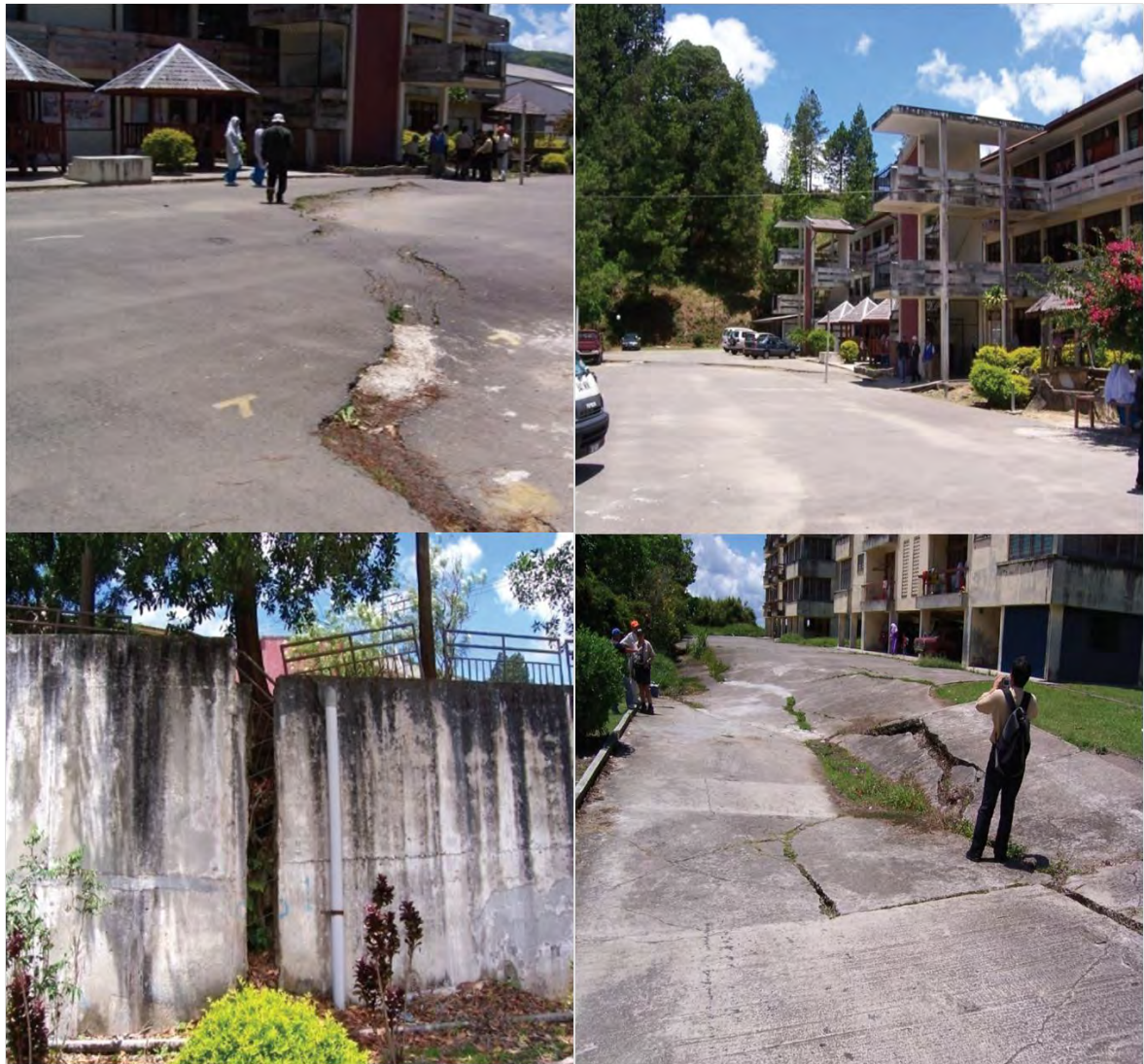
Figure 2.4 Non-structural damages captured at the Kundasang High School attributed by the Mensaban and Loubo-Loubo active faults (MOSTI, 2009)

2.2.3 Seismic Research in Malaysia

Following the 2001 Gujarat earthquake event, seismic research in Malaysia has received full support from the government since 2002. It all started following a cabinet note, featuring the 2001 Gujarat earthquake, which was presented by MMD before the Prime Minister and his cabinet members. The cabinet note briefly explained how distant shock waves during the 2001 Gujarat earthquake spread and travelled 600 km from the epicenter and caused devastation to many cities (Bendick *et al.*, 2001). The cabinet note has managed to convey

an important message to the government administration that distant earthquakes are indeed devastating and cannot be disregarded. Having been affected by both local and distant ground shakings, Malaysia has come to realize that seismic hazard in the country is real and has the potential to threaten the public safety and welfare, and may cause damages to properties. Such a concern is attributed to the fact that less than one percent of buildings in Malaysia are seismic resistant (Taksiah Abdul Majid, 2009). Taksiah Abdul Majid (2009) mentioned that among the very few structures, which were designed to seismic requirement are the Penang Bridge, the KOMTAR tower in Penang, and the Petronas Twin Tower in Kuala Lumpur.

The December 26, 2004 Sumatera earthquake has also become a revelation to the people in Malaysia that distant earthquakes should not be ignored. Following this earthquake event, the public's awareness and concern on the impacts of earthquakes has significantly improved. The public has since demanded assurance, from the government, of the stability, and capability of existing structures to withstand seismic forces. Hence, since 2005, the government of Malaysia has taken various efforts, through the Ministry of Science, Technology, and Innovation (MOSTI), to assess and address the risks associated with potential earthquake events.

Research on reduction and mitigation of earthquake risk in Malaysia started immediately, and by January 2009 MOSTI has published the final report entitled *Seismic and Tsunami Hazards and Risks Study in Malaysia* (MOSTI, 2009). Some important publications, which were mentioned in the report included the macrozonation contour maps based on peak ground acceleration (PGA) at 10% and 2% probabilities of exceedance in 50 years for bedrock of Malaysia (Adnan *et al.* 2005); and the assessment on the vulnerability of public buildings (Adnan et *al.*, 2006). In the study on the vulnerability assessment of public buildings by Adnan *et al.* (2006), a total of 65 buildings across the country was subjected to earthquake forces. The assessment was performed to ATC 21 *Rapid Screening of buildings for Potential Seismic Hazards: a Handbook* (Applied Technology Council, 2002), and ATC 22 *A Handbook for Seismic Assessment of Existing Buildings* (Applied Technology Council, 1989). The study concluded that the vertical element design provision was inadequate for at least 50% of the buildings, hence posing higher earthquake damage risk.

Malaysia, like many other countries, concerned with seismic hazard, has worked on developing macrozonation and microzonation maps. The macrozonation mapping for

several major cities in Malaysia was completed, in 2005, by a team of researchers headed by Associate Professor Azlan Adnan of Universiti Teknologi Malaysia. These maps give estimates of expected ground motions, which can be readily used in the design of structures. They are synonymously called the peak ground acceleration (PGA) maps of Malaysia. The PGA values derived from the macrozonation maps were later adopted by PWD in its proposal for seismic design guidelines for concrete buildings in Malaysia (PWD, 2007). This proposal has been submitted, for review, to the Institution of Engineers Malaysia; however, it has yet to be published. The PGA values adopted in the draft document for seismic design guidelines have been challenged as impractical and relatively high, by at least a researcher who suggested that the analysis philosophy utilized to derive the PGA values might have to be reviewed (Chiang, 2008). The microzonation map for Kuala Lumpur City Centre was published in 2008 (Adnan, 2008).

2.3   Fundamentals of Performance-based Seismic Design

In the United States of America, performance-based design started as an attempt at developing systematic guidelines for seismic rehabilitation of buildings (Chen and Lui, 2006). A growing interest in performance-based design is attributable to many observations of structural behavior following disastrous destruction brought upon by large earthquakes in seismically active countries, such as in Japan and the United States of America. It is probably not an overstatement to say that the performance-based design was an outcome following observations of substantial losses, of life and monetary, impacted by earthquake events. Large earthquake events, which have caused tremendous damage and losses, such as the 1989 Loma Prieta, and the 1995 Kobe earthquake, have made researchers realized of the significance of seismic performance levels. Consequently, in 1994 the California Department of Transportation (CALTRAN) incorporated the performance-based design approach, emphasizing on capacity design, in the Caltrans Bridge Design Specifications (BDS). BDS relates to performance-based design by adopting the two-level seismic performance in its design provision. The Applied Technical Council (ATC) recommendations ATC-32 recognizes the significance of relative displacement in the seismic performance of bridges where bridges are classified based on their importance.

Japan has also learnt from observations of many earthquake disasters that losses can be reduced with the implementation of performance-based design. A year after the 1995 Kobe earthquake, bridge design procedures, Part V: Seismic Design of Highway Bridges (JRA,

1996) has shifted from the conventional design concept using the seismic coefficient method (SCM) to the ductility method. Two seismic performances were introduced: the level 1 performance with SCM remaining as the design method; and the level 2 performance where the ductility design method must be used. Level 1 and 2 performances in both Japan and the United States of America refer to the performance of bridges in small but frequent earthquakes, and large but rare earthquake occurrences, respectively.

2.3.1　Displacement-based Design Approach

Bridges are important lifelines, which must remain operational in an earthquake event. Therefore, since decades ago, seismic design of these structures has been emphasizing on no-collapse performance. For this purpose, prior to the 1970s, designers have conventionally worked to achieve no-collapse state by first utilizing the elastic method. However, observations of damage in bridges, which were designed and constructed to the elastic method, indicated some critical deficiencies of the elastic method (Priestley *et al.* 1996). These deficiencies are attributed to the fact that the elastic method ignores ductility and consideration of appropriate strength. Consequently, the elastic method was replaced by the force-based design approach. The force-based design approach has played a major role in the development of seismic design codes across the globe. However, since three decades ago, as the earthquake engineering community welcome the performance-based design philosophy, researchers and designers began to notice the importance of the displacement-based design approach.

While force-based approach focuses on "strength", the performance-base approach (in which the displacement-based design approach is based upon) emphasizes on "performance". The shift from force-based to performance-based was prompted when researchers recognized that damage can be appropriately related to strain, and therefore is better represented by displacement, rather than by force. It is immediately recognized that damage is a function of displacement demand, and as such, structural damage can be effectively controlled by specifying displacement limit in the design of a bridge structure (Calvi and Kingsley, 1995).

The displacement-based design has been in development since almost two decades ago with the aim to address deficiencies in the force-based design method. In the displacement-based design, nonlinear forces are obtained for a desired performance level: the serviceability limit state or the ultimate limit state. This method has become such an

appealing method of design mainly because stakeholders are allowed to specify the structural levels of performance in bridges, hence resulting in cost effective and economical design and construction.

The displacement-based approach focuses on displacement demand based on the assumption of a displaced shape, and uses predefined displacement response spectrum to determine the target period of vibration. The target period of vibration will then be used to calculate the force distribution for use in bridge design, or to determine seismic demand and capacity. The displacement-based approach incorporates the *Substitute Structure* approach developed by Gulkan and Sozen (1974) to approximate the displacement of an inelastic system with equivalent linear elastic system. As can be seen from Figure 2.5, the *Substitute Structure* approach emphasizes the significance of two parameters: secant stiffness, K_{eff} (rather than initial stiffness), and equivalent viscuous damping value, ξ_{eff}. Essentially, this method is capable of estimating the base shear and the ductility of a bridge, given the target displacement and material properties of structural elements.

The displacement-based design procedures have been utilized in seismic design of single-degree-of-freedom (SDOF) bridges (Kowalsky *et al.*, 1995), and multi-degree-of-freedom (MDOF) bridge structures (Calvi and Kingsley, 1995). Both literatures outlined procedures on obtaining the target displacement and lateral force distribution. The procedures to calculate displacement demands and lateral load distribution, or base shear values for various types of structure are also discussed by Priestley *et al.* (2007).

In both SDOF and MDOF systems, displacement-based design procedures begin with the selection of performance level to identify acceptable damage level in bridge structures. Damage levels are represented, among others, in terms of first yield, cracking, plastic rotation, or concrete crushing. The next step is to evaluate the target displacement, Δ_u for use in seismic design. For MDOF system, it is essential to define the target displacement for each column in the bridge system so that the critical column can be identified. The shortest column is usually the critical column, and governs the selection of the displacement pattern, however, depending on the bridge geometry; other columns can appear as the critical column (Kowalsky, 2002).

For a SDOF system, Δ_u can be estimated by referring to the drift limit value recommended in seismic design codes, or the strain limits prescribed when defining the damage level.
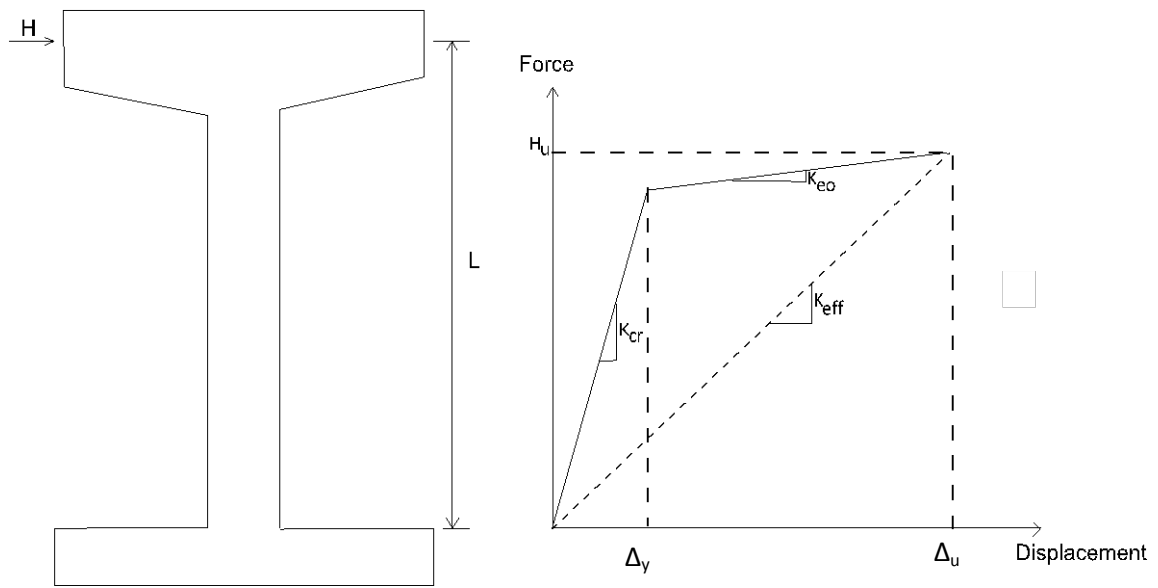
Figure 2.5 Substitute Structure approach for seismic response of a bridge structure (adopted from Kowalsky *et.al*, 1995)

2.4 Seismic Design Motion

Earthquake prone countries require seismic resistant procedures to ensure acceptable structural seismic performance. As such, it is the duty of engineers, within the Human Security Engineering framework, to ensure safety of bridge structures, and avoid severe damages, which may cause collapse. This is because bridge structures are important lifeline features, which need to remain operational during an earthquake, i.e. bridges must be seismic resistant. Seismic resistant provisions generally begin with the definition of a seismic design motion, an engineering model, which may be used to predict strong ground motion amplitude for use in the design and assessment of bridges. Conventionally, estimates of strong ground motion for engineering practice are derived from strong motion records, which are gathered by strong motion network.

Seismic design motion is one of the seismic resistant elements used, in building codes across the globe, to protect public safety and welfare (Hamburger, 2002). In seismically active countries of the United States of America and Japan, building codes were originally developed to provide design recommendations to avoid collapse of structures. These early recommendations were strictly based on experience and observations of structures during

23

damaging earthquakes, such as the 1868 Hayward earthquakes. The early twentieth century saw the introduction of lateral load, also known as the equivalent lateral force (ELF) rule, as a measure to provide structures with sufficient strength. According to the record, following the devastating 1906 San Francisco earthquake, San Francisco city was the first state in the United States of America to include the ELF concept in the building code (Hamburger, 2002).

In the context of Japan, Toshikata Sano was responsible for introducing the concept of seismic coefficients for use in the analysis of buildings in 1916. He estimated maximum ground accelerations brought about by the 1855 Ansei-Edo earthquake in the Honjo, Fukugawa, and Yamanote areas. However, it was not until the 1923 Kanto earthquake devastation, that the Japan Urban Building Law Enforcement Regulations was revised, in 1924, to include a seismic coefficient of 0.10 (Otani, 2004). Japan introduced its first seismic provision for bridges in 1926, incorporating the use of a lateral load equivalent to 20 percent of the gravity load (superstructure dead weight) as the resisting seismic force.

Modern earthquake engineering started with the advent of the accelerograph, developed by M. Ishimoto in 1931. Since then, records of accelerograph have been used by many researchers, whose works have bloomed into significant engineering applications, for engineering evaluation. Some names worth mentioning are Biot (1933) who introduced the response spectrum; and Veletsos and Newmark (1960) who emphasized the importance of system ductility to resist base shear due to ground motions.

A seismic design motion represents the engineering demand in the form of design spectrum, capacity spectrum, seismic hazard map or peak ground acceleration map, attenuation relationships, or seismic coefficient. It indicates the amount of seismic forces, sometimes defined as inertial forces or base shear, which a structure must resist to survive potential earthquake forces. In modern seismic design, an acceptable and reliable evaluation of seismic design motions is dependent upon understanding the behavior of a structure under dynamic loads. Therefore, an effective estimate of a seismic design motion, relies heavily on ground motion records from past earthquake events. While seismically active countries may have ample data to develop design motions, low seismicity areas have obvious challenges in developing reliable design motion. In the instance of insufficient ground motion data, an alternative approach to inelastic dynamic analysis to evaluate structural response is necessary. An analysis tool capable of predicting nonlinear response of a structure by utilizing static loading is the nonlinear static pushover analysis (Lawson,

1994; Kim and D'Amore; 1999, Elnashai, 2001). The nonlinear static pushover (NSP) procedures have the capabilities to predict nonlinear structural response, deformation, and provide force-deformation relationship in terms of base shear. Nevertheless, one should be cautious when using NSP, as it requires careful definition of analysis inputs, such as realistic target displacement estimate, and reliable lateral load distribution, which will ensure accurate evaluation of the deformation of a structure. A brief review of NSP is as discussed below in section 2.4.2.

2.4.1   Open System for Earthquake Engineering Simulation (OpenSees)

Computer simulation through OpenSees, Open System for Earthquake Engineering (OpenSees, 2009) is gaining popularity since its introduction to the earthquake engineering community over a decade ago. OpenSees is a finite element framework software developed by the Pacific Earthquake Engineering Research Centre (PEER) specifically for earthquake engineering simulation. It is capable of modeling and analyzing nonlinear response of systems under earthquake excitation. Users start by building the model of a system to analyze, by creating nodes and elements; identifying materials, and defining boundary constraints. What follows next is the definition of load patterns; selection of solver algorithm, constraint handlers, and integrators for analysis procedures; and specifying the outputs to observe during simulation in appropriate recorders.

OpenSees appeals to users because it is downloadable from the internet, free of charge, fully programmable, and modeling is very flexible. For example, OpenSees allows users to 'build' their own material. Detail information on OpenSees is available at http://opensees.berkeley.edu. This website provides, among others, source codes, examples, command language manual, and a community board for online support to users who need consultation on solving problems related to simulation.

2.4.2   Nonlinear Static Pushover Analysis (NSP)

Pushover analysis first manifests itself in earthquake engineering through the work of Gulkan and Sozen (1974), which derived an equivalent linear elastic single degree of freedom (SDOF) system to represent a nonlinear multi-degree of freedom (MDOF) system. Over the years, when engineers came to recognize the importance of inelastic assessment, pushover analysis has begun its application as an analysis tool to observe inelastic response

and damage in structures. Similar to other proposed analysis, pushover analysis also has disadvantages and setbacks (Krawinkler *et al.*, 1998). Krawinkler *et al.* (1998) mentioned some of the difficulties involving pushover procedures, mainly in defining the target displacement and load pattern; and the errors incurred with the omission of higher mode effect in tall buildings and irregular bridges.

Pushover analysis can be categorized into two groups: conventional, and advanced. In brief, conventional pushover analysis involves a procedure, whereby three critical elements are considered. These elements are the nature of the forcing function (constant lateral load or displacement), the distribution of the forcing function, and its magnitude. In conventional pushover analysis, the structure is first applied with gravity load before it is subjected to constant monotonically increasing forcing function, i.e. a set of displacements or forces, until a predetermined target displacement is reached at a monitoring point. At each increment in force the resistance of the structure to the applied force is evaluated using static equilibrium equations, whereby stiffness matrix is updated, and unbalanced force is reapplied until convergence, and predefined limit state is achieved (Elnashai, 2001). The estimates of target displacement and lateral load distribution may be derived from displacement response of piers, and the mode shape recorded during dynamic analysis. Alternatively, procedures for obtaining target displacement and force distribution are as explained in section 2.3.1.

In contrast to the conventional analysis, the adaptive analysis deals with possible changes in force distribution, i.e. the forcing function is not constant. Pushover analysis methods, which belong to this group, are the *multi-mode pushover* (Sasaki *et al.*, 1998), *adaptive pushover method* (Gupta and Kunnath, 2000), *N2 method* (Fajfar, 2000), *modal pushover analysis* (Chopra and Goel, 2001), and *adaptive pushover analysis* (Elnashai, 2001). The advanced pushover analysis differs from that of conventional as it accounts for the effects of higher modes of vibration and progressive degradation of stiffness (Elnashai, 2001; Antoniou and Pinho, 2004). Various researchers have demonstrated the importance of accounting for the effects of higher modes, especially in tall structures (Sasaki *et al.*, 1998; Elnashai, 2001; Moghadam *et al.*, 2002). Calvi and Kingsley (1995) have shown the significance of mass participation factor in the analysis of irregular or asymmetrical bridges.

In keeping up with recent development in performance-based design, NSP has found its application in seismic evaluation of structures mainly because of its simple-to-perform, and less time-consuming attributes. It has gained significance because despite its simplicity it is

capable of providing critical regions of inelasticity, such as plastic hinge locations, and sequence of failure.

NSP procedures are simple enough that they have been adopted by well-known seismic codes, such as EC8, FEMA 273/356 (Building Seismic Safety Council; American Society of Civil Engineers, 2000), and ATC-40 (Applied Technology Council, 1996). Since the past decade, NSP has become an increasingly popular tool for assessment of building structures. However, application of NSP in assessment of bridges has been rather limited. Some studies on reinforced concrete bridges include those conducted by Karim and Yamazaki (2001), Abeysinghe *et al.* (2002); Chiorean (2003), and Mwafy *et al.* (2007).

References

Abeysinghe, R.S., E. Gavaise, M. Rosignoli, and T. Tsaveas (2002). Pushover analysis of inelastic seismic behavior of Greveniotikos Bridge. *Journal of Bridge Engineering*, Vol. 7, No. 2, 115-126, March/April.

Adnan, A., Hendriyawan, A. Marto, and I. Masyhur (2005). Seismic hazard assessment for Peninsular Malaysia using Gumbel Distribution Method. *Jurnal Teknologi* 42(B) Jun 2005:57-73, Universiti Teknologi Malaysia.

Adnan, A., S. Suradi, P.N Selvanayagam, Z. Darus (2006). Vulnerability of public buildings subjected to earthquake by Finite Element Modelling. *Proceedings of the 6th Asia-Pacific Structural Engineering and Construction Conference (APSEC 2006)*, 5–6 September 2006, Kuala Lumpur, Malaysia.

Adnan, A. (2008). Development of microzonation maps of Kuala Lumpur City Centre for seismic design of buildings. *Bulletin of the Institution of Engineers Malaysia*, March.

Antoniou, S., and R. Pinho (2004). Advantages and limitations of adaptive and non-adaptive force-based pushover procedures. *Journal of Earthquake Engineering*, Vol.8, No.4, 497-522.

Applied Technology Council (2002). *Rapid Screening of buildings for Potential Seismic Hazards: a Handbook*, *Report No. ATC21*, California.

Applied Technology Council (1989). *A Handbook for Seismic Assessment of Existing Buildings*, *Report No. ATC22*, California.

Applied Technology Council (1996). *Improved Seismic Design Criteria for California Bridges:Provisional Recommendations*, *Report No. ATC32*, California.

Applied Technology Council (1996). *Seismic Evaluation and Retrofit of Concrete Buildings, Report No. ATC40,* California.

Bendick, R., R. Bilham, E. Fielding, V. Gaur, S.E. Hough, G. Kier, M. Kulkarni, S. Martin, and M. Mukul (2001). The January 26, 2001 Bhuj, India earthquake. *Seismological Research Letters*, 72, 3.

Biot, M.S. (1933). Theory of elastic systems vibrating under transient impulse with an application to earthquake-proof buildings. Proc. National Academy of Sciences, *Vol. 19*, No. 2, 262-268.

British Standards Institution (1978). *Specification for Load, BS 5400: Part 2*, British Standards Institution, London.

Caltrans (1994). *Bridge Design Specifications*, California Department of Transportation, Sacramento, California.

Calvi, G.M., and G.R. Kingsley (1995). Displacement-based seismic design of multi-degree-of-freedom bridge structures.earthquake. *Engineering and Structural Dynamics*, *Vol.24*, 1247-1266.

Chai, M.F., Zamuna Zainal, D. Ramachandran, Zaty Aktar Mokhtar, Asmadi Abdul Wahab, and Mohd Rosaidi Che Abas (2011). *Study on Hypocenter Relocation of the Local Earthquakes in Malay Peninsular Using the Modified Joint Hypocenter Determination and HYPOCENTER Programs.*, Malaysian Meteorological Department, MOSTI, Research Publication *2/2011*.

Chen, W.F., and E.M. Lui (2006). *Earthquake Engineering for Structural Design*. Taylor & Francis Group, USA.

Chiang, J. (2008). Design for Seismic Action – A far field effect in Malaysia experience. *The 3rd ACF International Conference- ACF/VCA* 2008, paper *E03*.

Chiorean, C.G. (2003). Application of pushover analysis on reinforced concrete bridge model: Part 1 – Numerical models. *Research Report No POCTI/36019/99.*

Chopra, A.K., and R.K. Goel (2001). A modal pushover analysis procedure to estimate seismic demands for buildings: Theory and preliminary evaluation. *Pacific Earthquake Engineering Research Center*, College of Engineering, University of Berkeley, California.

Elnashai, A.S. (2001). Advanced inelastic static (pushover) analysis for earthquake applications. *Structural Engineering and Mechanics*, *Vol.12*, No. 1:51-69.

Eurocode 8 (2003), *Design of Structures for Earthquake Resistance*, European Committee for Standardization, 2000.

Fajfar, P.A. (2000). Nonlinear analysis method for performance-based seismic design. *Journal of Earthquake Spectra*, 16:573-592.

Federal Emergency Management Agency (1997). *NEHRP Guidelines for the Seismic Rehabilitation of Buildings. FEMA 273*, Washington D.C.

Gulkan, P., and M. Sozen (1974). Inelastic response of reinforced concrete structures to earthquake motions. *ACI Journal*, December 1974.

Gupta, B., S.K. Kunnath. (2000). Adaptive spectra-based pushover procedure for seismic evaluation of structures. *Earthquake Spectra*, Vol.16, No.2, pp 367-392.

Hamburger, R.O., Chapter 11 (2003). Building code provisions for seismic resistance, Ee*arthquake Engineering Handbook*, ed. Chen, W.F., and C. Scawthorn, CRC Press, Boca Raton, Florida.

Japan Road Association, *Design Specifications for Highway Bridges, Part V: Seismic Design.*

Karim, R., and F. Yamazaki (2001). Effect of earthquake ground motion on fragility curves of highway bridge piers based on numerical simulation. *Earthquake Engineering and Structural Dynamics*, 30:1839-1856.

Kim, S., and E. D'Amore (1999). Pushover analysis procedures in earthquake engineering. *Earthquake Spectra*, 15(3), August, 417-434.

Kowalsky, M.J., M.J.N. Priestley, and G.A. MacRae (1995). Displacement-based design of RC bridge columns in seismic regions. *Earthquake Engineering and Structural Dynamics*, 24: 1623-1643.

Kowalsky, M.J. (2002). A performance-based approach for the seismic design of concrete bridges. *Earthquake Engineering and Structural Dynamics*, Vol. 29, No. 3 pp. 719-747.

Krawinkler, H., and G.D. Seneviratna (1998). Pros and cons of pushover analysis of seismic performance evaluation, *Eng. Struct.*, 20(4-6), 452-464.

Lawson, R.S., V. Vance, and H. Krawinkler (1994). Nonlinear static pushover analysis, why, when and how?, *Proc. Of 5th US Nat. Conf. on Earthquake Engineering*, Chicago, 1, 283-292.

Malaysian Meteorological Department. (2010). http://www.met.gov.my/.

Minerals and Geoscience Department Malaysia (2006). *Study on the seismic and tsunami hazards and risks in Malaysia: Report on the geological and seismotectonic information of Malaysia*, Kuala Lumpur.

Ministry of Science, Technology and Innovation of Malaysia (2009). *Seismic and Tsunami Hazards and Risks Study in Malaysia: Final Report*, prepared by the Academy of Science Malaysia, Kuala Lumpur for the Inter Agency Committee and Tsunami Risk Management, Kuala Lumpur, Malaysia.

Moghadam, A.S., and W.K. Tso (2002). A pushover procedure for tall buildings. *Proc. Of the twelfth European Conference on Earthquake Engineering*, London, United Kingdom, paper No. 395.

Ismail Mohamed Taib, (2009). Personal communication via e-mail.

Mustaffa Kamal Shuib, (2009). The Recent Bukit Tinggi Earthquakes and their Relationship to Major Geological Structures. *Geological Society of Malaysia*, Bulletin 55, Nov. 2009, pp 67-72.

Mwafy, A., A. Elnashai, and W.H. Yen (2007). Implications of design assumptions on capacity estimates and demand predictions of multispan curved bridges. *Journal of Bridge Engineering*, American Society of Civil Engineering, pp 710-717.

Open System for Earthquake Engineering Simulation (OpenSEES) (2009). *Pacific Earthquake Engineering Research Center*, University of California, Berkeley, http://opensees.berkeley.edu/.

Otani, S. (2004). Earthquake resistant design of reinforced concrete buildings: Past and Future. *Journal of Advanced Concrete Technology*, Vol.2, No. 1, 3-24, February.

Pan. T.C., and J. Sun (1996). Historical earthquakes felt in Singapore. *Bulletin of the Seismological Society of America*, Vol. 86, p. 1173–1178.

Pan, T.C. (1997). Site-dependent building response in Singapore to long-distance Sumatra earthquakes. *Earthquake Spectra*, Vol. 13, p. 475–488.

Pan, T.C., K. Megawati, J.M.W. Brownjohn, and C.L. Lee (2001). The Bengkulu, Southern Sumatra, earthquakes of 4 June 2000 (Mw = 7.7) - Another warning to remote metropolitan areas. *Seismological Research Letters*, Vol. 72, pp. 171–185.

Public Works Department of Malaysia (2006) (rev. 2008). *Terms of Reference for Bridges and Viaduct Structures*, Public Works Department of Malaysia, Kuala Lumpur.

Public Works Department of Malaysia (2006). *Seismic Design Guidelines for Concrete Buildings* (unpublished), Public Works Department of Malaysia, Kuala Lumpur.

Priestley, M.J.N., F. Seible, G.M. Calvi (1996). *Seismic Design and Retrofit of Bridges*, J. Wiley & Sons, Canada.

Sasaki, K.K., S.A. Freeman, and T.F. Paret (1996). Multi-modal pushover procedure (MMP) – A method to identify the effects of higher modes in a pushover analysis, *Proc. O f 5th US Nat. Conf. on Earthquake Engineering*, EERI, Oakland, California.

Taksiah Abdul Majid (2009). *Less Than One Per Cent Of Buildings In Malaysia Have Earthquake Preventive Measures*. http://www.bernama.com.my/bernama/v5/newsindex.

The Highways Agency (2002). *Loads for Highway Bridge, BD 37/01*. London, The stationery office.

United States Geological Survey (USGS), http://www.geohazards.cr.usgs.gov

Veletsos, A. S., and N. M. Newmark (1960). Effects of inelastic behavior on the response of simple system to earthquake motions. *Proceedings of the 2nd World Conference on Earthquake Engineering*, Japan, Vol. 2, pp. 895-912.

Chapter 3

Assessment of Possible Ground Motions in Peninsular Malaysia

3.1   Introduction

Seismic resistant design emerges as a solution for better and acceptable designs to minimize the destructive effects of earthquakes. Prior to establishing a seismic design motion, it is essential to assess earthquake occurrences and the hazard associated with the magnitude of ground motions. For a country such as Malaysia, where historical data is scarce, seismic activities are low, and where information on geologic structures is absent, the assessment of possible ground motion and seismic hazard may be represented by any of the attenuation models previously established by past researchers. In addition, seismic hazard may also be defined as maximum magnitude earthquakes, which may occur within inland area.

This chapter is dedicated to investigating the characteristics of distant ground motions in Peninsular Malaysia, which originated from the active tectonic plates of Sumatera. The methodology employed is by comparing recorded peak ground acceleration (PGA) and peak ground velocity (PGV) values of ground motions recorded by the Malaysian network of seismic stations with those estimated using established attenuation models. The investigation of attenuation characteristics of ground motion shall consider that of the rock site condition.

In addition, this chapter discusses about estimating the maximum magnitude earthquakes, which are expected to occur within inland Malaysia, based on historical earthquake records. PGA and PGV values are evaluated using attenuation equations, which can consider near-source effect.

These assessments are significant to estimate the ground motion at a site, due to an earthquake at an epicenter, for structural design. In many cases, engineers are also interested to know the maximum magnitude earthquakes to define the hazard at a seismic source.

3.2 Selection of Attenuation Models for Earthquakes

Peninsular Malaysia is located within the low seismicity region of the stable Sunda tectonic plate. However, for the past 25 years strong ground motions have affected Malaysia several times. Sources of these strong ground motions include the Sumatran subduction zone, the most active plate tectonic margins in the world (Petersen *et al.*, 2004), and the 1650 km long Sumatran fault. While no real structural damage has been reported following these earthquake tremors, there have been reports of swaying motion and panicked-attack suffered by occupants of tall buildings in densely populated cities such as Kuala Lumpur, Putrajaya, Penang, and Johor Bharu. Such reports have motivated a good number of researches on seismic hazard assessment, and have reflected the importance of deriving a seismic design motion for engineering evaluation and design in Malaysia.

The development of a design motion requires ample information on the characteristics of ground motions, which may affect a structure. This information may be found by analyzing important time-domain parameters, such as the peak ground acceleration (PGA) and, or peak ground velocity (PGV). However, for a country, such as Malaysia, where historical data is scarce and seismic activities are low, previously established attenuation models may be utilized to examine the characteristics of ground motions at site. This entails the selection of appropriate attenuation models, which best represent the seismicity of Malaysia.

In determining the characteristics of ground motions, PGA has become the most widely used parameter simply because strong motion seismometers record time history accelerations. Hence, PGA values can be instantly read off the accelerograms. In addition to using PGA, Chandler and Lam (2004) suggested that the characteristics of low frequency, long period seismic waves, resulting from large and distant earthquakes, as are typically recorded across Malaysia, may be better described by using PGV.

Thus, the selection of attenuation model for Malaysia depends on input parameters such as PGA and PGV derived from locally recorded accelerograms, distance, and magnitude. It is important to mention that the context of discussion within this chapter is restricted to PGA and PGV values in reference to rock site conditions.

3.2.1 Dataset for Study

Malaysia has a national network of seismic stations to gather information on seismic activities within the country and from around the region. In 2008, the network comprises of 14 three-component real time stations, six in Peninsular Malaysia, five in Sabah, and three in Sarawak. Figure 3.1 depicts the locations of seismic stations across Malaysia. The Malaysian Meteorological Department (MMD) monitors and gathers information on seismic activities within Malaysia and from around its region. MMD also keeps records of earthquake event dated more than a century ago; however, compilation of digital ground motion records has only started in 2004. Thus, the ground motion records used for analysis come from 171 earthquake events, which occurred between May 2004 and July 2007. These records are as tabulated in Table 3A-1, in Appendix 3A, at the end of the chapter. However, due to the constraints set about by all four attenuation relationships selected for study, the original set of 171 ground motion records were reduced to a maximum of 46 accelerograms. This 'filtered' dataset, with their accompanying ground motion parameters, are as shown in Table 3A-2 in appendix 3A. Accelerograms corresponding to the dataset are as tabulated in Appendix 3B. This dataset are visible records, which are free from background noises. Insignificant waveforms have been excluded by applying a resolution value of 0.2 gal for PGA, and 0.05 cm/s for PGV.

In this study, only horizontal components of the accelerograms were considered for analysis, whereby recorded PGA and PGV values have been derived by taking the larger of the North-South (N-S) and East-West (E-W) components.

Between May 2004 and July 2007, 15 interplate earthquake events of magnitude $M_w \geq 5.0$, and shallow hypocentral depth $h_{hypo} \leq 40$ km were recorded. Out of these 15 events, three were shallow strike-slip events, which occurred along the Sumatran fault, while the remaining 12 events occurred within the subduction zone. The hypocenters of all 15 events were adopted from the National Earthquake Information Center (NEIC) of the United States Geological Survey (USGS) and the MMD. Figure 3.1 illustrates the epicenters of the 15 earthquake events chosen for this study, and their profiles are briefly summarized in Table 3-1. Data distribution with respect to earthquake magnitudes and source-to-site distances is as demonstrated in Figure 3.2, which clearly shows that distant ground motions recorded in Malaysia have distances ranging from 450 to 2300 km.
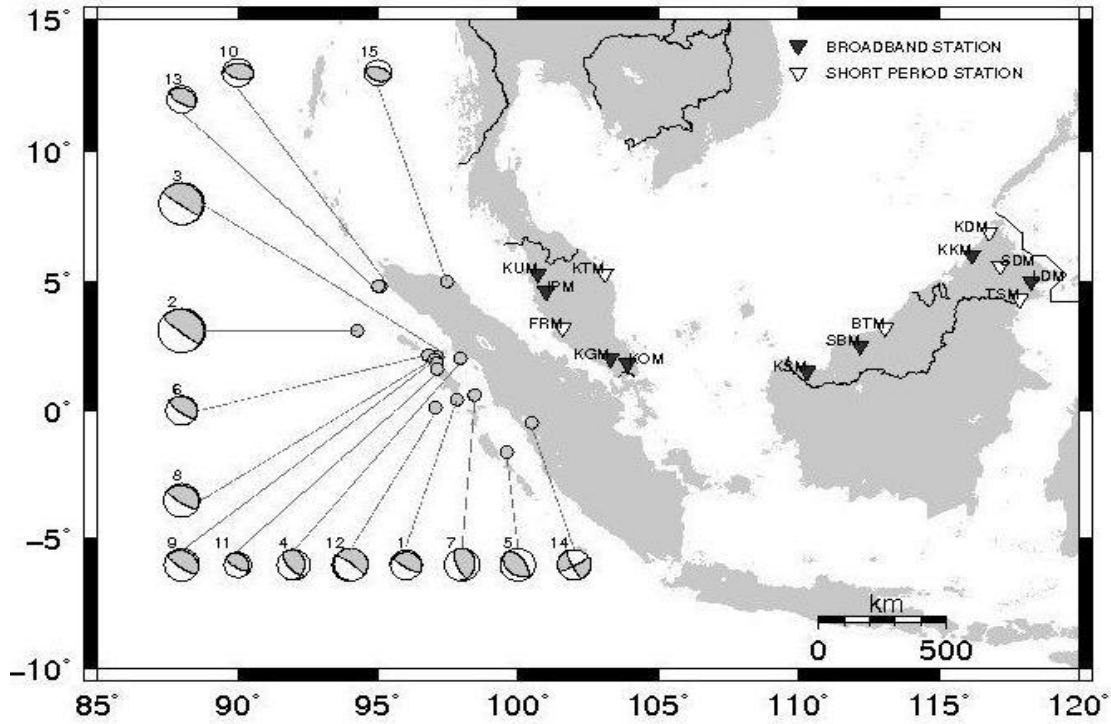
Figure 3.1   Seismic station network across Malaysia (as in 2007) which recorded 15 earthquake events selected for the study. Epicenters of earthquakes are shown as grey circles, while their focal mechanisms are displayed as black and white "beach ball" symbols.
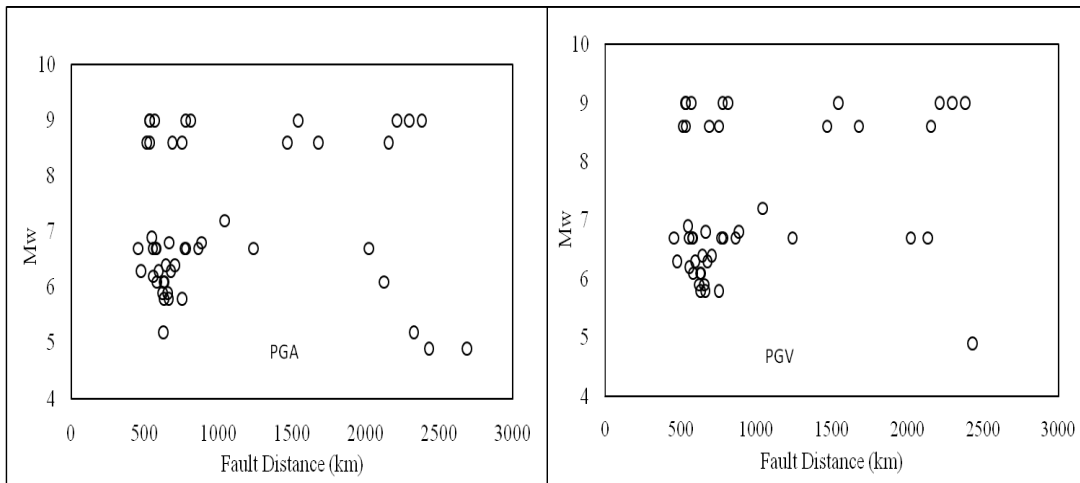
Figure 3.2   Distribution of data between May 2004 and July 2007. A total of 46 data was available for PGA analysis, whereas 44 data were incorporated in PGV analysis.

36

Table 3-1. Profile of 15 earthquake events recorded between May 2004 and July 2007

Ref. Number	Date	M_w	Latitude (°)	Longitude (°)	Source Depth (km)	Number of Recordings
1	2004/05/11	6.1	0.415	97.8	21	4
2	2004/12/26	9.0	3.295	95.982	30	9
3	2005/03/28	8.6	2.085	97.108	30	8
4	2005/04/03	6.3	2.022	97.942	36	3
5	2005/04/10	6.7	-1.644	99.607	19	5
6	2005/04/28	6.2	2.132	96.799	22	1
7	2005/05/14	6.7	0.587	98.457	34	2
8	2005/05/19	6.9	1.989	97.041	30	1
9	2005/07/05	6.7	1.819	97.082	21	2
10	2005/10/11	5.9	4.82	95.098	30	2
11	2006/02/06	5.2	1.607	97.101	26	1
12	2006/05/16	6.8	0.093	97.05	12	2
13	2006/12/17	5.8	4.815	95.018	36	3
14	2007/03/06	6.4	-0.493	100.498	19	2
15	2005/07/21	5.2	5.003	97.456	30	1

3.2.2 Selection of Attenuation Models

The selection of attenuation model(s) that best describes the seismicity of Malaysia involves the comparison between estimated PGA and PGV values with those recorded by the seismic stations. Estimated PGA and PGV values are obtained from attenuation functions, which are presented in an attenuation model. For this purpose, four existing attenuation models have been selected: the Atkinson and Boore (1995), Toro *et al.* (1997), Dahle *et al.* (1990), and Si and Midorikawa (1999). Their selections were based on the types of tectonic environment i.e. for shallow crustal earthquakes and subduction zone; and source-to-site distance.

The Atkinson and Boore (1995) attenuation relationship was developed using the stochastic method, for tectonically stable, low seismicity regions of Eastern North America (ENA). The model provides expressions to estimate PGA and PGV values and is intended for applications within r_{hypo} of 10 to 500 km, and for M_w ranging from 4.0 to 7.25. The attenuation function is represented by the following expression:

$$\ln Y = f_1 (M_w, r_{hypo}) + f_2 (S) \tag{3.1}$$

where Y is the horizontal component of PGA or PGV, and

$$f_1 (M_w, r_{hypo}) = c_1 + c_2 (M_w - 6) + c_3 (M_w - 6)^2 - \ln r_{hypo} + c_4 r_{hypo} \tag{3.2}$$

$$f_2 (S) = c_5 S_{Deep} \tag{3.3}$$

The values of regression coefficients c_1, c_2, c_3, c_4, c_5, and S_{Deep} are presented in Atkinson and Boore (1995).

Similarly, the Toro *et al.* (1997) attenuation relationship was derived to estimate strong ground motions for ENA. It only provides expressions to estimate PGA values, which are applicable for M_w between 4.5 and 8.0; and Joyner-Boore distance r_{jb} of up to 500 km. The representation of the model is as shown below:

$$\ln Y = c_1 + c_2 (M - 6) + c_3 (M - 6)^2 - c_4 \ln R + c_5 f (R) + c_6 R \tag{3.4}$$

where Y is the horizontal component of PGA, $M = M_w$ or m_{Lg}, and

$$f (R) = \begin{cases} 0 & \text{for } R \leq 100 \text{ km} \\ \ln (R/100) & \text{for } R > 100 \text{ km} \end{cases} \tag{3.5}$$

$$R = \sqrt{(r^2_{jb} + c^2_7)} \tag{3.6}$$

Regression coefficients c_1, c_2, c_3, c_4, c_5, c_6, and c_7 are as tabulated in Toro *et al.* (1997).

Due to the constraints posed by the Atkinson and Boore (1995) and the Toro *et al.* (1997) models, it is obvious that these models are able to represent only four percent of the field data. This is due to the fact that majority of the data used in this study are distant ground motions with epicenters exceeding 300 km.

Dahle *et al.* established an attenuation model in 1990 for the stable tectonic region of Europe. It incorporated worldwide database from 56 intraplate earthquakes in North America, Europe, China, and Australia. This model gives expressions to predict PGA values for earthquake magnitudes between 3.0 and 6.9 and is applicable for source-to-site distances

of up to 1000 km. Thus, the Dahle *et al.* (1990) model can represent 71 percent of the observed data. Estimates of ground motion by this model are represented by the following expression:

$$\ln Y = c_1 + c_2\, M_s + \ln R + c_3\, r_{hypo} \tag{3.7}$$

where Y is the largest component of PGA, and

$$R = \begin{cases} 1/r_{hypo} & \text{for } r_{hypo} \leq 100 \text{ km} \\ (1/100)(100/\, r_{hypo}) & \text{for } r_{hypo} > 100 \text{ km} \end{cases} \tag{3.8}$$

c_1, c_2, and c_3 are regression coefficients listed in Dahle *et al.* (1990).

Si and Midorikawa (1999) derived the attenuation relationship for Japan to predict PGA and PGV values. They treat earthquakes into three types of faulting: crustal, interplate, and intraplate. Attenuation expressions for Si and Midorikawa (1999) model are presented as follows:

$$\text{Log } A = b - \log (X + c) - k X \tag{3.9}$$

where A is maximum amplitude of PGA (cm/s^2), and PGV (cm/s), and M_w is earthquake magnitude.

$$b = a\, M_w + h\, D + \sum d_i\, S_i + e + \varepsilon \tag{3.10}$$

$$c = 0.0055 \times 10^{0.50M_w} \qquad \text{for PGA} \tag{3.11}$$

$$c = 0.0028 \times 10^{0.50M_w} \qquad \text{for PGV} \tag{3.12}$$

Some of the parameters used in the model are:

D= hypocentral depth (km)

X = shortest distance from hypocenter (km)

S_i = fault type

a, b, c, d, e, h, and k = regression coefficients

Si and Midorikawa (1999) suggested application of their model with a cutoff fault distance R of 300 km. Although, it is clear that ground motion records for Malaysia represent fault distances larger than 300 km, this model has been included in the analysis mainly to avoid deducing a 'biased' conclusion on PGV characteristics. This is because the comparison for PGV values is provided only by the Atkinson and Boore (1995) model.

The Si and Midorikawa (1999) model was also utilized to compare estimated PGA values with recorded ones. Table 3-2 lists important ground motion parameters of the selected attenuation models used in the present study.

Table 3-2   Summary of four attenuation models selected for study

Region	Types of Earthquake	M_w	Supporting range (km)	Literature Reference
Stable Continental Region	Shallow crustal earthquake in ENA	4.0-7.25	r_{hypo} 10-500	Atkinson & Boore (1995)
	Shallow crustal earthquake in ENA	4.5-8.0	r_{jb} 1-500	Toro *et al.* (1997)
Stable tectonic region of Europe	Intraplate worldwide	3.0 –6.9	r_{hypo} 6-1000	Dahle *et al.* (1990)
Active Tectonic Region of Japan	Crustal, intraplate and interplate	5.8 -8.2	R 0-300	Si & Midorikawa (1999)

3.2.3   Methodology

The first step in analysis is to determine PGA and PGV values of 171 available accelerograms. For this purpose, horizontal components of ground motions were processed with a band-pass filter between 0.1 and 50 Hz for PGA. PGV values were obtained by integrating the accelerograms. At this stage, waveforms for all accelerograms were plotted, and insignificant ones were identified and excluded by introducing resolution values: 0.2 gal for PGA and 0.05 cm/s for PGV.

What follows next is the determination of estimated PGA and PGV values using expressions given by each attenuation model. However, prior to calculating these values, estimates of source-to-site distances, such as r_{hypo}, r_{jb}, and R were calculated. r_{hypo} is a term commonly used in both the Dahle *et al.* (1990), and Atkinson and Boore (1995) models. Toro *et al.* (1997) used r_{jb} in their model; while Si and Midorikawa (1999) used the term R to define source-to-site distance. The value of r_{hypo} is reasonably easy to estimate by using the familiar expression:

$$r_{hypo=} \sqrt{(r^2_{epi} + h^2_{hypo})} \qquad\qquad (3.13)$$

where r_{epi} is the epicentral distance. Campbell (2003), however, suggested that r_{hypo} is a poor representation of distance for "earthquakes with large rupture areas". The distance measure r_{jb} i.e. the closest horizontal distance to the vertical projection of the rupture plane was introduced by Joyner and Boore (1981). Figure 3.3 shows the various distance measures, which are widely used in characterizing ground motions: r_{rup} or the closest distance to the rupture plane was introduced by Schnabel and Seed (1973), while r_{seis} or the closest distance to the seismogenic part of the rupture plane was first used by Campbell (1987, 2000b).

The distance R is defined as the closest distance from the station or site to the rupture plane. In this study, the values R were derived by considering the source rupture model of the December 26 2004, M_w 9.0 earthquake, proposed by Megawati and Pan (2009). This rupture model was considered because the M_w9.0 earthquake was the largest earthquake recorded in Sumatera in the modern age of ground motion recording.

Reference to Megawati and Pan (2009) has facilitated us to assume a rupture plane located between 2.1ºN and 6.1ºN. The rupture model measuring 410 x 170 km, has a strike of N329ºE and a dip angle of 8º. The rupture plane was subdivided into 6 x 8 grid system, and the shortest distance from the station to the rupture plane can be determined. The present study accounts for PGA and PGV values calculated for rock site conditions as all seismic stations in Peninsular Malaysia are sited on rock areas.

The correlation between recorded and estimated PGA values is presented using all four attenuation models, while comparison of PGV values was examined using the Atkinson and Boore (1995), and the Si and Midorikawa (1999) models.

For analysis purposes, an attenuation model is assumed to give a good estimation of PGA and PGV values, if the observed values fall within the prediction ranges i.e. within the attenuation curve. Further verification of a good agreement between observed and estimated values is confirmed if both the observed and estimated values fall on or very close to the straight line making a 45-degree angle, which run through the axes of the plot.
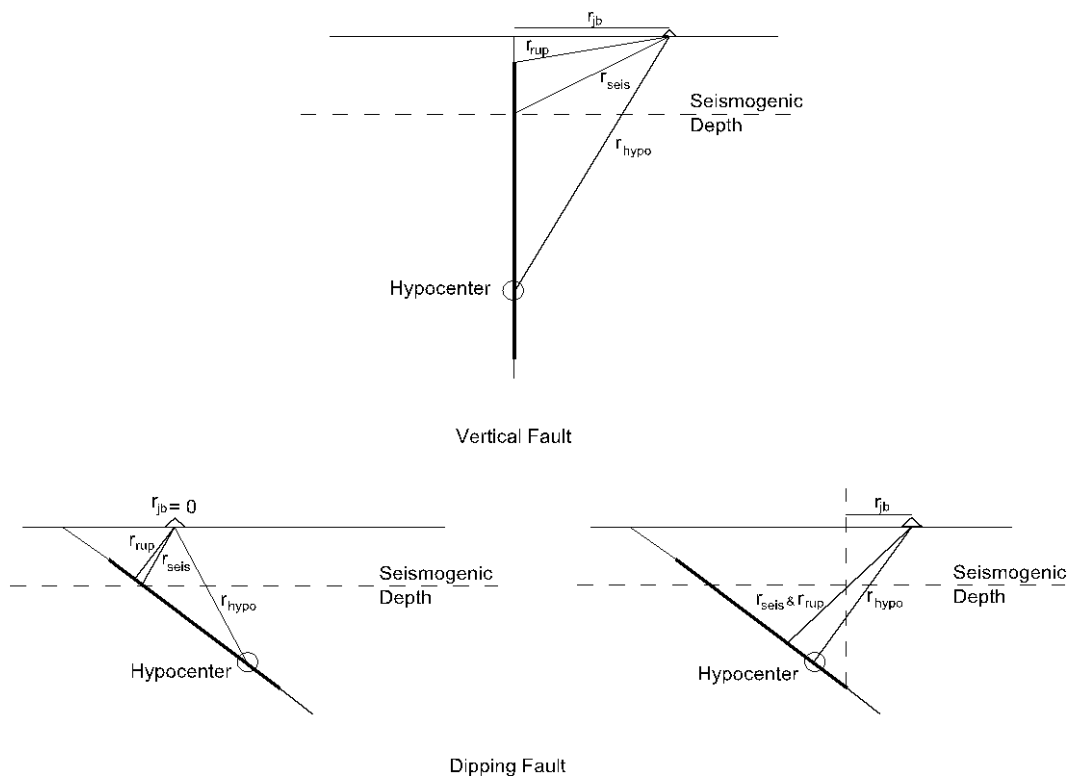
Figure 3.3 Comparison of distance measures (Abrahamson, N.A. and Shedlock, K.M. 1997. "Overview", Seismol. Res. Lett., 68, 9-23.).

3.2.4   Results and Discussion

Following seismic analysis on 15 earthquake events between May 2004 and July 2007, it was revealed that minimum value of PGA is approximately 0.3 gal corresponding to the March 6, 2007 M_w 6.4 earthquake, recorded in the E-W direction at station KUM. Minimum

PGV value of 0.05 cm/s was recorded by the October 11, 2005 M_w 5.9 earthquake in the E-W direction at station IPM, 656 km from the epicenter. Maximum PGA and PGV values are 20 gal and 15 cm/s, respectively. These correspond to the March 28, 2005 M_w 8.6 earthquake recorded in the N-S direction at FRM station near Kuala Lumpur, located approximately 515 km away from the fault plane. Comparisons between recorded and estimated PGA and PGV values are as presented in Figures 3.4 through 3.10.

3.2.4.1   Peak Ground Acceleration (PGA)

Figure 3.4 shows the plots of observed PGA values on the Atkinson and Boore (1995) attenuation curves for magnitudes M_w 6.3 and 6.7. Observation indicates that the Atkinson and Boore (1995) attenuation model estimated the data well for both earthquakes since observed data fall within the prediction range.

Similarly, Figure 3.5 indicates that the Toro *et al.* (1997) model predicted earthquakes M_w 6.3 and 6.7 well as observed PGA values fall very close to the attenuation curves. The same trend can be seen in Figure 3.6, whereby most of the observed PGA values lie on or clustered around the Dahle *et al.* (1990) attenuation curves for earthquakes M_w 6.1, 6.7, 8.6 and 9.0. Observation on Figure 3.7 indicates that the Si and Midorikawa (1999) model estimated PGA values fairly well, within the first order, for earthquake magnitudes M_w 5.9, 6.1, 6.7, 8.6, and 9.0, up to a distance of 700 km.

As suggested by Figures 3.4 through 3.7, the selected attenuation models provide relatively good estimates of PGA values for distant ground motions originated in Sumatera. The analysis has shown that recorded PGA values, for earthquake magnitude between 5.9 and 9.0, seem to agree well with the values predicted using the Atkinson and Boore (1995), the Toro *et al.* (1997) and the Dahle *et al.* (1990) models. The results show that the Dahle *et al.* (1990) model estimates PGA values most accurately. Figure 3.8 shows that the majority of the data points, representing recorded and estimated PGA values, fall on or close to the 45-degree line through the axes. This further confirms that the Dahle *et al.* (1990) model would best represent the attenuation characteristic of ground motions in Peninsular Malaysia.
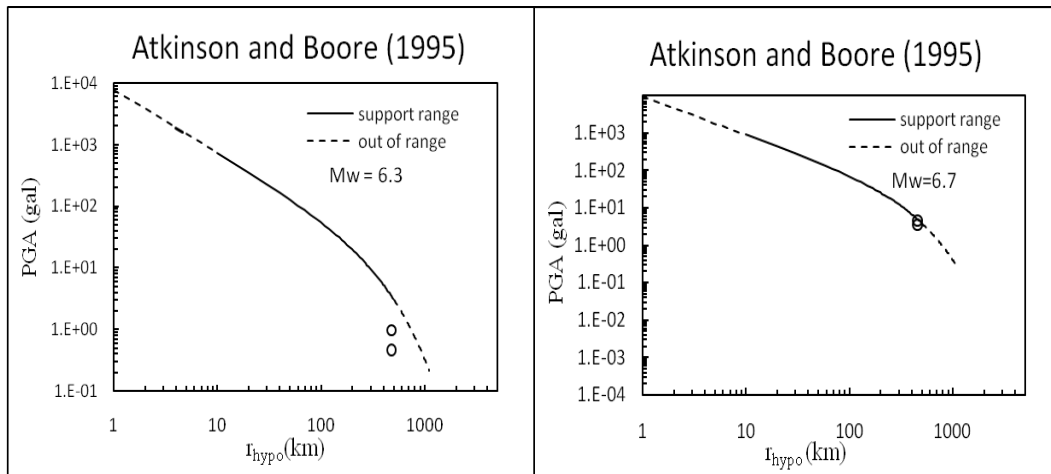
Figure 3.4 Comparison of recorded PGA with estimated PGA using the Atkinson and Boore (1995) model, for M_w 6.3 and 6.7.
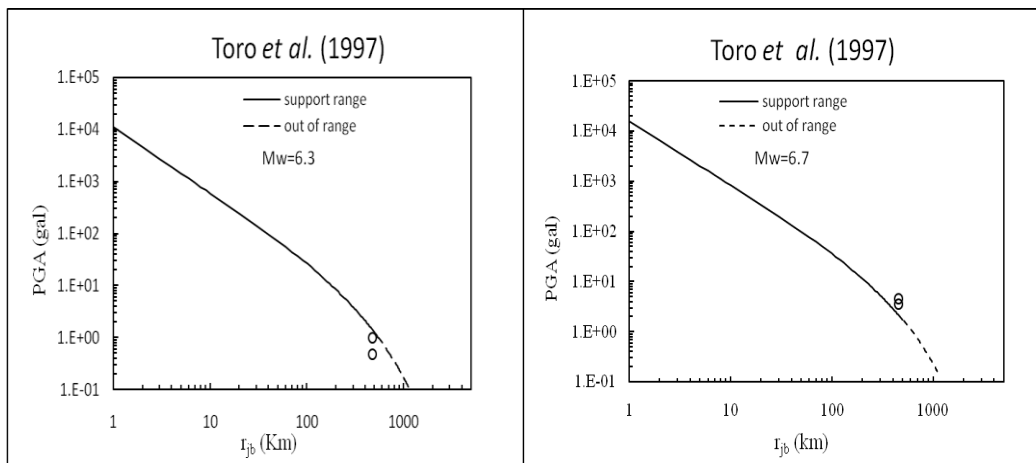
Figure 3.5 Comparison of recorded PGA with estimated PGA using the Toro *et al.* (1997) model for M_w 6.3 and 6.7.
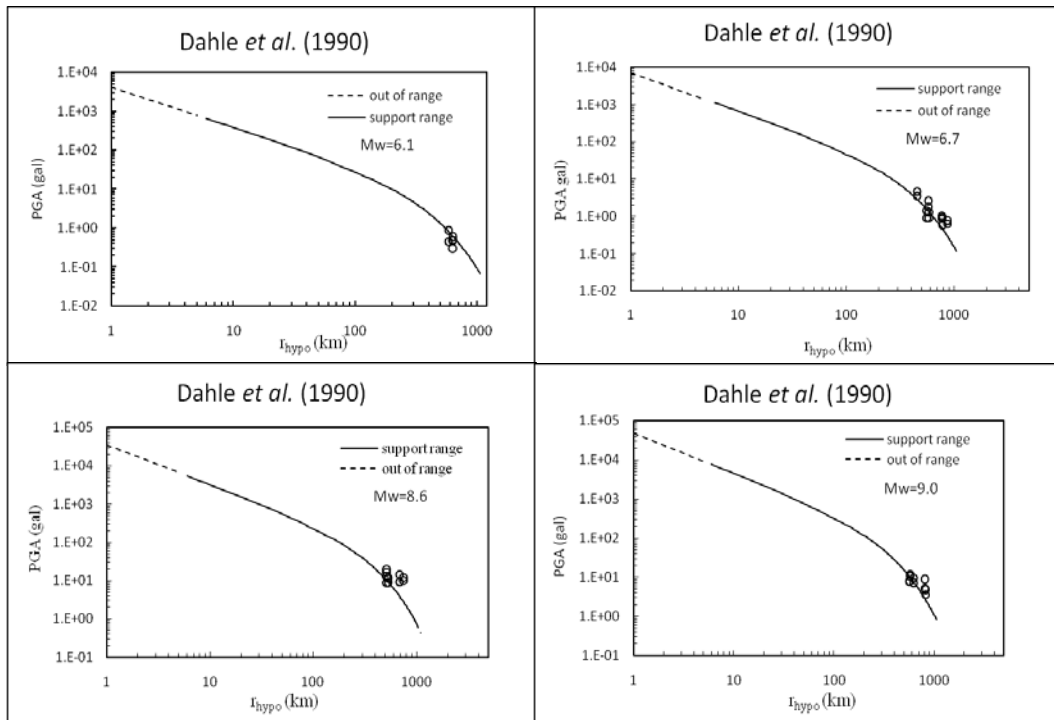
Figure 3.6   Comparison of recorded PGA with estimated PGA using
the Dahle *et al.* (1990) model for M_w between 6.1 and 9.0.

The Si and Midorikawa (1999) model, on the other hand, only gave good PGA predictions for earthquake magnitudes Mw 5.9, 6.1, 6.7, 8.6, and 9.0, for distances up to 700 km. A possible explanation for this is that the Si and Midorikawa (1999) model was developed to predict ground motions for source-to-site distances up to 300 km and as such is out of range for estimating distant ground motions resulting from the Sumatran earthquakes.
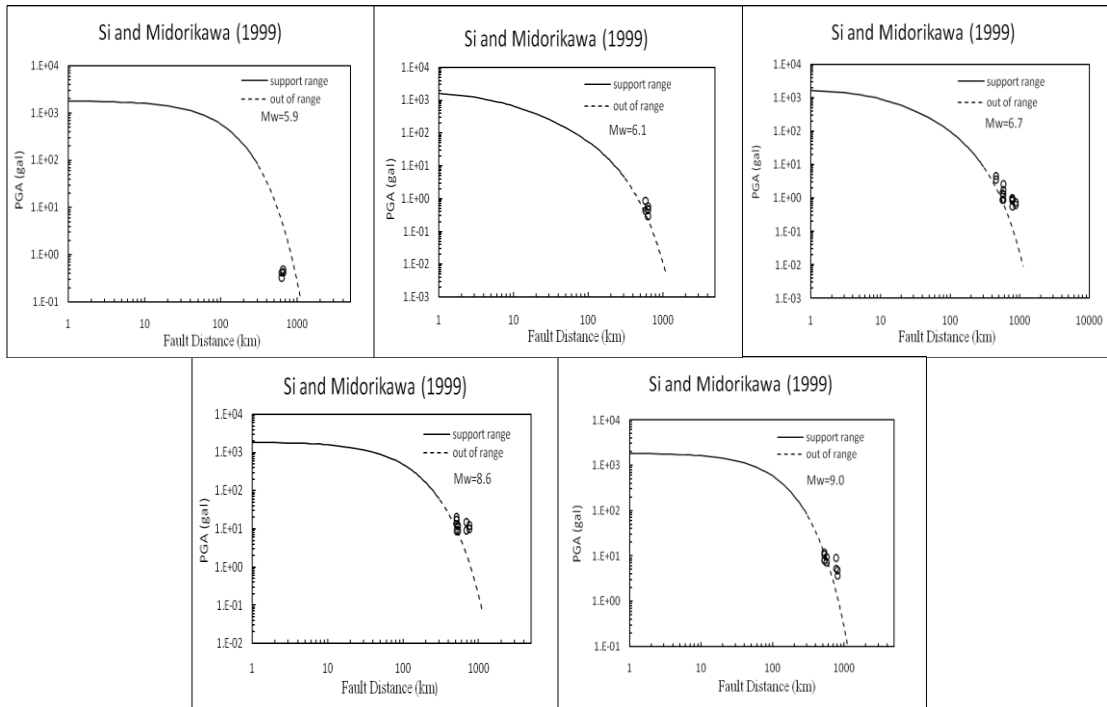
Figure 3.7   Comparison of recorded PGA with estimated PGA using Si and Midorikawa (1999) model for M_w between 5.9 and 9.0
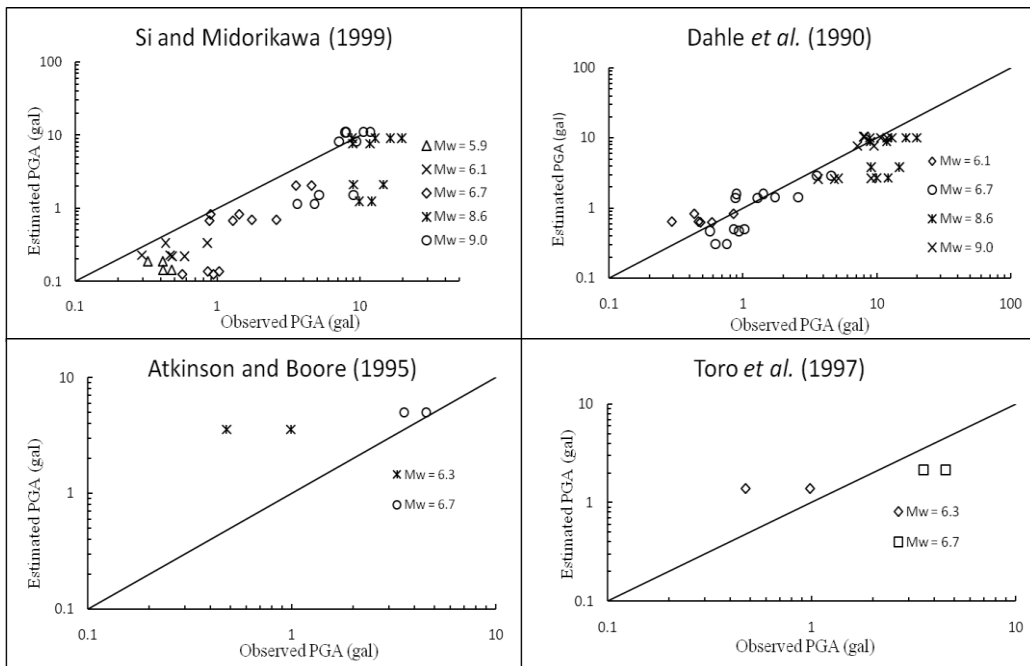
Figure 3.8   Comparison between estimated and observed PGA values.

3.2.4.2 Peak Ground Velocity (PGV)

Comparisons of recorded PGV with those estimated using attenuation models of Atkinson and Boore (1995), and Si and Midorikawa (1999) are as demonstrated in Figures 3.9 and 3.10, respectively. Results of comparison using the Atkinson and Boore (1995) model in Figure 3.9 show that the model predicted the Sumatran earthquakes well since recorded values fall very close or on the attenuation curves for both M_w 6.3 and 6.7 earthquakes.
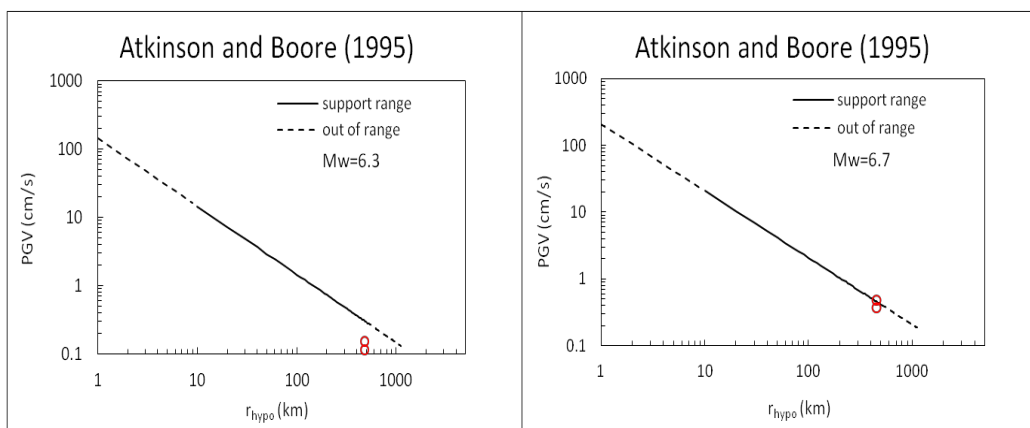
Figure 3.9 Comparison of recorded PGV with estimated PGV using the Atkinson and Boore (1995) model for M_w 6.3 and 6.7.

Comparison using the Si and Midorikawa (1999) model, as shown in Figure 3.10, illustrates that the model underestimated PGV values for all earthquake magnitudes under study. Again, as have been discussed earlier in section 3.2.4.1, a possible explanation for this is that, ground motions recorded by seismic stations in Peninsular Malaysia have source-to-site distances beyond 300 km and therefore, are out of range for this model. The Si and Midorikawa (1999) model was developed using near-field strong ground motions of the seismically active region of Japan and therefore is not appropriate to represent distant ground motions of Sumatera. Figure 3.11 further supports the deduction whereby the observed and estimated PGV data points lie at the lower portion of the 45-degree line. On the other hand, the comparison of recorded PGV with those estimated using the Atkinson

and Boore (1995) attenuation relationship suggested that the Atkinson and Boore (1995) model predicted PGV values well for earthquakes of magnitudes M_w 6.3 and 6.7.
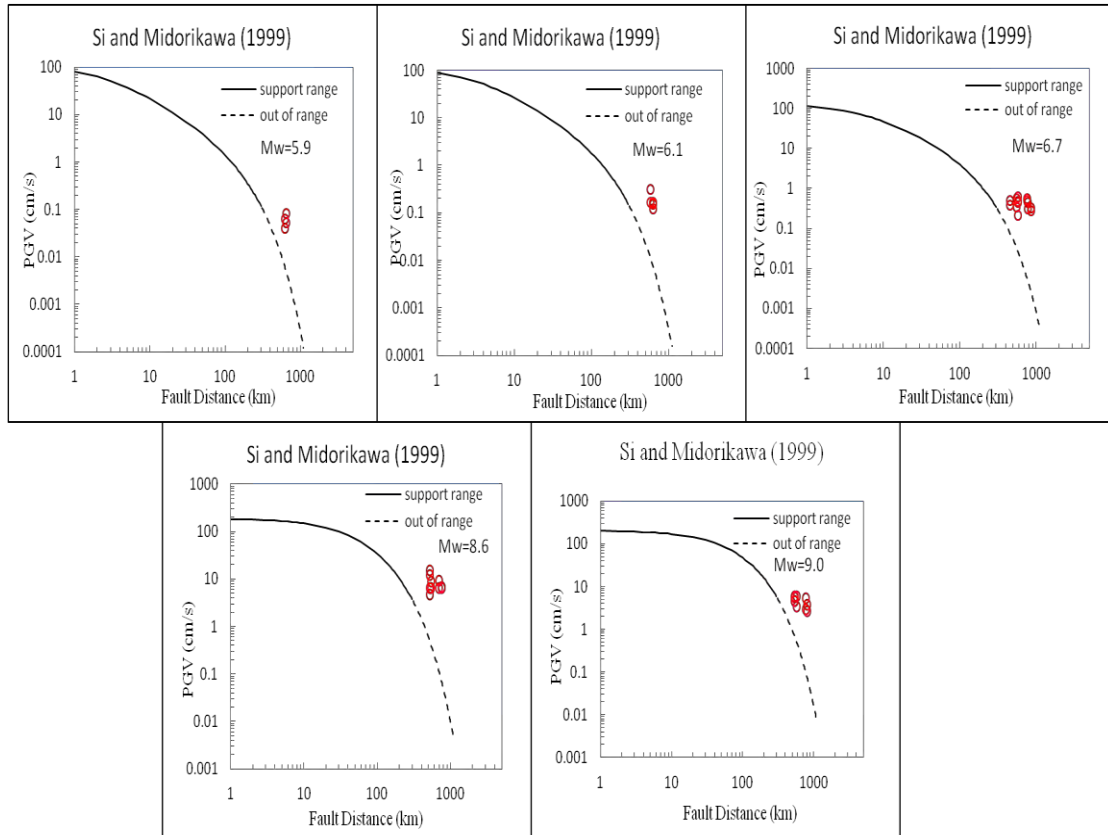
Figure 3.10   Comparison of recorded PGV with estimated PGV using the Si and Midorikawa (1999) model for M_w between 5.9 and 9.0.
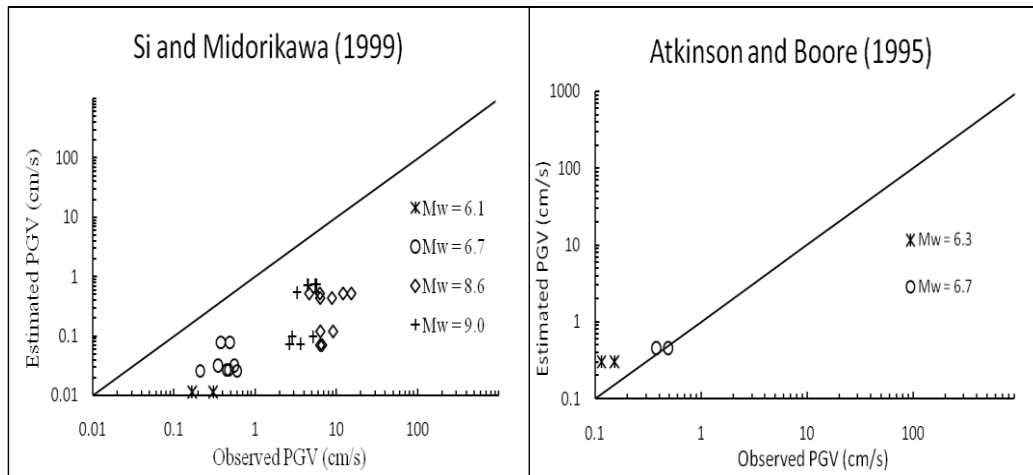
Figure 3.11   Comparison between estimated and observed PGV values.

3.3   Maximum Magnitude Earthquake within Inland Malaysia

It is important to assess the maximum magnitude earthquake for a seismic source, as this parameter may dominate the ground motion assessment in low seismicity regions (Bender, 1984). For a country with insufficient historical earthquake data; and a lack of information on geologic structures and recognizable earthquake faults, area sources may be employed to estimate maximum magnitude earthquake. For the case of low seismicity regions, it is assumed that the largest historical earthquake is the minimum value for a maximum earthquake estimate (Tenhaus *et al.*, 2003). This research regards that it is significant to estimate the maximum magnitude earthquake because this value may influence the design earthquake ground motion chosen for an engineering evaluation of structures including bridges.

From section 2.2.2, it can be identified that the maximum magnitude earthquake observed in Malaysia within a period of 136 years, beginning 1874, is 6.5 M_b, which was recorded in the state of Sabah. At an instance, one may assume a maximum magnitude earthquake as 6.5 M_b, however, to estimate a maximum magnitude earthquake with a return period of 1000 years, it is predicted that larger earthquakes may occur in Malaysia. This is considering the claim of reactivation of the Bukit Tinggi fault due to the occurrences of several earthquakes in Sumatera (Mustaffa Kamal Shuib, 2009). As such, it is assumed that the minimum earthquake magnitude expected in Malaysia is an earthquake, which will result in a surface rupture. Based on the knowledge that an earthquake of magnitude 6.5 and

49

larger is capable of producing surface rupture, it is thus decided that the maximum magnitude earthquake expected for Malaysia shall be 6.5, with a recurrence interval of 1000 years. Note that, as the M6.5 earthquake may be associated with surface rupture, we cannot predict where the earthquake would occur.

It would be interesting to estimate the ground motion at a chosen site, some distance away from a seismic source, for seismic performance assessment. For this purpose, the Samudera Bridge, located 30 km away from the Bukit Tinggi fault, has been chosen for study. The Bukit Tinggi fault is selected on the capacity that it recorded 32 small magnitude earthquakes between November 2007 and December 2009. In section 3.2.4.1, it has been shown that the Dahle *et al.* (1990) attenuation model predicts PGA values in Malaysia most accurately, and thus, the ground acceleration at the Samudera Bridge is estimated using this model. Considering that the Bukit Tinggi fault would generate a 6.5 magnitude earthquake, and assuming a shallow earthquake of 5 km depth, the ground acceleration at the Samudera Bridge, which is sited on rock, is predicted as 135 gal. However, if the earthquake occurs at a nearer location its ground acceleration will be larger.

Another important parameter, which describes the characteristics of possible ground motions, is the peak ground displacement (PGD). This parameter can determine the maximum allowable displacement that a bridge may resist to avoid failure. PGD can be estimated from the peak ground velocity (PGV) attenuation models.

Considering the near fault scenario as described above, the PGV value may be best estimated by using the Si and Midorikawa (1999) model. This model is selected because it accounted for near source data, unlike other attenuation models discussed in this chapter, which did not incorporate near source data well.

For these parameters: M=6.5, D=10 km, X=1 km, the PGV value is calculated, using the Si and Midorikawa (1999) model, to be approximately 60 cm/s. PGD can now be estimated as:

$$\omega = 2\pi f \tag{3.14}$$

where

ω = natural angular frequency (sec^{-1})

f = natural frequency = 1/T (Hz)

T = natural period of structure (sec)

Assume the worst case scenario, whereby the damage anticipated during the 6.5 magnitude earthquake, would occur during the predominant period in the range of 1.5 to 2.0 seconds, as with the case during the 1995 Kobe earthquake. Taking the predominant period as 1.5 seconds will result in ω equivalent to 4.2 sec^{-1}. With PGV of 60 cm/s, and ω = 4.2 sec^{-1}, the peak ground displacement is estimated at approximately 15 cm. Thus, it is safe to deduce that the allowable ultimate displacement for Malaysia is 150 mm.

The next important task is choosing input ground motions for seismic performance evaluation of the Samudera Bridge based on the ground acceleration estimate. In addition to subjecting the bridge to the largest ground motion recorded in Malaysia i.e. the 2005 Sumatera earthquake, this study proposes to employ the 1995 Kobe and the 1940 El Centro ground motions to evaluate the seismic performance of the Samudera Bridge to observe its response to larger ground motions. The selection of the Kobe ground motion is justified considering the location of the bridge, which is within a short distance from the Bukit Tinggi fault. The shortest distance from the fault to the bridge is 15 km.

3.4 Conclusions

Understanding the attenuation characteristics of ground motions is crucial for optimized seismic hazard assessment or design of seismic resistant structures. For this reason, researchers have heightened their efforts to gather information on earthquake motions over the decades. In earthquake engineering, PGA and PGV are two most important strong motion parameters used in seismic hazard assessment, estimation of acceleration response spectra, and dynamic analysis. PGA has been widely used in studying the characteristics of any strong ground motion, whereas PGV has found its application in estimating possible damage. In addition, PGD is also important to evaluate allowable ultimate displacement to consider non-linear response.

Seismic activities in Malaysia are low, resulting in limited historical data for the development of an attenuation relationship. In addition, developing an attenuation model for Malaysia is a great challenge due to uncertainties in identifying seismic sources within the country. Therefore, an appropriate approach, which can be used to predict the characteristics of ground motions in Malaysia, is by selecting an attenuation model, from a list of

established models, which would best describe its seismicity. Section 3.2 of this chapter has described a methodology for selection of attenuation model(s) for Peninsular Malaysia.

Results of analysis show that attenuation characteristics of ground motions for Peninsular Malaysia can be appropriately represented by attenuation models established for stable tectonic region, used herein. As such, these models may be used to estimate or predict ground motion amplitudes across Peninsular Malaysia, for application in seismic hazard assessment, seismic design or engineering assessment of structures. In conclusion, the Dahle *et al.* (1990) model best represents the attenuation characteristics of ground motion in terms of PGA, while the Atkinson and Boore (1995) model may appropriately estimate ground motion in terms of PGV for distant earthquakes.

It is also worth noting that estimating a maximum magnitude earthquake within a near inland area is essential to help understand the seismic hazard in a low seismicity region. Engineering evaluation or structural design may refer to this value for future design of both bridges and buildings. In reference to the available historical earthquake data, it is proposed that the maximum magnitude earthquake for Peninsular Malaysia is 6.5. Based on this magnitude, the PGV is estimated at 60 cm/s, and the PGD is calculated as 150 mm. Therefore, it is proposed that the seismic performance evaluation of the bridge, in chapter 4 of the thesis, should employ large acceleration ground motion, such as that recorded by the 1995 Kobe earthquake.

Acknowledgements

References

Atkinson, G.M., and D.M. Boore (1995). New ground motion relations for Eastern North America. *Bulletin of the Seismological Society of America* 85, 17-30.

Bender, B. (1984). Incorporating Acceleration Variability into Seismic Hazard Analysis. *Bulletin of the Seismological Society of America* 74, 1451-1462.

Campbell, K.W. (2003). Engineering models of strong ground motion. In *Earthquake Engineering Handbook.* Chen, W.F. and Scawthorn, C. (Eds), CRC Press, London, chap 5.

Chandler, A., and N. Lam (2004). An attenuation model for distant earthquakes. *Earthquake Engineering and Structural Dynamics* 33, 183-210.

Dahle, A., H. Bungum, and L.G. Dvamme (1990). Attenuation models inferred from intraplate earthquake recordings. *Earthquake Engineering and Structural Dynamics* 19, 1125-1141.

Megawati, K., and T-C. Pan (2009). Regional seismic hazard posed by the Mentawai segment of the Sumatran Megathrust. *Bulletin of the Seismological Society of America* 99, 566-584.

Mustaffa Kamal Shuib, (2009). The Recent Bukit Tinggi Earthquakes and their Relationship to Major Geological Structures. *Geological Society of Malaysia*, Bulletin 55, Nov. 2009, pp 67-72.

National Earthquake Information Center Database. USGS. http://neic.usgs.gov/.

Petersen, M.D., J. Dewey, S. Hartzell, C. Mueller, S. Harmsen, A.D. Frankel, and K. Ruskstales (2004). Probabilistic seismic hazard analysis for Sumatra, Indonesia and across the Southern Malaysian Peninsular. *Techtonophysics* 390, 141-158.

Si, H., and S. Midorikawa (1999). New attenuation relationships for peak ground acceleration and velocity considering effects of fault type and site condition. *Journal of Struct. Constr. Eng.*, AIJ 523, 63-67.

Tenhaus, P.C., and K.W. Campbell (2003). Seismic Hazard Analysis. In *Earthquake Engineering Handbook.* Chen, W.F. and Scawthorn, C. (Eds), CRC Press, London, chap 8.

Toro, G.R., N.A. Abrahamson, and J.F. Schneider (1997). Model of strong ground motions from earthquakes in Central and Eastern North America: Best estimates and uncertainties. *Seismological Research Letters* 68, 41-57.

Appendix 3A

Table 3A-1   Raw data obtained from the Malaysian Meteorological Department

	(Y/M/D)	STATION	Peak Ground Acceleration (PGA)	
			EW (gal)	NS (gal)
1	20040511	BTM	1.3747440	1.7307780
2	20040511	FRM	1.1661020	2.3541560
3	20040511	IPM	0.8468180	0.4318860
4	20040511	KDM	0.1064280	0.1082900
5	20040511	KGM	0.4804940	0.5851580
6	20040511	KKM	0.6608140	0.4193420
7	20040511	KSM	0.1594460	0.2565640
8	20040511	KTM	1.5284080	1.0727080
9	20040511	KUM	0.4640300	0.2940000
10	20040511	SDM	0.4075820	0.5001920
11	20040511	TSM	0.5152840	0.5029360
12	20040725	BTM	3.3721800	3.2356660
13	20040725	FRM	0.8704360	1.8697420
14	20040725	IPM	0.4410000	0.5274360
15	20040725	KDM	2.1428680	3.6247260
16	20040725	KGM	2.7548780	2.9634220
17	20040725	KKM	5.7105580	3.9878160
18	20040725	KSM	1.0562440	2.3298520
19	20040725	KTM	1.0280200	1.0406620
20	20040725	KUM	0.4537400	0.3732820
21	20040725	SDM	3.9819360	2.9120700
22	20040725	TSM	3.4561660	2.1277760
23	20041226	BTM	1.4867580	1.2762540
24	20041226	FRM	7.1367520	9.4571960
25	20041226	IPM	11.8248760	10.6155560

26	20041226	KDM	0.6234760	0.6874700
27	20041226	KGM	3.6360940	4.7922000
28	20041226	KKM	1.0241980	0.6464080
29	20041226	KSM	1.3901300	1.8608240
30	20041226	KTM	5.1529380	9.0207040
31	20041226	KUM	8.0402140	7.9019360
32	20041226	SDM	1.0040100	0.7364700
33	20041226	TSM	0.7323540	0.5724180
34	20050205	BTM	5.3374720	5.3584440
35	20050205	FRM	3.1784340	2.7924120
36	20050205	IPM	0.1308300	0.0764400
37	20050205	KDM	0.7427420	0.7253960
38	20050205	KKM	9.2667820	6.9242880
39	20050205	KSM	0.2416680	0.3054660
40	20050205	KTM	0.3086020	0.4530540
41	20050205	KUM	0.0564480	0.0416500
42	20050205	SBM	0.6695360	0.6096580
43	20050205	SDM	2.0427120	1.9570600
44	20050205	TSM	1.1000500	1.0641820
45	20050328	BTM	0.2208920	0.2767814
46	20050328	FRM	16.4412640	19.7693440
47	20050328	IPM	8.8303880	12.8717120
48	20050328	KDM	8.8731158	12.7537199
49	20050328	KGM	9.0482420	14.6857900
50	20050328	KKM	1.8187820	0.8097740
51	20050328	KSM	3.9353860	4.0614140
52	20050328	KTM	9.9553300	12.1240700
53	20050328	KUM	11.7982200	8.9319160
54	20050328	SBM	2.3226980	5.0986460
55	20050328	SDM	12.5881003	8.9775839

56	20050328	TSM	12.5881003	8.9775839
57	20050403	FRM	2.6920600	5.5933500
58	20050403	IPM	53.4149980	2.2378300
59	20050403	KDM	0.2208920	0.2767814
60	20050403	KGM	1.2171600	0.8299620
61	20050403	KTM	1.1285680	0.8943480
62	20050403	KUM	0.4768680	0.9844100
63	20050410	BTM	0.9634380	0.8793540
64	20050410	FRM	2.0729940	1.9735240
65	20050410	IPM	36.1656260	0.7810600
66	20050410	KDM	0.1273020	0.1875720
67	20050410	KGM	2.5800460	1.7348940
68	20050410	KKM	1.3690600	1.7442040
69	20050410	KSM	0.6134800	0.6199480
70	20050410	KTM	0.7551880	0.6213200
71	20050410	KUM	0.9324700	0.5641860
72	20050410	SDM	0.1443540	0.1039780
73	20050410	TSM	0.1320060	0.1088780
74	20050419	BTM	5.3676560	4.9267540
75	20050419	FRM	12.5881003	8.9775839
76	20050419	IPM	12.5881003	8.9775839
77	20050419	KDM	12.5881003	8.9775839
78	20050419	KKM	0.2407860	1.2556740
79	20050419	KSM	0.0556640	0.3535840
80	20050419	KTM	12.5881003	8.9775839
81	20050419	KUM	12.5881003	8.9775839
82	20050419	SBM	1.4892080	1.3139840
83	20050419	SDM	0.0692860	0.2855720
84	20050419	TSM	12.5881003	8.9775839

85	20050428	FRM	0.8072260	1.1411120
86	20050428	IPM	21.5732300	0.4768680
87	20050428	KGM	0.2593080	17.2293800
88	20050428	KTM	0.3128160	0.2743020
89	20050428	KUM	0.9182600	0.3648540
90	20050514	BTM	0.2208920	0.2767814
91	20050514	FRM	4.5550400	3.5418180
92	20050514	IPM	37.8043820	1.3062420
93	20050514	KGM	0.2208920	0.2767814
94	20050514	KTM	1.6703120	1.9921440
95	20050514	KUM	1.2771360	0.8746500
96	20050519	FRM	2.0681920	3.8545360
97	20050519	IPM	18.0714940	1.0698660
98	20050519	KGM	0.2208920	0.2767814
99	20050519	KTM	0.8362340	0.8374100
100	20050519	KUM	1.3148660	0.9162020
101	20050523	BTM	1.5069460	2.0251700
102	20050523	KDM	1.5461460	1.7987900
103	20050523	SBM	0.3323180	0.5817280
104	20050523	SDM	7.6554660	8.6048900
105	20050523	TSM	0.7272580	0.5906460
106	20050630	BTM	1.2732160	0.9564800
107	20050630	KKM	0.7525420	0.7246120
108	20050630	KSM	0.1588580	0.1871800
109	20050630	SBM	0.1155420	0.1246560
110	20050630	SDM	0.1035860	0.0919240
111	20050630	TSM	0.0592900	0.0568400
112	20050705	FRM	2.1359100	3.5637700
113	20050705	IPM	36.5642900	1.1972660
114	20050705	KGM	0.2208920	0.2767814

115	20050705	KTM	1.0232180	0.8511300
116	20050705	KUM	1.4139440	0.8905260
117	20050724	FRM	0.8207500	1.6044560
118	20050724	IPM	0.3721060	0.3495660
119	20050724	KGM	0.2208920	0.2767814
120	20050724	KTM	0.4184600	0.3701460
121	20050724	KUM	1.4009100	0.2764580
122	20051011	IPM	0.4142460	0.4774560
123	20051011	KGM	0.2208920	0.2767814
124	20051011	KTM	0.2579360	5.1016840
125	20051011	KUM	0.3234980	0.4128740
126	20060127	BTM	2.2351840	2.8693420
127	20060127	KDM	1.1286660	1.6167060
128	20060127	KKM	8.9948320	5.9997560
129	20060127	KSM	0.5514460	0.3204600
130	20060127	SBM	2.3052540	1.3109460
131	20060127	SDM	1.2573400	1.2339180
132	20060127	TSM	1.5336020	2.4679340
133	20060206	KDM	0.0996660	0.1147580
134	20060206	KKM	0.1866900	0.4556020
135	20060206	SDM	0.0752640	0.1491560
136	20060206	TSM	0.2950780	0.3727920
137	20060516	IPM	0.7009940	0.8323140
138	20060516	KGM	2.0034140	18.1178480
139	20060516	KTM	0.8379000	0.5601680
140	20060516	KUM	0.9913680	0.9717680
141	20060928	KDM	0.3301620	0.2286340
142	20060928	KKM	1.0136140	0.9915640
143	20060928	TSM	0.2670500	0.2964500

58

144	20061201	FRM	3.3045600	2.6671680
145	20061201	IPM	11.7012980	3.4757660
146	20061201	KGM	1.0152800	7.8273580
147	20061201	KTM	1.2091240	0.6208300
148	20061201	KUM	2.1266980	2.2335180
149	20061201	SBM	0.1920800	0.1604260
150	20061217	FRM	10.1601500	6.3039480
151	20061217	IPM	1.9078640	0.9489340
152	20061217	KGM	3.8948140	9.0579440
153	20061217	KTM	1.2818400	1.0215520
154	20061217	KUM	1.0208660	0.4799060
155	20070306	FRM	6.1694920	9.1875980
156	20070306	IPM	8.2128900	0.4678520
157	20070306	KTM	0.8689660	0.5548760
158	20070306	KUM	0.5215560	0.3190880
159	20070306	FRM	4.8434540	2.4152100
160	20070306	IPM	1.0294900	0.7935060
161	20070306	KUM	1.0018540	0.7589120
162	20070721	IPM	3.1787280	0.6534640
163	20070721	KTM	0.3216360	0.3261440
164	20070724	IPM	0.7187320	0.6849220
165	20070724	KTM	0.3908240	0.2805740
166	20070724	KUM	0.3874920	0.4046420
167	20070808	BTM	1.3459320	2.3412200
168	20070808	IPM	0.7999740	2.4974320
169	20070808	KKM	2.1538440	1.5398740
170	20070808	KSM	0.6272000	0.9578520
171	20070808	KTM	0.8787660	2.0793640

Table 3A-2   Dataset used in analysis, after filtering of insignificant waveform

Entry	Date	Station	Location Of Site (Station)		Epicentre		R_{epi}(M)	Magnitude	Rhypo (M) /Fault Dist
			Lat	Long	Lat	Long			
1	20040511	IPM	4.6 N	101.0 E	0.415	97.825	583.68	6.1	584
2	20040511	KGM	2.0 N	103.3 E	0.415	97.825	634.03	6.1	634
3	20040511	KUM	5.3 N	100.7 E	0.415	97.825	629.83	6.1	630
4	20041226	FRM	3.2 N	101.6 E	3.295	95.982	624.50	9.0	570
5	20041226	IPM	4.6 N	101.0 E	3.295	95.982	575.43	9.0	534
6	20041226	KDM	6.9 N	116.8 E	3.295	95.982	2335.30	9.0	2297
7	20041226	KGM	2.0 N	103.3 E	3.295	95.982	826.80	9.0	813
8	20041226	KKM	6.0 N	116.2 E	3.295	95.982	2258.42	9.0	2215
9	20041226	KSM	1.5 N	110.3 E	3.295	95.982	1605.80	9.0	1543
10	20041226	KTM	5.3 N	103.1 E	3.295	95.982	819.93	9.0	779
11	20041226	KUM	5.3 N	100.7 E	3.295	95.982	568.58	9.0	535
12	20041226	TSM	4.3 N	117.9 E	3.295	95.982	2435.56	9.0	2383
13	20050328	FRM	3.2 N	101.6 E	2.085	97.108	514.35	8.6	515
14	20050328	IPM	4.6 N	101.0 E	2.085	97.108	514.39	8.6	515
15	20050328	KGM	2.0 N	103.3 E	2.085	97.108	688.94	8.6	690
16	20050328	KKM	6.0 N	116.2 E	2.085	97.108	2157.47	8.6	2158
17	20050328	KSM	1.5 N	110.3 E	2.085	97.108	1469.50	8.6	1470
18	20050328	KTM	5.3 N	103.1 E	2.085	97.108	754.04	8.6	755
19	20050328	KUM	5.3 N	100.7 E	2.085	97.108	535.01	8.6	536
20	20050328	SBM	2.5 N	112.2E	2.085	97.108	1679.02	8.6	1679
21	20050403	KGM	2.0 N	103.3 E	2.022	97.942	596.09	6.3	597
22	20050403	KTM	5.3 N	103.1 E	2.022	97.942	677.56	6.3	679
23	20050403	KUM	5.3 N	100.7 E	2.022	97.942	475.51	6.3	477
24	20050410	KGM	2.0 N	103.3 E	-1.644	99.607	577.31	6.7	578
25	20050410	KKM	6.0 N	116.2 E	-1.644	99.607	2022.59	6.7	2023
26	20050410	KSM	1.5 N	110.3 E	-1.644	99.607	1240.36	6.7	1241
27	20050410	KTM	5.3 N	103.1 E	-1.644	99.607	863.83	6.7	864
28	20050410	KUM	5.3 N	100.7 E	-1.644	99.607	782.18	6.7	782

29	20050410	TSM	4.3 N	117.9 E	-1.644	99.607	2134.76	6.7	2135
30	20050428	KUM	5.3 N	100.7 E	2.132	96.799	557.71	6.2	558
31	20050514	FRM	3.2 N	101.6 E	0.587	98.459	454.08	6.7	455
32	20050514	KUM	5.3 N	100.7 E	0.587	98.459	579.97	6.7	581
33	20050519	KUM	5.3 N	100.7 E	1.989	97.041	547.70	6.9	549
34	20050705	KTM	5.3 N	103.1 E	1.819	97.082	771.02	6.7	771
35	20050705	KUM	5.3 N	100.7 E	1.819	97.082	557.31	6.7	558
36	20050724	IPM	4.6 N	101.0 E	7.920	92.190	1042.54	7.2	1043
37	20051011	IPM	4.6 N	101.0 E	4.820	95.098	655.30	5.9	656
38	20051011	KUM	5.3 N	100.7 E	4.820	95.098	623.30	5.9	624
39	20060516	IPM	4.6 N	101.0 E	0.093	97.050	665.94	6.8	666
40	20060516	KTM	5.3 N	103.1 E	0.093	97.050	885.99	6.8	886
41	20060928	KKM	6.0 N	116.2 E	11.79	95.001	2431.96	4.9	2432
42	20061217	FRM	3.2 N	101.6 E	4.815	95.018	753.11	5.8	754
43	20061217	IPM	4.6 N	101.0 E	4.815	95.018	664.15	5.8	665
44	20061217	KUM	5.3 N	100.7 E	4.815	95.018	632.19	5.8	633
45	20070306	_KTM	5.3 N	103.1 E	-0.493	100.498	705.54	6.4	706
46	20070306	KUM	5.3 N	100.7 E	-0.493	100.498	645.17	6.4	645

64

71
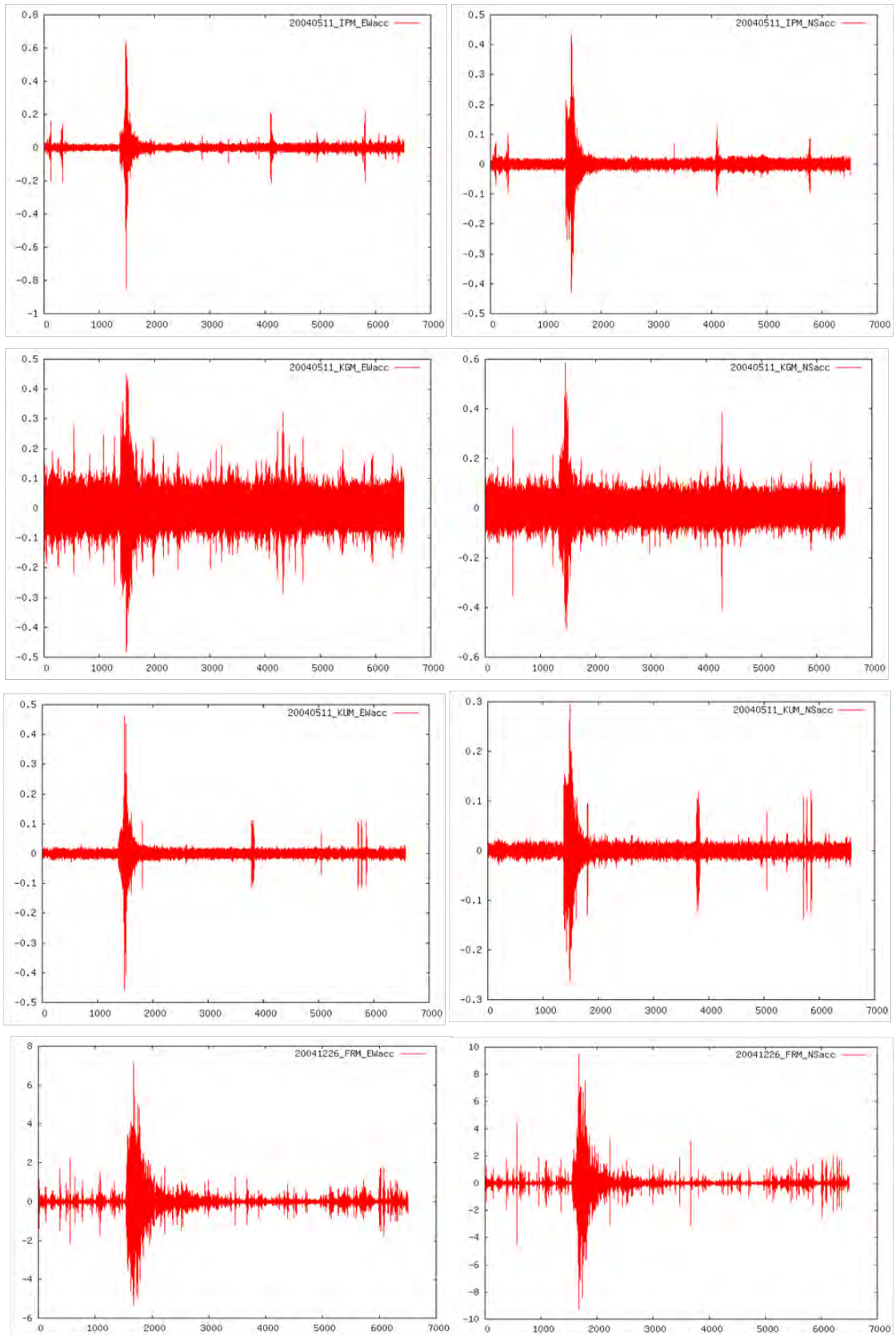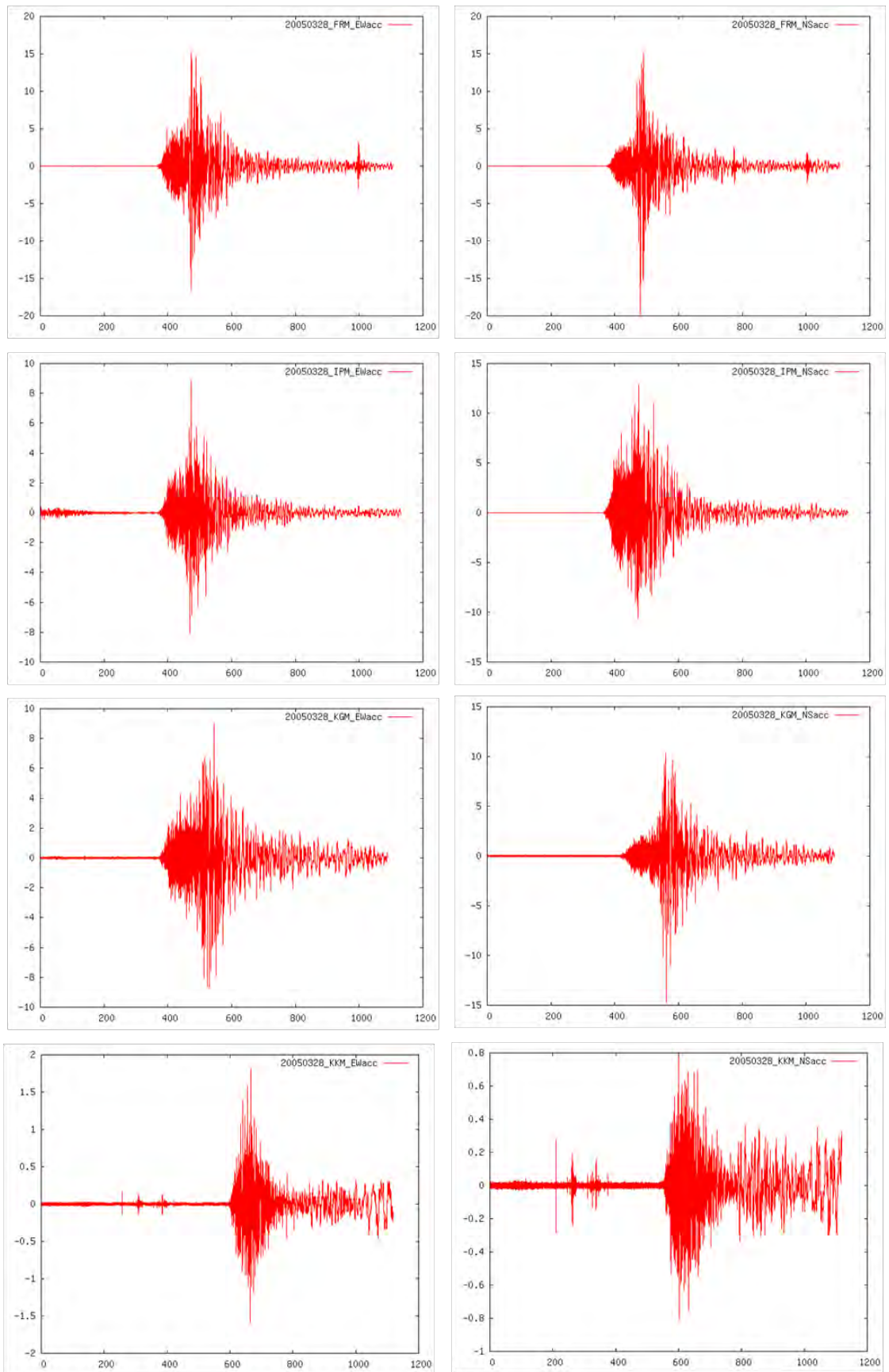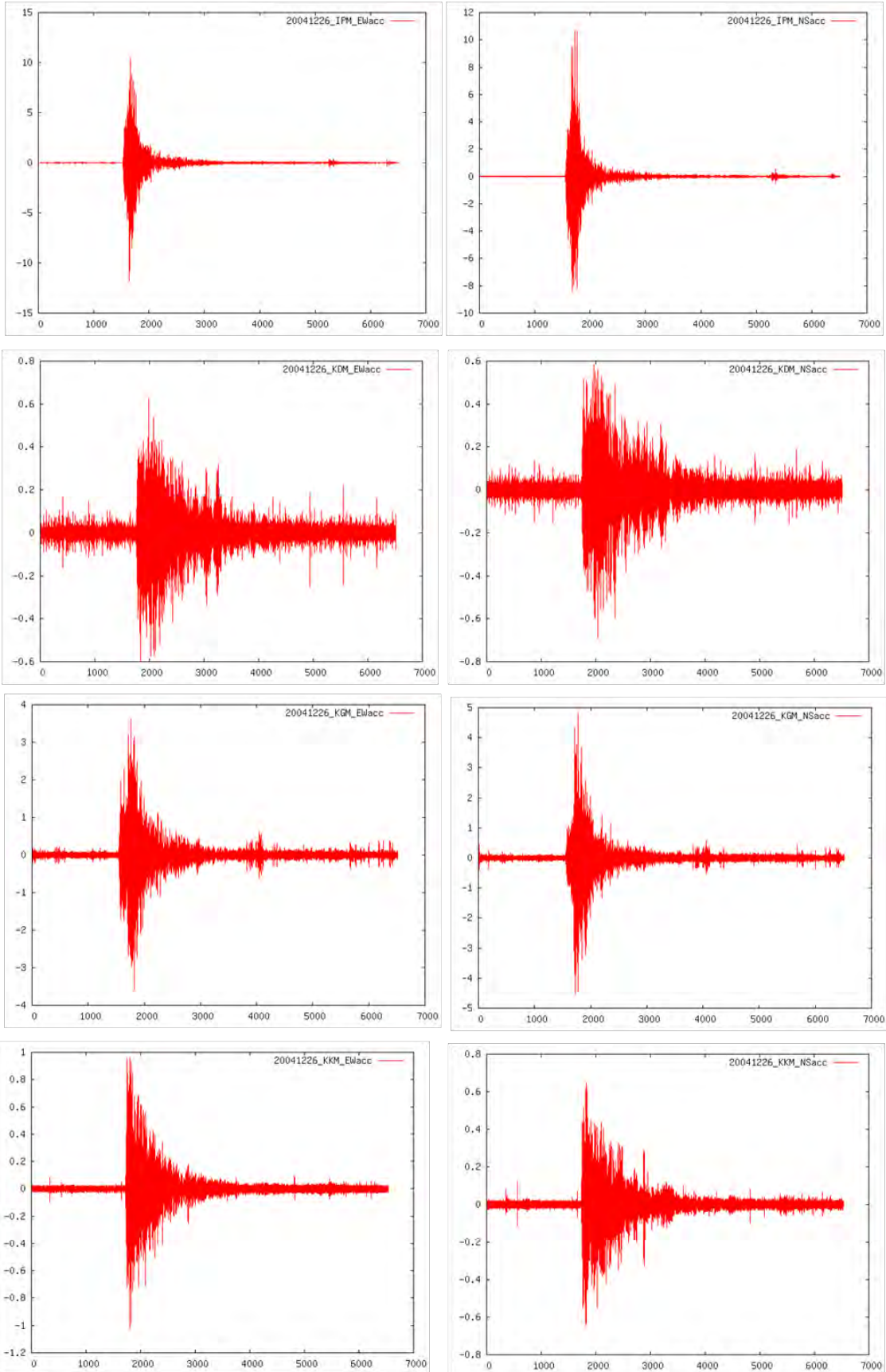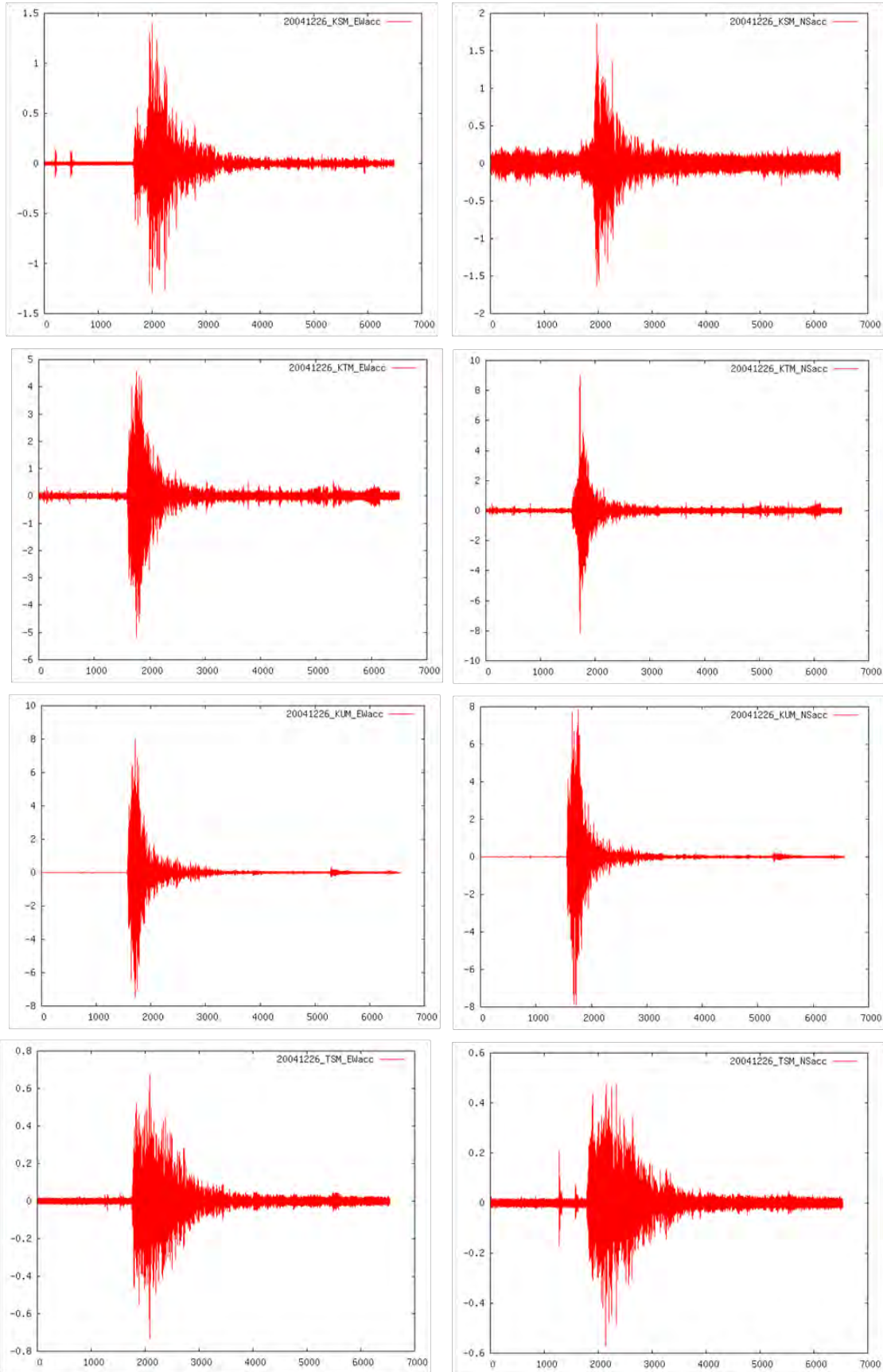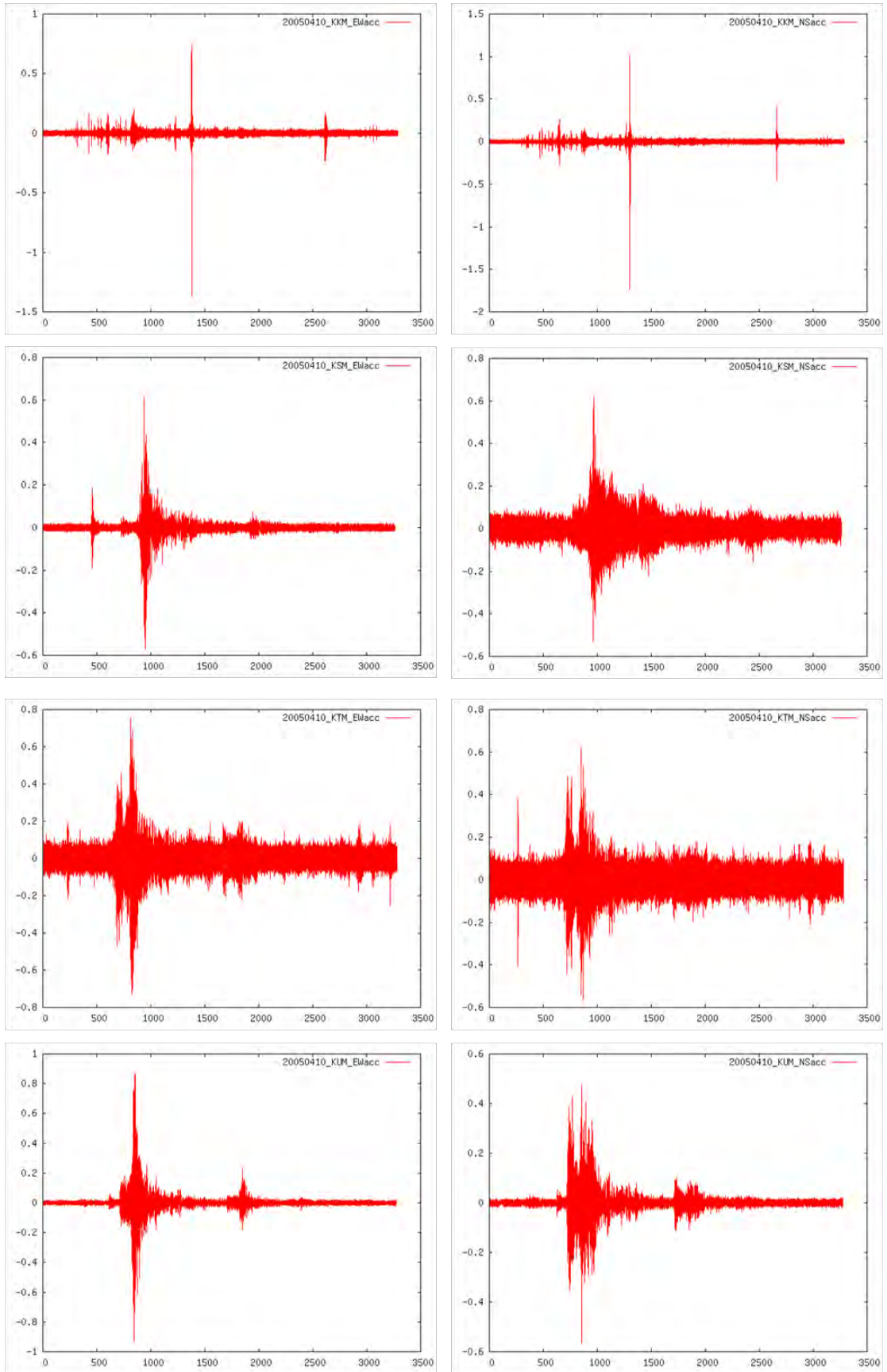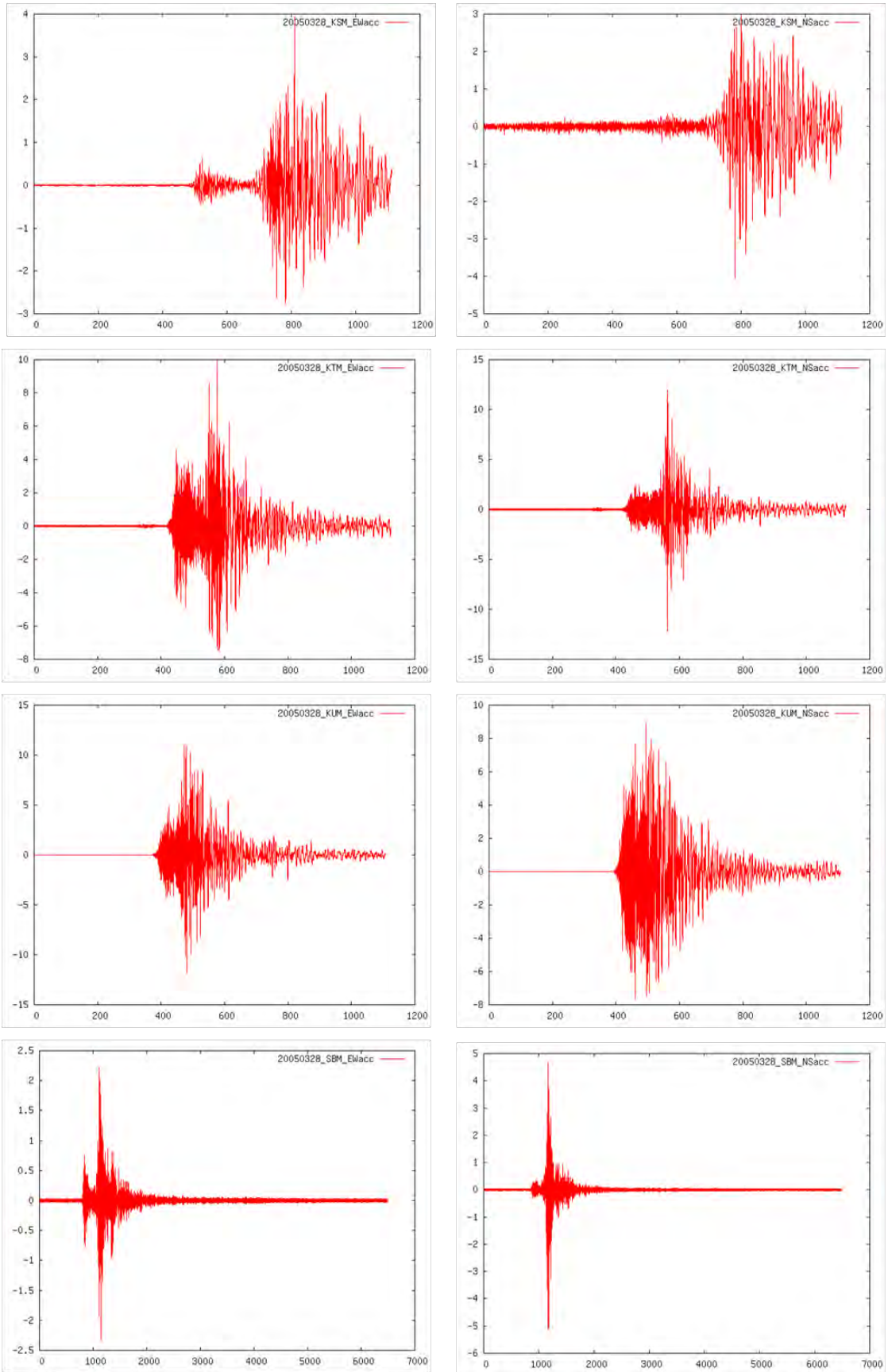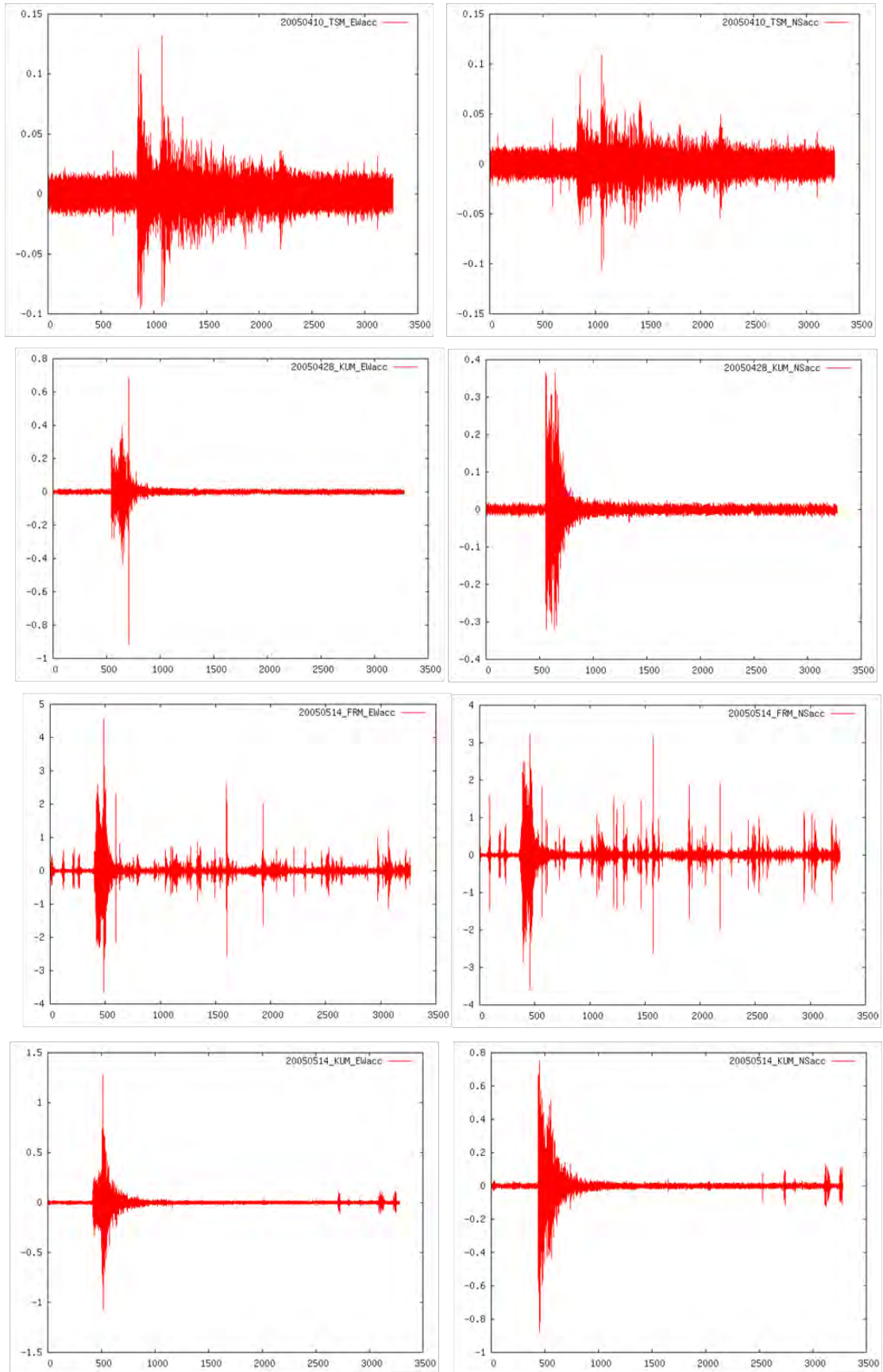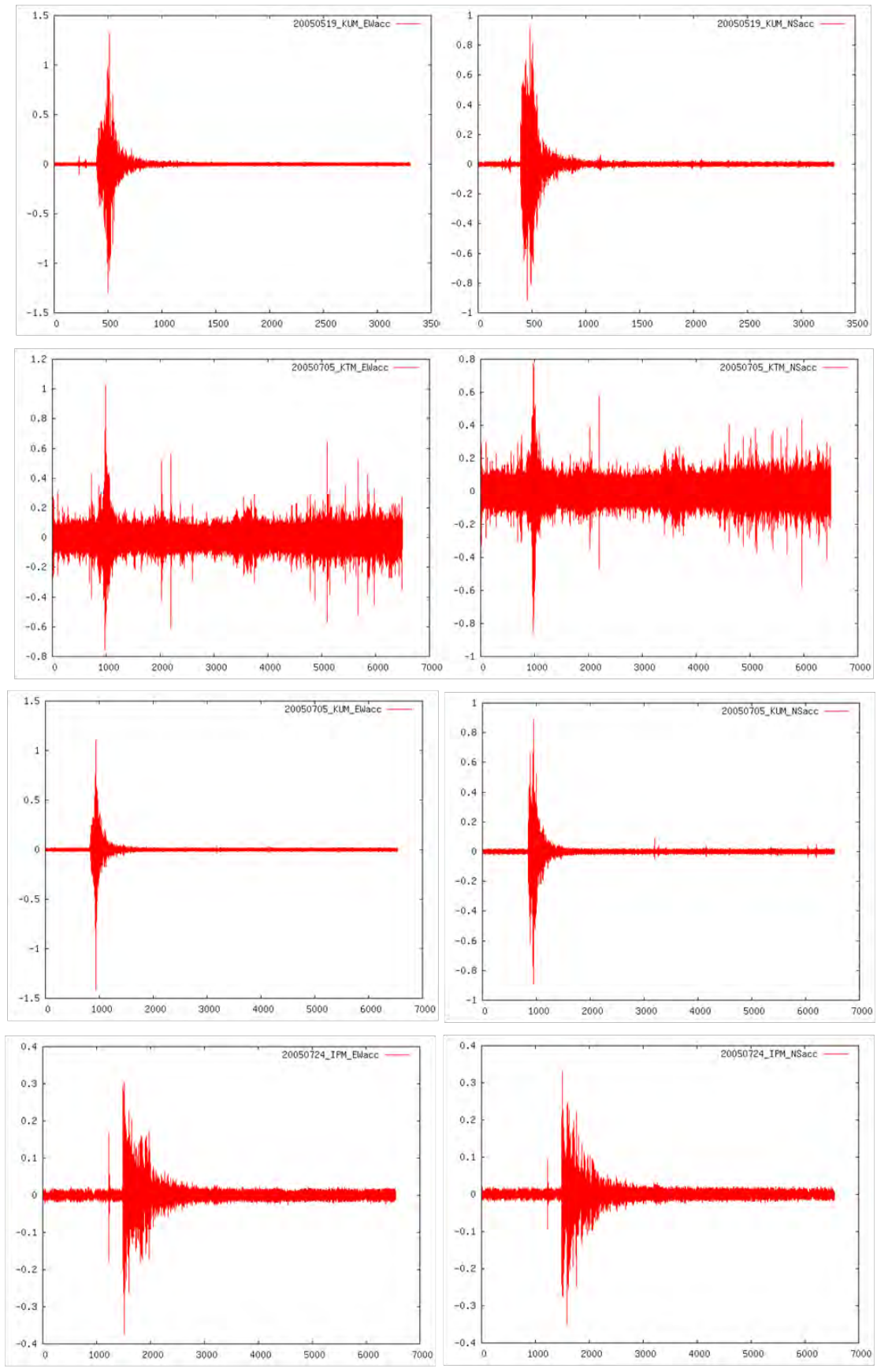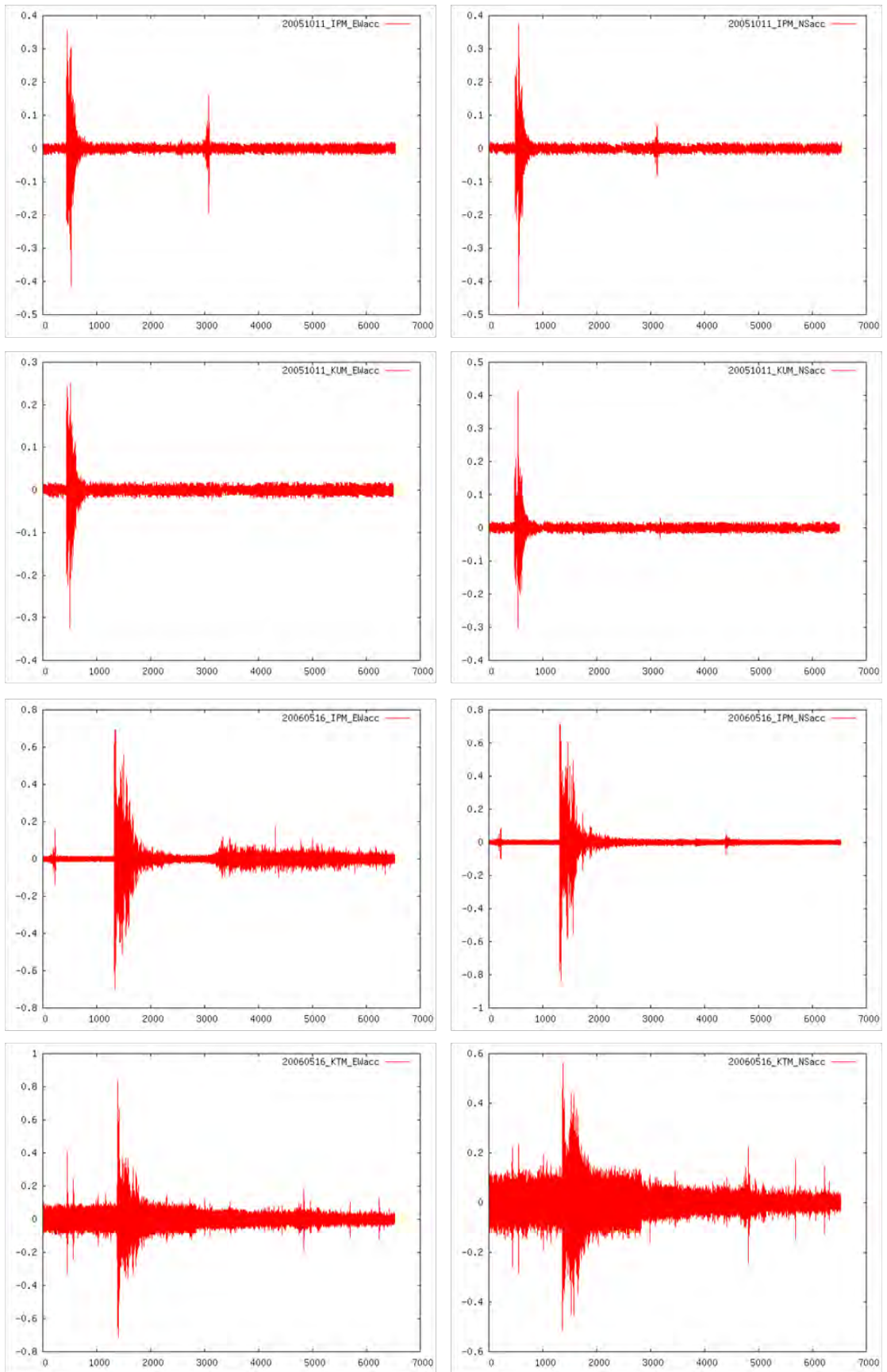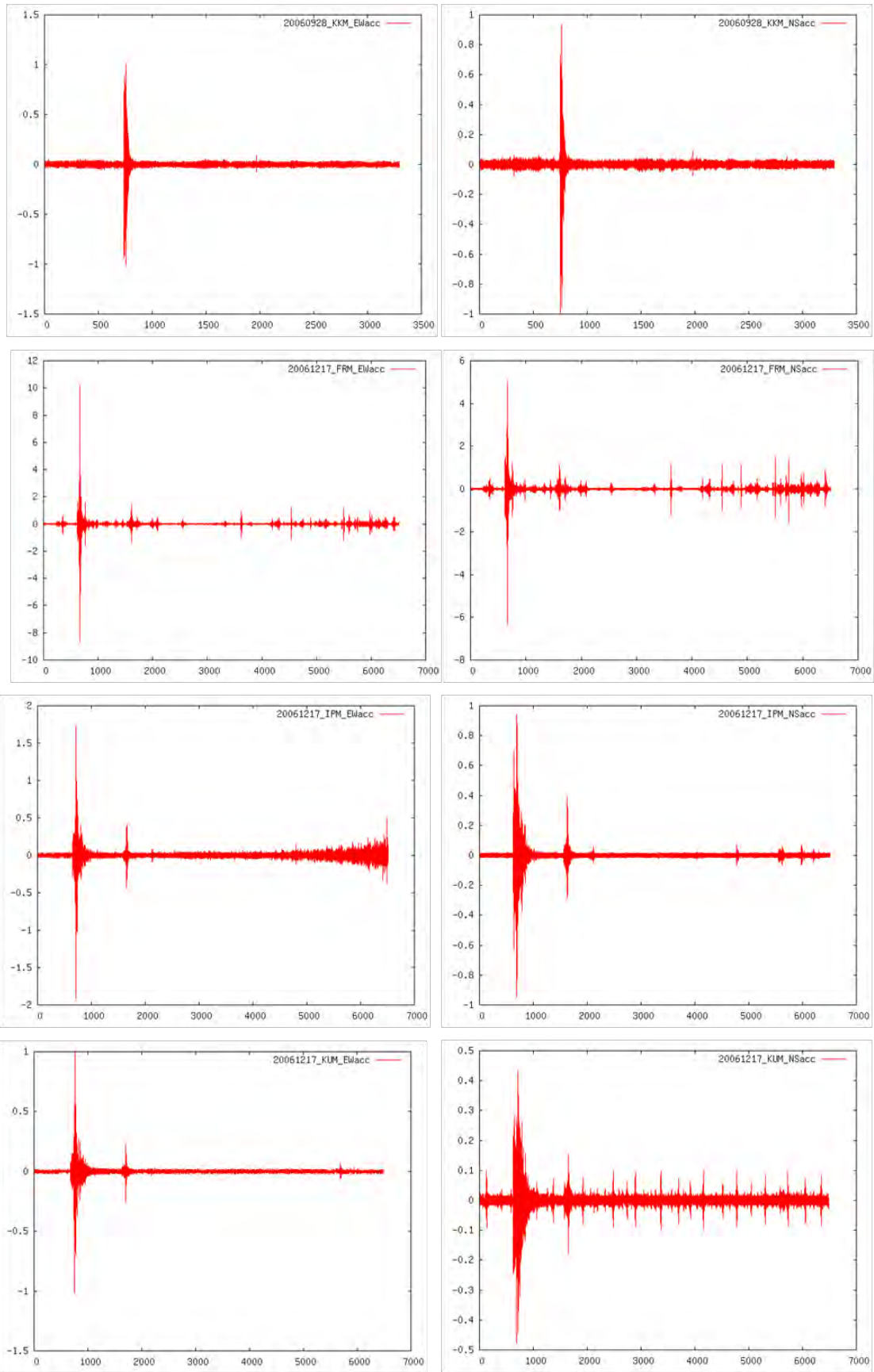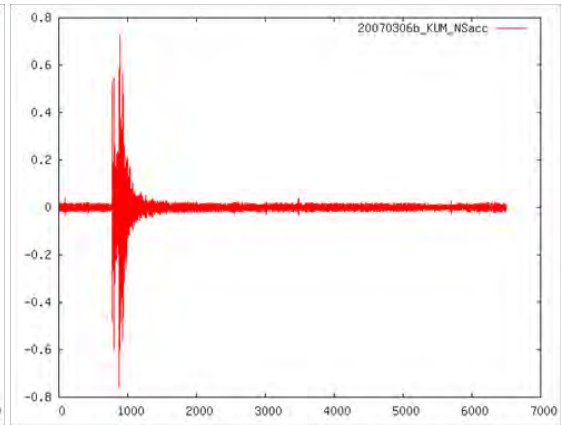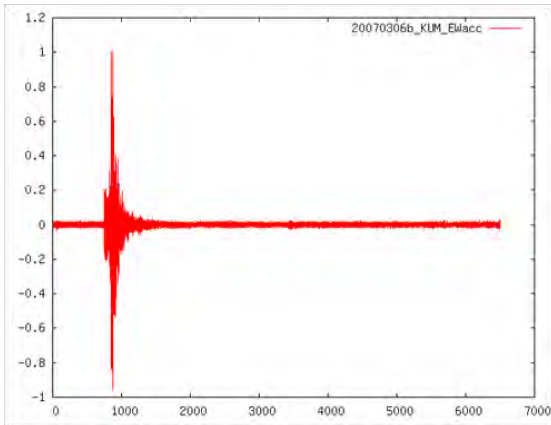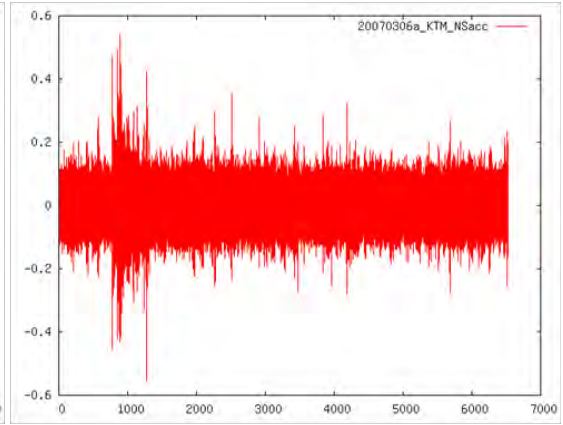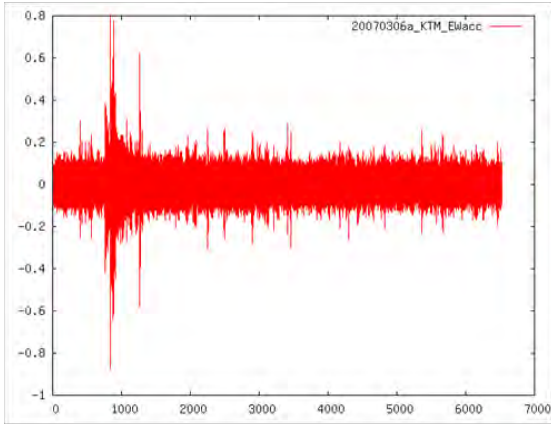
Chapter 4

Bridge Modeling and Procedures of Seismic Performance Investigation

4.1   Introduction

One of the main concerns among the structural and earthquake engineering community is how well a bridge performs under the seismic force. Such concern prompted various researchers to investigate the seismic demand by which ground motions may generate on existing bridges. This is because, the information on seismic demand and capacity can provide some insights into the possibilities of estimating suitable seismic design motion for use in the design of new bridges and retrofitting existing bridges.

The mapping of historical seismic activities within Malaysia and from distant seismic sources, since a century ago, provides evidence of low to moderate seismic hazard in Malaysia. Notwithstanding, the design of bridges in Malaysia has always been guided by the design requirements outlined in the British Standard BS 5400, which does not include the provision for seismic loading. Although seismic hazard in Malaysia is categorized as low to moderate, it should not be disregarded especially when most bridge structures in Malaysia lack seismic resistance. This is more so, especially knowing that earthquakes have occurred and continue to occur on "unknown" or "inactive" faults (Scawthorn, 2003). Thus, immediate evaluation of a seismic design motion is necessary to ensure the public welfare and safety against the potential damaging effects of ground motions. Equivalently important is the need for seismic assessment of existing bridges in Malaysia.

One of the many tools, which can be used for earthquake risk mitigation is through a revamp of the existing code of practice by including seismic provisions for the design of new bridges, and assessment of existing bridges. This calls for, among others, an estimation of a seismic design motion in the form of a design spectrum or a formulation of a seismic coefficient as have been largely used in the seismic design codes.

73

The development of a design motion incorporates the knowledge of seismic demand and capacity of a bridge. In modern earthquake engineering, and with the advent of performance-based engineering, the evaluation of the capacity and demand of a bridge calls for the use of nonlinear analysis. Such is because researches have managed to show that structures would deform into the inelastic range in the event of severe earthquakes. In general, seismic demand in a bridge is determined by evaluating its structural response under earthquake excitations. One of the most commonly used analysis tool to acquire seismic demand is the dynamic analysis, which employs nonlinear time-history analysis (Priestley *et al.*, 1996).

In order to achieve the aforementioned objective, an existing multi-span reinforced concrete bridge structure has been selected for study, modeled for dynamic simulation, and analyzed to static and ground motion loadings. In this context, the nonlinear dynamic analysis has a two-fold objective: to evaluate the seismic performance of the bridge system in order to understand the seismic risk of the bridge, and to estimate the seismic demand in the bridge system.

Reliable seismic analysis of a bridge structure requires the integration of these critical components: structural modeling, definition of performance limit states, and determination of loading combinations. Thus, this chapter is dedicated to describe each of these components in the following subsections. The bridge was conceptualized as a three-dimensional system, and structural elements have been modeled, as accurately as possible, to account for all information as have been laid out in the 'as-built' structural drawings. Where information is absent, reference and assumptions have been made based on existing literatures.

The seismic performance is evaluated to satisfy the limit states conditions, by which a designer would like the structure to demonstrate when subjected to ground motions. This corresponds to no-collapse state or acceptable damages.

This chapter deals with modeling of the Samudera Bridge prior to performing dynamic simulation to assess its seismic performance.

4.2 Procedure for Conducting Seismic Performance Evaluation

The analysis procedure incorporated in this study includes four main phases:

(i) Develop a three-dimensional analytical model for nonlinear dynamic analysis in the

(ii) open source software called Open System for Earthquake Engineering Simulation or OpenSees (McKenna and Fenves, 2006). The modeling shall refer to the 'as-built' structural drawing, and carefully include all elements in the selected bridge, which may influence its dynamic response under earthquake excitation;

(iii) Perform moment-curvature analysis to study the force-deformation characteristics of pier sections, which have been discretized into concrete and steel fibers. The theoretical moment-curvature relationship is developed based on selected stress-strain relations for concrete and steel. This analysis accounts for axial load due to gravity, the effects of concrete confinement, and steel strain hardening on pier cross sections;

(iv) Perform nonlinear dynamic simulation of the bridge system to observe its response to input ground motions, resulting deformation, and hysteresis. Horizontal components of the 1940 El Centro, 1995 Kobe and the 2005 Sumatera ground motions are applied in three different patterns: the transverse and longitudinal directions simultaneously; in the longitudinal direction only; and in the transverse direction only. P-Δ effect is considered during the analysis by using the OpenSees command for 'geometrical transformation' to include P-Δ effect; and

(v) Develop absolute acceleration response spectrums for all three ground input motions to evaluate their frequency contents. This procedure is necessary to understand the simulation results as well as the behavior of the structure under chosen excitations.

A pictorial description of the procedure is as illustrated in Figure 4.1.
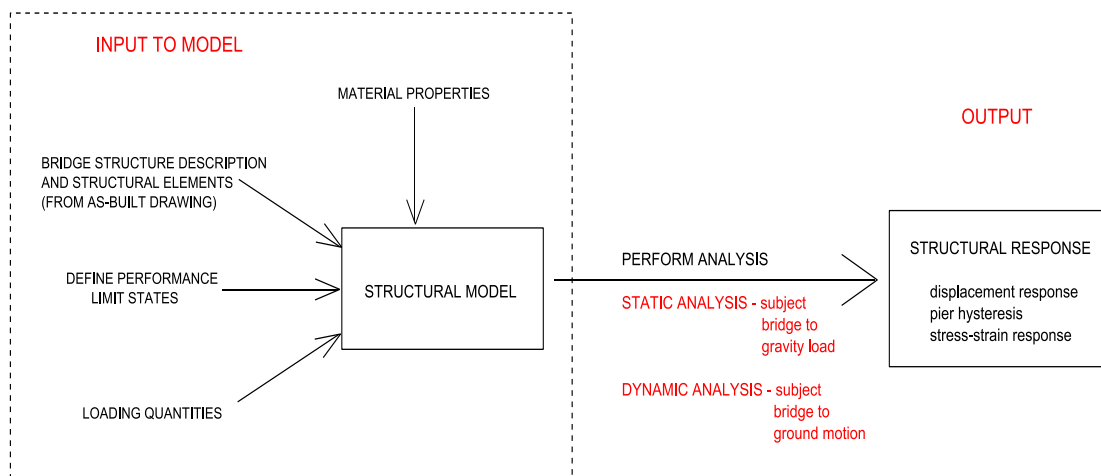
Figure 4.1   Procedure for evaluation of seismic performance

4.3   Description of the Bridge Structure

The Samudera Bridge, which was selected for the study, is located approximately 15 km away from the Kuala Lumpur city center. It was designed approximately a decade ago, according to the British Standards BS 5400:Part 2:1978 (British Standards Institution, 1978), BS 5400:Part 4:1990 (British Standards Institution, 1990), and BD 37/01 (the Highways Agency, 2002). It is noteworthy that seismic loading was not considered at the design stage mainly because there was no such provision in the design code.

The Samudera Bridge is a six-lane, dual carriageway viaduct structure located along the Federal Route 28, Middle Ring Road II, which serves the Batu Caves Industrial area and the residential area of Taman Samudera. The bridge system is a 28-span structure of 38 m centre to centre, with pier heights ranging from 4.5 m to 10.4 m.

The superstructure carries a 25.6 m wide, 200 mm thick reinforced concrete deck on eight prestressed U-beam girders, each mounted on laminated elastomeric rubber bearings. The deck, between piers P12 and P22, is slightly curved to suit the right of way (ROW) path, and this curvature has been taken into consideration during the modeling phase. According to BS 5400:Part 9 (British Standards Institution, 1983), bearings in bridges function as connections to control the interaction of loadings and movements between the superstructure and the substructure. As such, bridge bearings were not designed as seismic isolators. Figure 4.2 depicts the layout, elevation, and pier section of the bridge system.

The substructure consists of 27 rectangular cantilever piers, seven of which are of fixed type labeled as P2, P6, P10, P14, P18, P22, and P26. Based on the as-built drawings, fixed piers are equipped with bearings, which allow rotation about the longitudinal axis. The remaining piers are of free type where longitudinal movement and rotation about the longitudinal axis are allowed. Expansion joints are located at piers P4, P8, P12, P16, P20, and P24. However, for seismic simulation, all piers are assumed as having no bearings i.e. the node at the top of the pier and the node at the bottom of the deck are not connected. Instead, free piers are constrained in translation by "EqualDOF" in the vertical and transverse directions, while fixed piers are constrained by "EqualDOF" in all degree of freedoms.

All piers are supported on either four or five-bored pile groups of different lengths, socketed into the limestone.
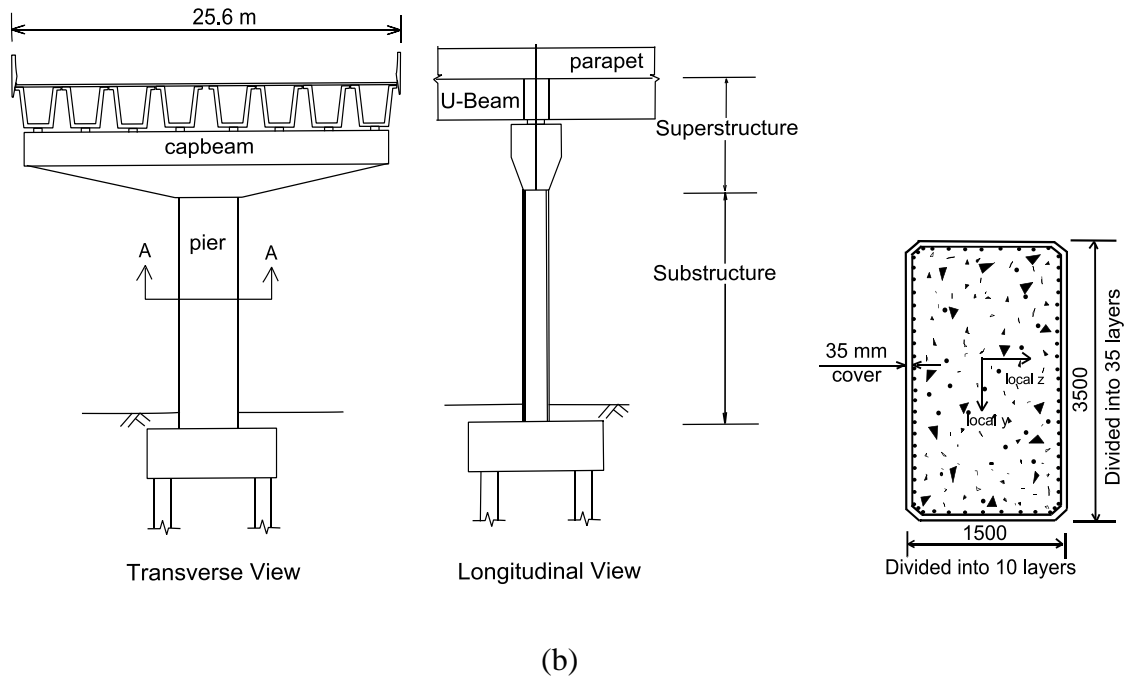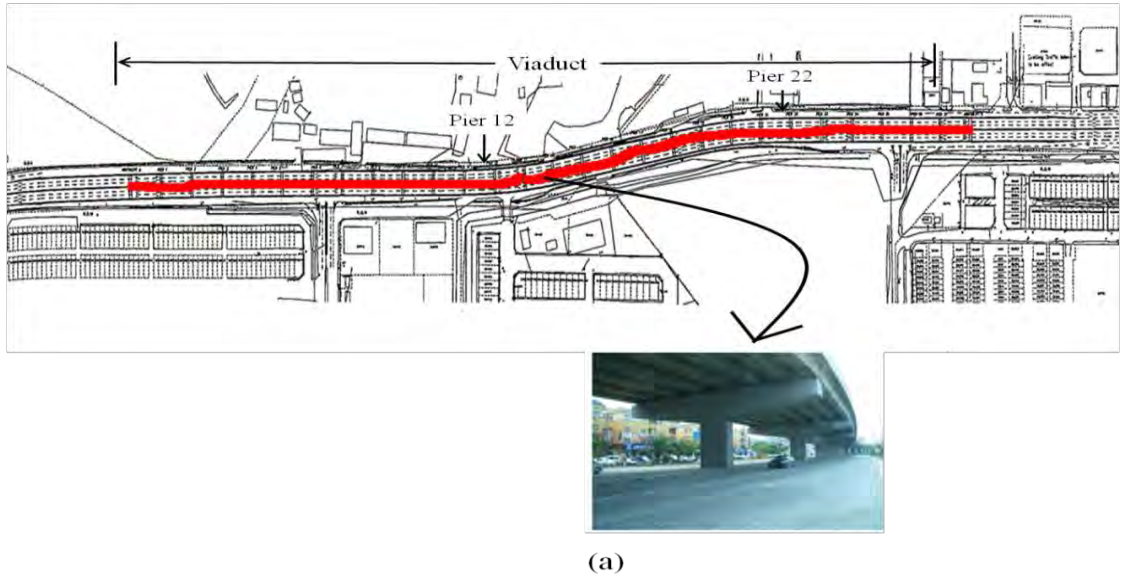
Figure 4.2 (a) Layout of the bridge structure, (b) transverse and longitudinal views of the bridge system, and idealized rectangular pier section.

4.3.1 Bridge Pier Detailing

Fixed and free piers are reinforced with basic longitudinal reinforcements equivalent to 68T40.

Fixed piers have been detailed with an additional 20T40 and 36T32 longitudinal steel bars (total main bar is 88T40 + 36T32). Confinement of piers is provided by high yield rectangular hoops, of 10 mm diameter, spaced at 250 mm and 150 mm in fixed and free piers, respectively. The sectional detailing of the fixed and free piers are as illustrated in Figure 4.3.

4.3.2 Fiber Configuration

Each pier has a rectangular cross-section with a depth of 3.5 m, width of 1.5 m, and a 35 mm concrete cover around the entire section. The concrete stress-strain curve adopted in this study was calculated using the model proposed by Mander *et al.* (1988). The number of steel layers corresponds to the number of longitudinal bars present in both fixed and free piers.

It is essential to determine the optimum number of concrete fibers to model the column section with, to effectively minimize simulation run-time. A suitable method to determine the optimum number of fibers for accurate and reliable results is by using the moment-curvature analysis. In this study, the configuration of fibers for concrete cover has been set to one layer. Therefore, a parametric study was focused on varying the number of fibers for concrete core to observe the differences, if any, in the moment-curvature capacity. Table 4-1 tabulates ten fiber configurations of the concrete core, which have been chosen for investigation.

The moment-curvature analysis was conducted on free pier sections only to determine which of the ten fiber configurations gives the optimum concrete core configuration for use in the dynamic simulation. Figure 4.4 shows the moment-curvature plots of each trial, and observation indicates very small improvement in the moment-curvature capacity even as the number of fibers was increased in both the weak and strong axes. When the number of fibers along the strong axis was kept constant between 7 and 20, and that of the weak axis was increased, no improvement in the moment capacity and strength was observed. This suggests that refinement of fiber size will not improve the simulation results of the bridge. Bearing in mind that increasing the number of fibers, unnecessarily, in a pier section would result in unfavorably longer simulation run-time, it was decided that the maximum number

78

of fibers in the local y, and z axes to be employed for analysis are 35 and 10, respectively. The discretization of the concrete section is as shown in Figure 4.2(b).
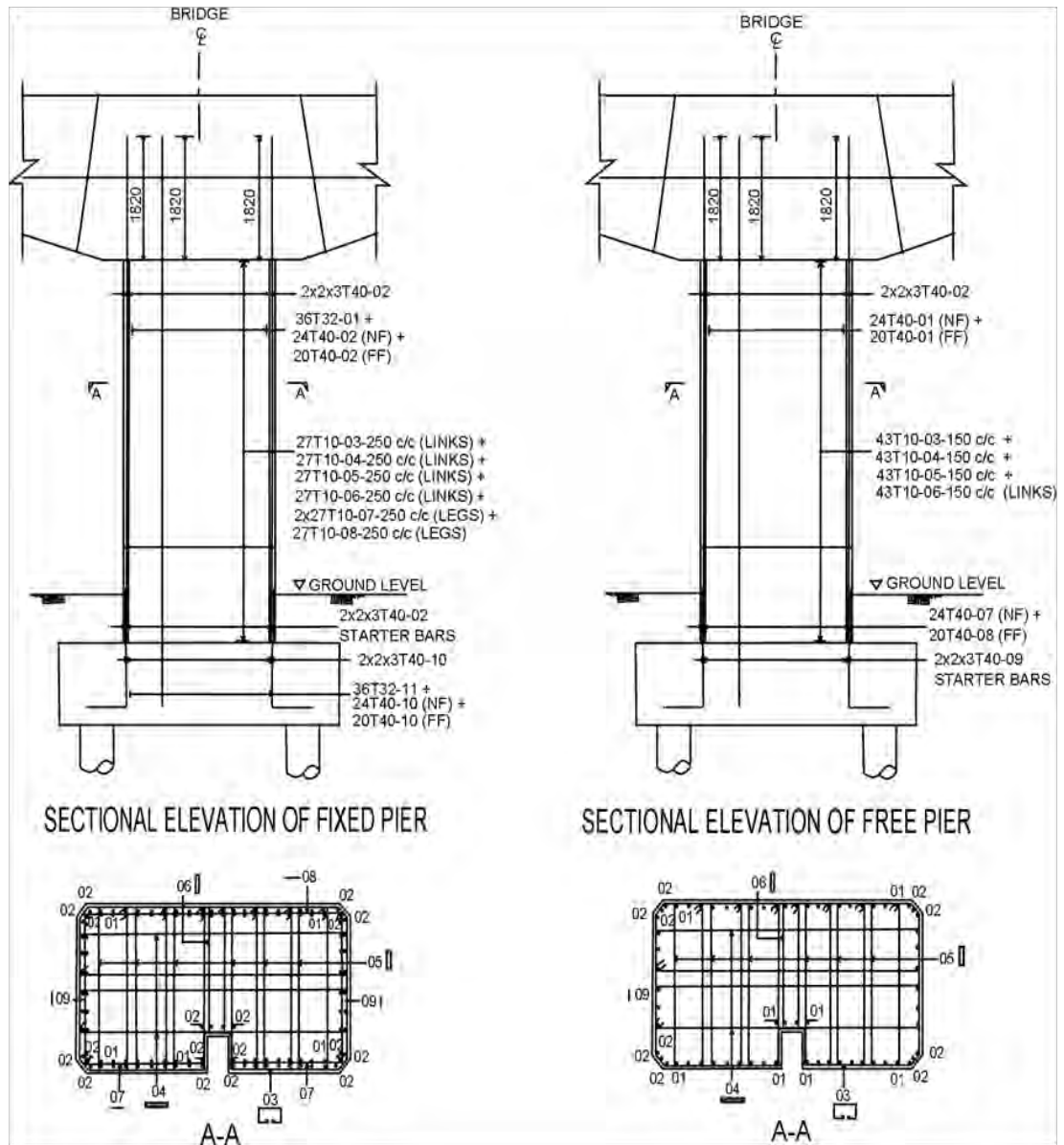
Figure 4.3 Sectional detailing of piers. Fixed piers have higher amount of longitudinal bars as that in free piers.

Table 4-1   Trials of fiber configurations to determine optimum number of fibers in concrete core

Trial Number	Number of fiber in local y axis	Number of fiber in local z axis
1	7	3
2	10	5
3	20	5
4	50	5
5	20	7
6	50	7
7	35	10
8	50	10
9	200	10
10	100	20
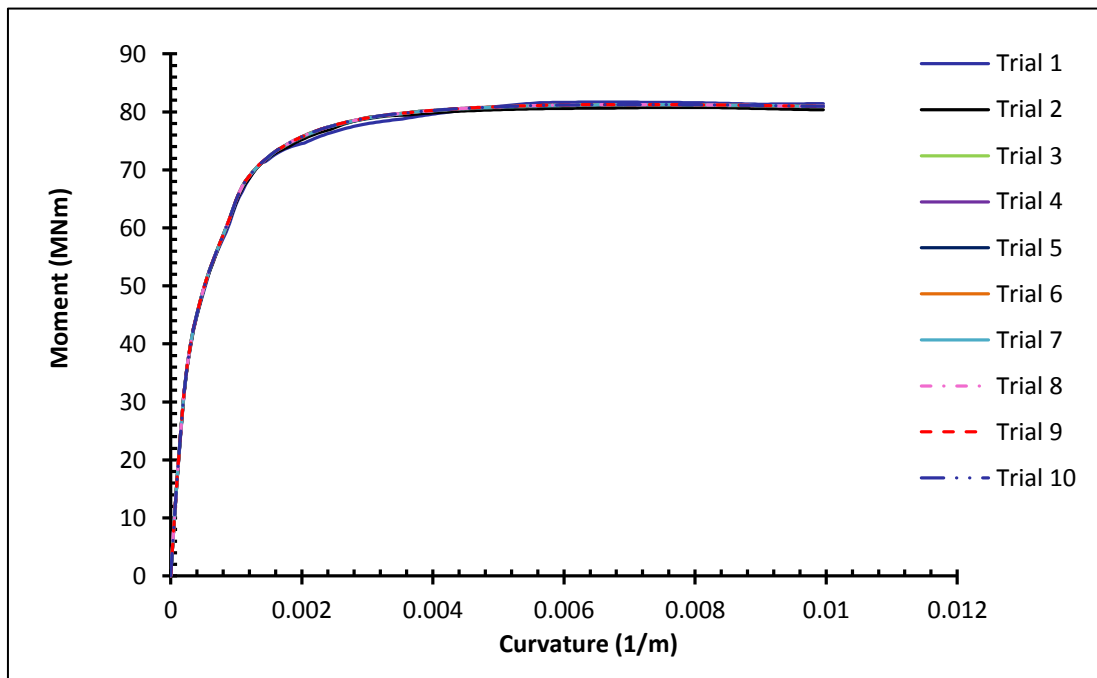
Figure 4.4   The moment-curvature relationship comparison for free pier sections having ten different fiber configurations.

4.4　Bridge Modeling and Idealization

This section describes the main assumptions and constitutive law of materials adopted in modeling the bridge structure. The aforementioned structure is an overpass bridge mounted on laminated rubber bearings. Hence, the bridge has been idealized as a multiple degree of freedom (MDOF) system. The bridge system was developed as a three-dimensional model, with each nodal point having six DOFs, using OpenSees. Masses were lumped at the neutral axis of the deck and neutral axis of the capbeam.

Typical in an earthquake engineering research of a bridge, structural elements at the superstructure level are expected to remain elastic, while its piers would deform into the nonlinear range under severe earthquake excitation. Thus, plastic hinges have been assumed to form only in the piers. In this study, the abutments and foundations have been assumed to behave infinitely rigid under seismic action, and boundary conditions have been fixed in all six DOFs. Soil-structure interaction was ignored mainly because the bridge structure had been constructed on limestone area. Thus, all pier bases were assumed fixed.

4.4.1　Material Properties and Performance Limit States

The prestressed U-beam girders have a concrete nominal strength of 50 N/mm^2 (grade 50 concrete), while other structural elements have a 28-day compressive concrete strength of 40 N/mm^2 (grade 40 concrete). The yield strength of both longitudinal and transverse steel reinforcements is 460 N/mm^2. Elastic moduli for grade 40 concrete and steel are 31000 N/mm^2 and 200000 N/mm^2, respectively.

In the analytical model, the prestressed girders, and other elements at the superstructure level have been modeled using linear-elastic elements at their neutral axis on the assumption that they remain elastic under seismic action. Similarly, the capbeam elements and vertical connections between the girder and the top of the pier have been represented by elastic elements.

To simulate and ensure linear-elastic behavior of the superstructure during dynamic simulation, the superstructure elements, capbeam elements, and the vertical connection between the girder and the top of the pier have been assigned a large elastic modulus value of 1.0×10^{10} N/mm^2.

The structural damping ratio of the bridge system was assumed at two percent (2 %). Figure 4.5 is an illustration of the idealized model of the bridge system in OpenSees.
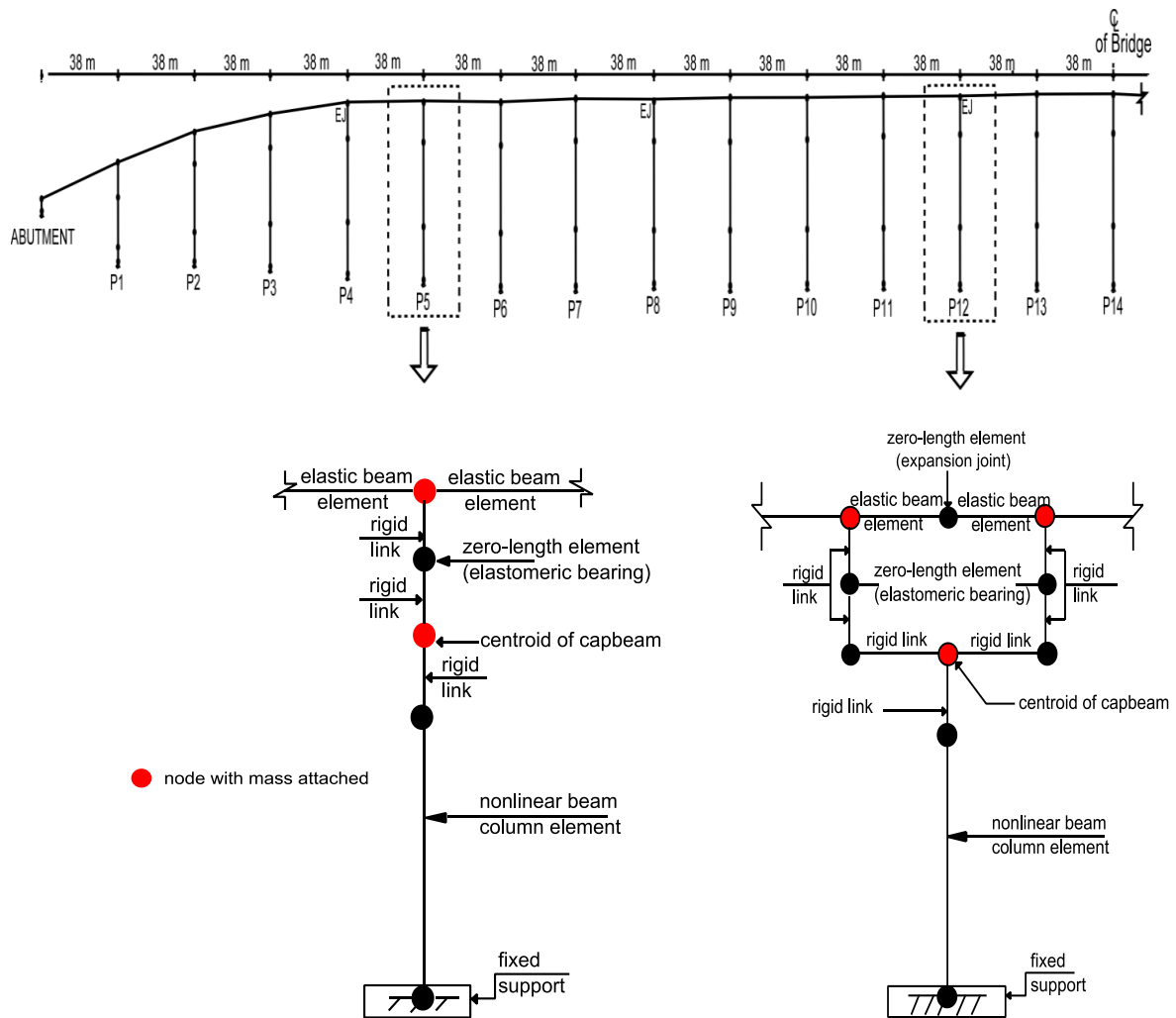
Figure 4.5 The bridge system as idealized in OpenSees.

As in any earthquake simulation, nonlinear response of piers is particularly of interest to researchers. In order to observe nonlinear behavior in pier sections, piers would have to be idealized using nonlinear beam-column elements with a focus to capture the nonlinear deformation. In OpenSees, there are basically two types of finite element model for evaluating

nonlinear response of beam-column members. These are the concentrated plasticity, and the distributed plasticity models. In the concentrated plasticity model, the nonlinear behavior of

82

pier elements can be observed by defining a rotational spring at the ends of an elastic element, or by using the "beamWithHinges" element. On the other hand, in the distributed plasticity model, plasticity is assumed to spread along the entire element section. The distributed plasticity model is constructed by assigning fiber elements in the entire pier element based on the assumption that potential plastic hinges may form at any location along the nonlinear element. Since the concentrated plasticity approach is deficient, because they separate axial-moment interaction from the element behavior (Scott *et al.*, 2003), the distributed plasticity model has been selected for analysis.

Within the distributed plasticity category, comparison was done between the force-based, and the displacement-based beam-column element approaches. Based on Neuenhofer and Filippou (1997), the modeling for nonlinear response using the force-based element approach is more favorable due to its simplicity and several advantages it has over the displacement-based element approach. The most appealing advantage being the ability to use only one forced-based element to simulate the nonlinear response, thus the number of DOF in a model can be kept to a minimum. For these reasons, in this research, pier elements were represented by the force-based distributed plasticity element, also known as the "nonlinearBeamColumn" element. Second-order P-Δ effect has also been considered by using the "PDelta transformation" command. Figure 4.6 depicts the distributed plasticity finite element model of bridge piers considered in the research.

The cross sections of the piers were defined using concrete and steel fibers. Each fiber was modeled with appropriate stress-strain relationships representing confined concrete (or concrete core), unconfined concrete (or concrete cover), and reinforcing steel. "Concrete 02" was selected to represent both the concrete core and cover. MacGregor and Wight (2005) suggested that concrete might have a tensile strength in the range of 8 to 15 percent, therefore in this study, concrete has been assumed capable of carrying a tensile stress equivalent to 10 percent of its compressive strength.
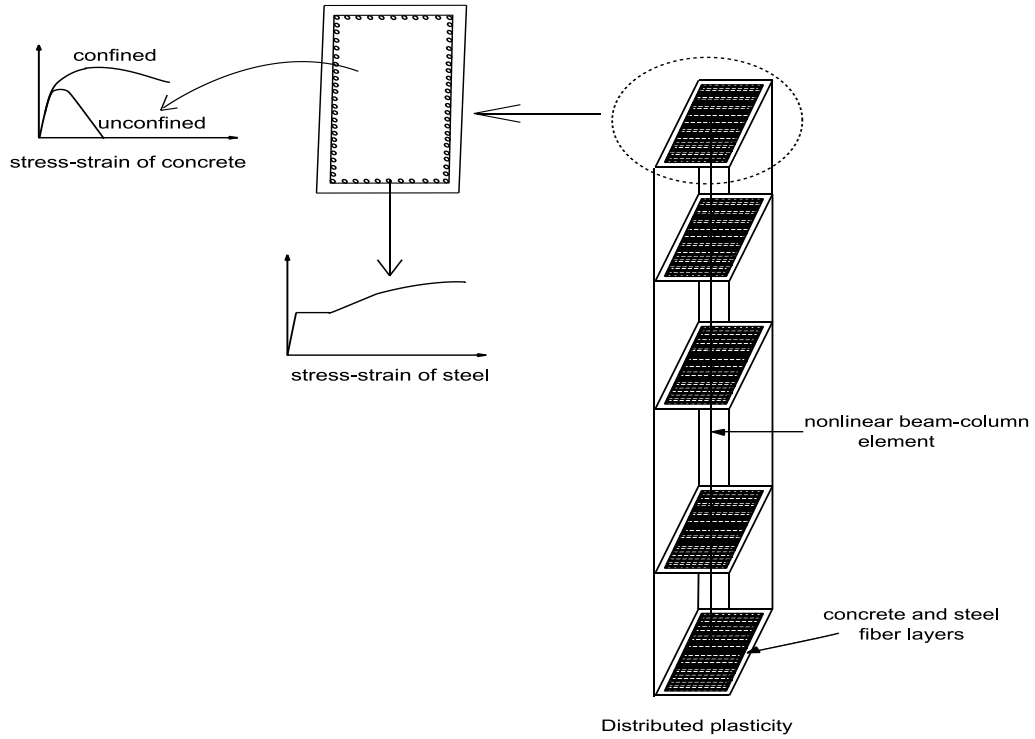
Figure 4.6 Finite element model for observing nonlinear reinforced concrete section, considering distributed plasticity.

The confined concrete properties have been estimated based on the constitutive model proposed by Mander *et al.* (1988). The stress-strain model is illustrated in Figure 4.7, and is based on the equation derived by Popovics (1973). Equation (4.1) has been derived for the longitudinal compressive concrete stress, f_c subjected to a slow (quasi-static) strain rate and monotonic loading.

$$f_c = \frac{f'_{cc}\, xr}{(r-1)+x^r} \tag{4.1}$$

where $f'_{cc} = f'_c \left(2.254\sqrt{(1 + \frac{7.94 f'_l}{f'_{co}})} - \frac{2 f'_l}{f'_{co}} - 1.254\right)$

$$x = \frac{\varepsilon_c}{\varepsilon_{cc}} \tag{4.2}$$

where

f'_l = effective lateral confining stress

f'_{co} = unconfined concrete compressive stress

ε_c = longitudinal compressive concrete strain

f'_{cc} = compressive strength (peak stress) of confined concrete.

The strain at maximum concrete stress ε_{cc} is given as

$$\varepsilon_{cc} = \varepsilon_{co} \left[1 + 5 \left(\frac{f'_{cc}}{f'_{co}} - 1\right)\right] \tag{4.3}$$

where strain at maximum stress f'_{co} of unconfined concrete, ε_{co} is generally taken as 0.002.

$$r = \frac{E_c}{E_c - E_{sec}} \tag{4.4}$$

$$E_{sec} = \frac{f'_{cc}}{\varepsilon_{cc}} \tag{4.5}$$

E_c and E_{sec} denote modulus of elasticity of concrete and secant modulus of confined concrete at peak stress, respectively.

Mander *et al.* (1988) recommended the use of equation (4.6) for estimating the (tangent) modulus of elasticity. However, in this research the modulus of elasticity, E_c, was assumed as 31000 N/mm^2, corresponding to the value used when the bridge was designed.

$$E_c = 5000\sqrt{f'_{co}} \ \ N/mm^2 \tag{4.6}$$

For rectangular sections, the effective lateral confining stresses in the x and y directions, f'_{lx} and f'_{ly}, can be calculated to consider different transverse reinforcement area ratios, ρ_x and ρ_y in the principal directions. The effective lateral confining stresses, f'_{lx} and f'_{ly}, have been derived by using the following relationships

$$f'_{lx} = K_e \rho_x f_{yh} \tag{4.7}$$

$$f'_{ly} = K_e \rho_y f_{yh} \qquad (4.8)$$

where the confinement effectiveness coefficient K_e is

$$K_e = \left(\frac{\left[1 - \sum_{i=1}^{n} \frac{(w'_i)^2}{6 b_c d_c} \right] \left(1 - \frac{s'}{2 b_c} \right) \left(1 - \frac{s'}{2 d_c} \right)}{(1 - \rho_{cc})} \right) \qquad (4.9)$$

$$\rho_x = \frac{A_{sx}}{S d_c} \qquad (4.10)$$

$$\rho_y = \frac{A_{sy}}{S b_c} \qquad (4.11)$$

The definitions for w'_i, b_c, d_c, s and s' are as shown in Figure 4.8. A_{sx} and A_{sy} are the total area of transverse bars running in the x and y directions, respectively. f_{yh} is the yield strength value of the transverse reinforcement.
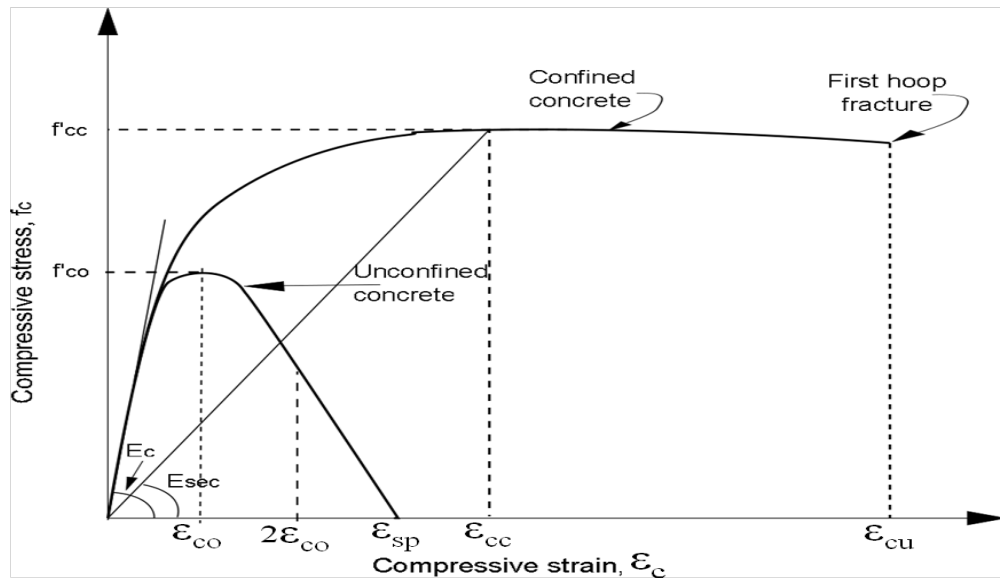
Figure 4.7   The stress-strain model for concrete in compression (Mander *et al.*, 1988).
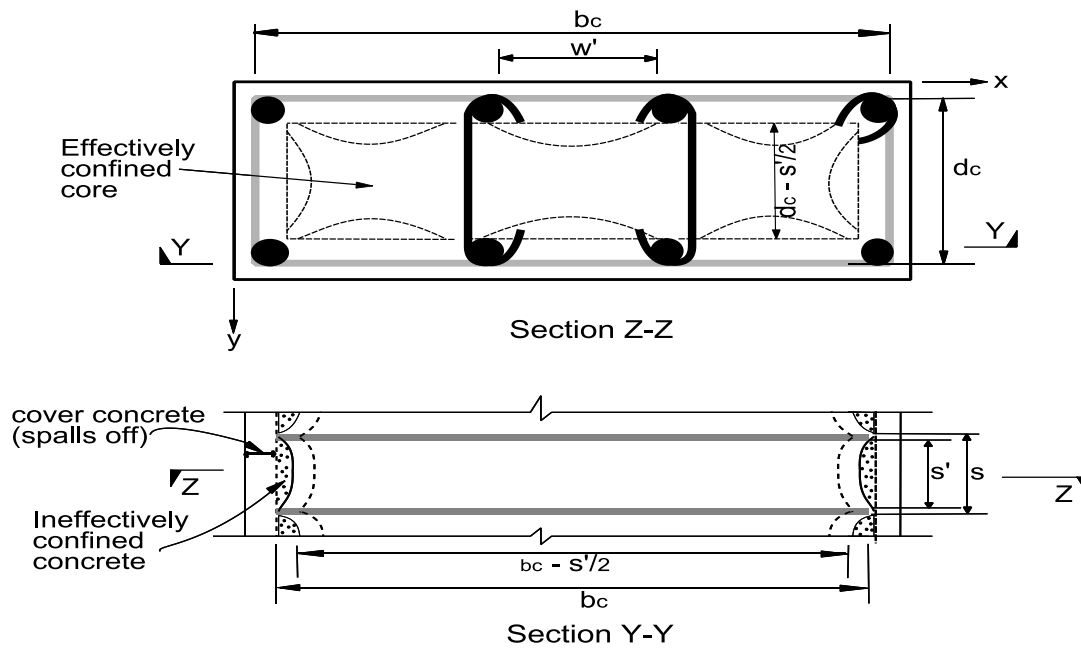
Figure 4.8 Effectively confined core for rectangular hoop reinforcement (Mander *et al.*, 1988).

The peak stresses of the confined concrete in free and fixed piers were calculated to be 46 and 45 N/mm^2, respectively. The compressive strains corresponding to these peak stresses were estimated at 0.0035 and 0.0032, respectively. For the ultimate confined concrete compression stresses, reference has been made to several literatures. A study performed by Mander *et al.* (1988) to observe stress-strain curves, of square columns confined by square and octagonal hoops, shows that first hoop fracture in square columns occurred at strains larger than 0.04. Reference on the typical ultimate compression strain values recommended by Paulay and Priestley (1992) indicates that typical values for strain at crushing of the concrete core, in rectangular sections, range from 0.012 to 0.05. Penelis and Kappos (1997) illustrated several analytical models for confined concrete by Park *et al.* (1982), Sheikh and Uzumeri (1982), and Kappos (1991). Among all literatures reviewed, Penelis and Kappos (1997) gave clear pictorial reference and relationship to calculate the confined concrete ultimate stress. Therefore, it was decided that the stresses at crushing of concrete would occur as recommended by Park *et al.* (1982), as shown in Figure 4.9.

87
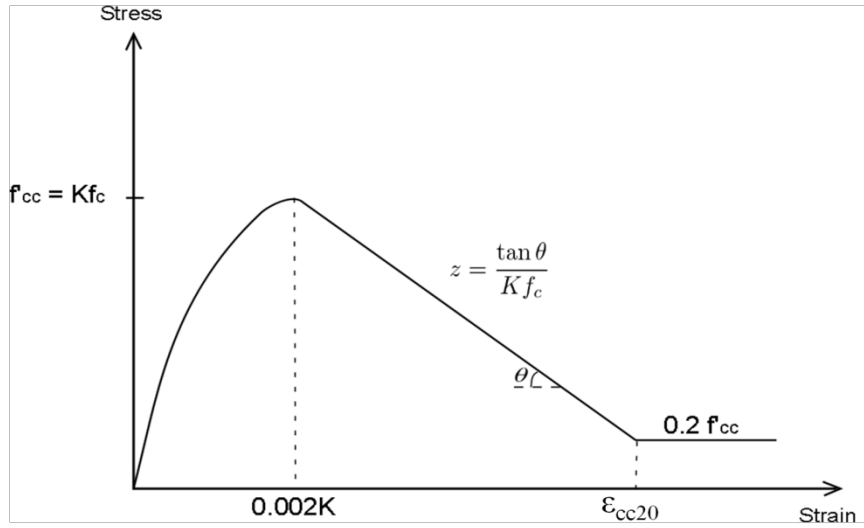
Figure 4.9 Park, Priestley and Gill (1982) model for confined concrete stress-strain.

In this study, the confinement index K is obtained from the relationship established by Mander *et al.* (1988). Park *et al.* (1982) model assumes that concrete crushes when the compressive stress drops to 20% of the confined concrete stress (i.e. analysis is carried out until the concrete stress reaches $0.2f'_{cc}$). The slope of the descending branch, which is linear, is calculated from the following relationship.

$$Z = \frac{0.5}{\varepsilon_{cc50} - \varepsilon_{cc1}} \qquad (4.12)$$

where

$$\varepsilon_{cc50} = \frac{3 + 0.29f_c}{145f_c - 1000} + 0.75 \, \rho_w \left(\sqrt[2]{\frac{b_c}{s}}\right) \qquad (4.13)$$

$$\varepsilon_{cc1} = 0.002K \qquad (4.14)$$

$$K = 1 + \frac{\rho_w f_y}{f_c} \qquad (4.15)$$

f_c, ρ_w, ε_{cc50}, b_c, f_y, and S denote concrete compressive strength, volumetric ratio of transverse reinforcement, strain at 50% confined compressive stress, size of confined core, yield strength of transverse reinforcement, and transverse reinforcement spacing, respectively.

As such, the ultimate compressive strains, i.e. ε_{cc20}, for free and fixed piers are 0.025 and 0.019, respectively. These values also correspond to the minimum possible values, which did not cause non-convergence issue during simulation, as did some lower trial values between 0.008 and 0.011. The peak stress of the concrete cover was assumed equal to the concrete compressive stress (i.e. 40 N/mm^2), where the peak strain was 0.002. The crushing of concrete cover was assumed to occur when the peak stress value drops 90% of the compressive stress at an ultimate strain value of 0.006.

The uniaxial material command "Steel02" was selected to construct the pier reinforcements, and strain hardening was assumed at a small value of 0.0001. According to the steel material properties mentioned earlier, yielding of reinforcements would start to occur at a strain value of 0.0023 i.e. the ratio of yield strength to elastic modulus.

4.5   Loading and its Application for Analysis

Prior to conducting seismic simulation, it is critical to determine input quantities such as the gravity load and ground motions, which make up the seismic load combination. These loading quantities are affecting parameters, which influence the response of the Samudera Bridge under earthquake loading. Thus, this section provides the assumptions considered in determining gravity load and the selection of ground motions as inputs in the seismic simulation.

4.5.1   Seismic Load Combination

The gravity load (or axial load) is defined to consider the dead load (DL), which makes up the bridge structure. The dead load included all primary superstructure weights, such as the prestressed U-beam girders, concrete deck, road pavement, and selfweight of the pier. It also accounted for the secondary weight, such as that of the road divider, parapet, railing, and diaphragm.

In the dynamic simulation, all piers have been applied a constant gravity load of 14000 kN at the deck level. In all piers, the capbeam level was subjected to a gravity load of

approximately 4000 kN. Meanwhile, the abutments were subjected to 50 percent of the value applied at the piers.

All nodes at pier bases were applied with similar earthquake excitation using three ground motion records from three earthquake events. They are the 1940 El Centro (hereafter called the El Centro), the 1995 Kobe (hereafter called the Kobe), and the largest locally recorded distant ground motion in Malaysia (until 2007), which corresponds to the March 28, 2005 Sumatera earthquake (hereafter referred to as the 2005 Sumatera earthquake).

The earthquake load is an application of the ground motion horizontal components bidirectionally as is illustrated in Figure 4.10. Bidirectional application of ground motions is considered in the analysis since seismic waves reach a particular site at a random manner and impact a structure in all directions.
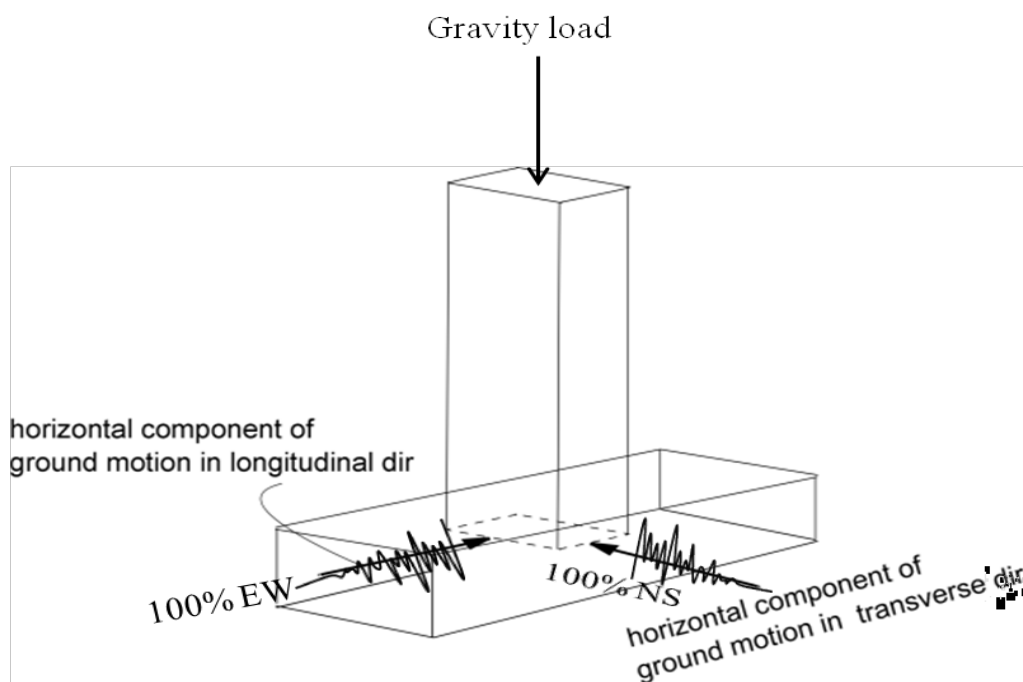
Figure 4.10   Seismic loading and its application

Thus, the seismic load combination considered in this research is illustrated by the following relationship:

$$\text{GRAVITY LOAD} + 1.0\ EQ_T + 1.0\ EQ_L \qquad\qquad (4.16)$$

GRAVITY LOAD, EQ_T and EQ_L are axial load calculated as described earlier, earthquake action in transverse and earthquake action in longitudinal directions, respectively.

The procedure of nonlinear dynamic simulation included two main loading steps: the bridge was first loaded with the gravity load in ten steps, after which structural responses were held still, before it was subjected to the ground motion. The input loading pattern employed in the dynamic simulation is the "uniform excitation", in which all bases are subjected with equal magnitude of input motion. The dynamic simulation was predetermined to continue until concrete stresses were reduced to 20 percent of the confined concrete compressive stress.

4.5.2 Ground Input Motion

The horizontal components of strong motion recordings of the El Centro (M_w 7.0), Kobe (M_J =7.3 or M6.9), and the distant 2005 Sumatera (M_s= 7.2) earthquakes were selected as the input motions in this study. Figure 4.11 depicts the El Centro acceleration time histories, recorded for 50 seconds, acquired from the website of the Pacific Earthquake Engineering Research Center, http://peer.berkeley.edu/research/motions. The acceleration amplitude observed during this earthquake was 0.35 g in the North-South direction.

The second set of input ground motions considered in this research was that of the Kobe earthquakes recorded between 25 and 75 seconds. Peak ground acceleration (PGA) value of approximately 0.8 g was observed in the North-South direction. These acceleration time histories were acquired from the Japan Meteorological Agency (JMA), and are as shown in Figure 4.12.

Comparison of acceleration pattern between the El Centro and Kobe ground motions shows that peak ground acceleration occurred earlier during the ground shaking i.e. between 2 and 12 seconds in the El Centro accelerograms, whereas the Kobe time histories show that strong motion was recorded between 8 and 12 seconds.
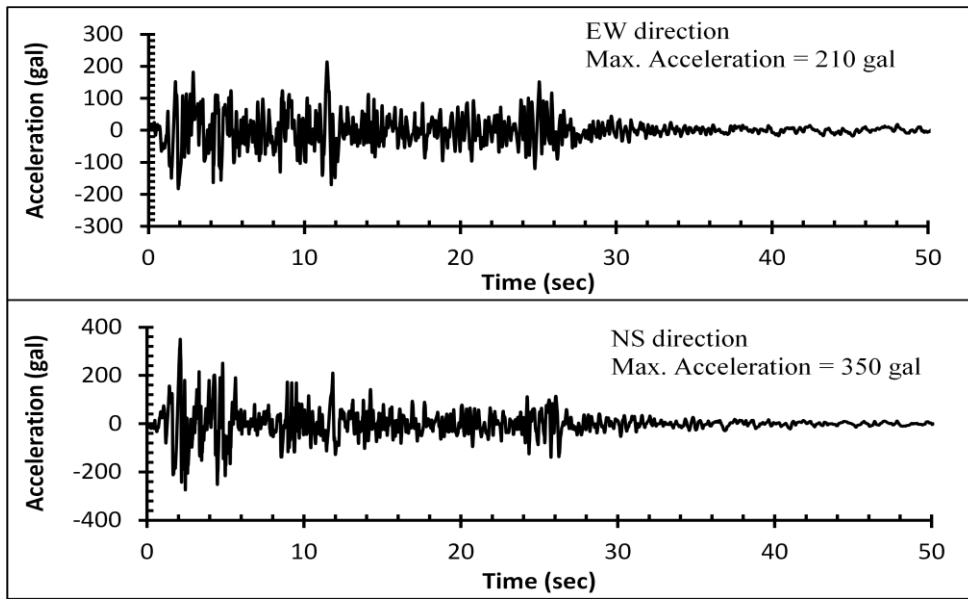
Figure 4.11   Horizontal components of the 1940 El Centro earthquake recorded at the Imperial Valley Irrigation District substation, El Centro, California.
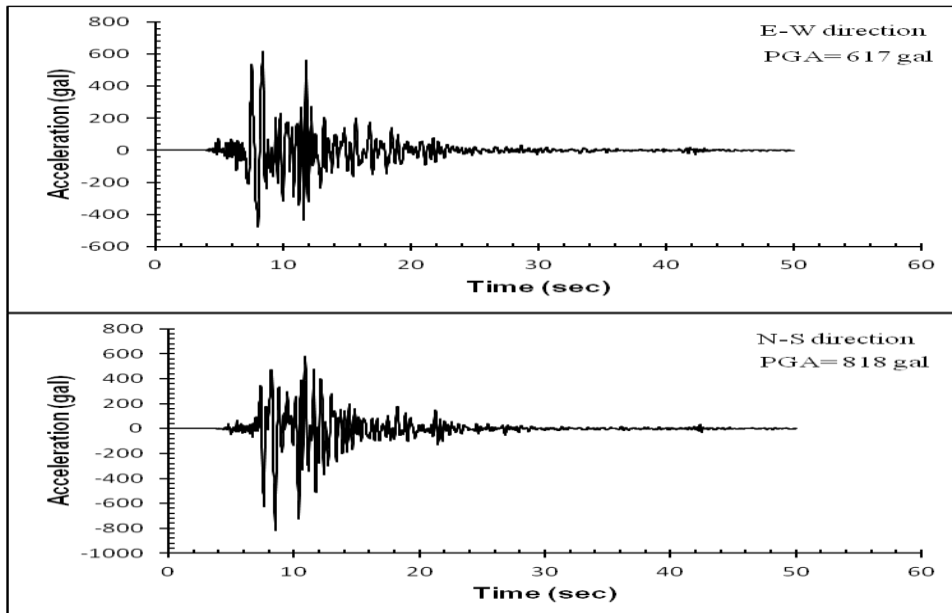
Figure 4.12   Horizontal components of the 1995 Kobe input ground motion recorded at the Kobe Marine Observatory.

From the suite of locally recorded acceleration time histories, collected by the Malaysian Meteorological Department (MMD) between 2004 and 2007, it was identified that the largest PGA value observed in Malaysia corresponds to the 2005 Sumatera earthquake. This earthquake event recorded PGA value of 0.02 g, at station FRM, which is coincidently located approximately 15 km away from the bridge site. The acceleration time histories are as shown in Figure 4.13. For the purpose of simulation, this input motion has been selected to run for 115 seconds. This is to account for acceleration amplitudes, which occurred at different times in both the horizontal components. A longer simulation period was allowed for, to appropriately include the significant time histories of both the horizontal components.
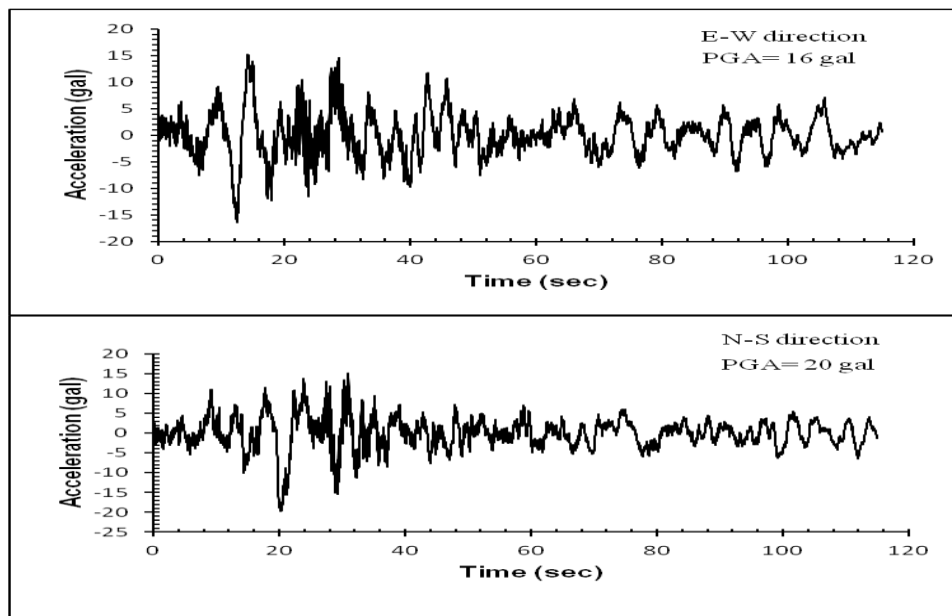
Figure 4.13   Horizontal components of the March 28, 2005 Sumatera
ground motion, recorded at station FRM, near Kuala Lumpur.

These ground motions have been selected as inputs to perform dynamic simulations to observe the bridge response to two levels of earthquake. The Kobe earthquake is an example of a typical large earthquake, which rarely occurs, with a high return period. It has been selected to study the dynamic response of the Samudera Bridge to account for

maximum magnitude earthquake, which is predicted to occur at the Bukit Tinggi fault, a seismic source located approximately 30 km from the bridge site.

In contrast, the 2005 Sumatera earthquake represents small earthquake events, which occur more frequently or in shorter return period. The El Centro ground motion was selected for investigation owing to the fact that it has become one of the most popular time histories ever used by researchers since decades ago before more recent accelerograms were considered.

The seismic performance of a bridge structure is meaningless without an evaluation of the frequency contents of the ground motions used in the analysis. Frequency content is a useful tool employed to understand the behavior of the structure under an earthquake excitation. As part of the seismic performance evaluation exercise, the frequency content of all three selected ground motions shall be investigated via absolute acceleration response spectrum. This is possible by employing a series of SDOF systems and subjecting them to the ground motions before constructing the response spectrum for each ground motion. Further detail of the procedure is outlined in chapter 6.

4.6   Conclusions

The inputs and procedures for use in the seismic performance investigation on the Samudera Bridge have been discussed in detail in this chapter. The structural response can be obtained by running nonlinear dynamic simulations on the bridge. The simulation results are discussed in detail in chapter 6.

References

British Standards Institution (1978). *Specification for Load, BS 5400: Part 2*, British Standards Institution, London.

British Standards Institution (1990). *Code of Practice for Design of Concrete Bridges, BS 5400: Part 4*, British Standards Institution, London.

British Standards Institution (1983). *Code of Practice for Design of Bridge Bearings,BS 5400: Part 9*. British Standards Institution, London.

Council of Standards Australia (2004). *Bearings and Deck Joints, AS5100.4-2004.* Australian Standards.

Elnashai, A. and L. Di Sarno (2008). *Fundamentals of Earthquake Engineering*, John Wiley & Sons, Ltd., West Sussex, United Kingdom

Japan Meteorological Agency (2009). http://www.jma.go.jp/.

MacGregor, J. and J.K. Wight (2005). *Reinforced Concrete Mechanics and Design*, 4th ed., Pearson Prentice Hall, Upper Saddle River, New Jersey.

Mander, J.B., M.J.N. Priestley and R. Park (1988). Theoretical stress-strain model for confined concrete. *Journal of the Structural Division, ASCE*, 114(8), 1804-1826.

Mander, J.B., M.J.N. Priestley and R. Park (1988). Observed stress-strain behavior of confined concrete. *Journal of the Structural Division, ASCE*, 114(8), 1827-1849.

Mc Kenna, F. and G.L. Fenves (2006). *The OpenSees Command Language Manual*, Pacific Earthquake Engineering Research Center, University of California at Berkeley, California (http://opensees.berkeley.edu/).

Malaysian Meteorological Department (2010). http://www.met.gov.my/.

Neuenhofer, A. and F.C. Fillipou (1997). Evaluation of nonlinear frame finite-element models. *Journal of Structural Engineering, ASCE*, Vol. 123 (7), 958-966.

Paulay, T. and M.J.N. Priestley (1992). *Seismic Design of Reinforced Concrete and Masonry Buildings*. John Wiley & Sons, Inc., New York.

Penelis,G.G, and A.J. Kappos (1997). *Seismic Earthquake-Resistant Concrete Structures,* Taylor& Francis, 2 Park Square, Milton Park, Abingdon, Oxon.

Popovics, S. (1973). A numerical approach to the complete stress-strain curves for concrete. *Cement and Concrete Research*, 3(5), 583-599

Priestley, M.J.N., F. Seible and G.M. Calvi (1996). *Seismic Design and Retrofit of Bridges*, J. Wiley & Sons, New York.

Scawthorn, C. (2003). Earthquakes: Seismogenesis, Measurement, and Distribution. *Earthquake Engineering Handbook*. Section II Chapter 4. CRC Press,Florida.

Scott, M.H., and G.L. Fenves (2006). Plastic hinge integration methods for force-based beam-column elements. *Journal of Structural Engineering*, ASCE, Vol. 132 (2), 244-252.

Chapter 5

Nonlinear Static Pushover (NSP) Analysis as a Tool to Estimate Seismic Capacity and the Seismic Coefficient Value

5.1 Introduction

A seismic evaluation performed on a bridge structure requires an incorporation of the nonlinear static pushover analysis (hereinafter called pushover analysis), as a tool to evaluate the displacement or deformation capacity. Such information is fundamental to identify the extent of damage in the bridge when it is subjected to ground motions during dynamic analysis. Pushover analysis is also a useful tool, which can be used to derive the seismic coefficient value of piers. Thus, this chapter discusses the pushover analysis performed on two types of pier, namely the free and fixed piers, and deduces the ultimate displacement values, which shall be used in the evaluation of the Samudera Bridge in Chapter 6.

5.2 One-pier Pushover Analysis to Determine Seismic Capacity

Prior to conducting the dynamic analysis of the Samudera Bridge, the pushover analysis was conducted on each type of pier i.e. free and fixed piers. Free pier P17 and fixed pier P18 have been selected to undergo pushover analysis because they represent the majority of the piers in the bridge system: they are similar in heights, and most piers have relatively similar heights with these two piers.

One-pier pushover analysis is a reliable method to understand the seismic capacity of the entire bridge system under nonlinear loading. The results provided by the pushover curve are fundamental to evaluate the seismic performance of the Samudera Bridge under dynamic loading, using ground motion records. Pushover analysis is capable of providing such information as 'at what displacement does the ultimate limit state occur?', and 'the

97

maximum curvature expected at the ultimate limit state'. By knowing these information, the seismic performance of the bridge, under a particular input motion, may be predicted and seismic resistant provisions may be designed to improve the bridge performance under a variety of earthquake levels.

A description of the Samudera Bridge and its modeling is explained in great detail in chapter 4. Important information on the bridge structure and its model are briefly summarized here, and related figures from chapter 4 are reproduced in this chapter to recall on the detailed modeling process, which has been conducted earlier.

5.3   Description of the Samudera Bridge

The Samudera Bridge is a 28-span, six-lane dual carriageway viaduct structure with varying pier heights, between 4.5 m and 10.4m (height measured to the neutral axis of the capbeam). The substructure consists of rectangular piers of size 3500x1500 mm. The sectional view of the bridge system is as illustrated in Figure 5.1.

Both piers are reinforced with basic longitudinal reinforcements equivalent to 68T40. Fixed piers have been detailed with an additional 20T40 and 36T32 longitudinal steel bars (total main bar is 88T40 + 36T32). Confinement of piers is provided by high yield rectangular hoops, of 10 mm diameter, spaced at 250 mm and 150 mm in fixed and free piers, respectively. The sectional detailing and cross sections through piers are as illustrated in Figure 5.2.
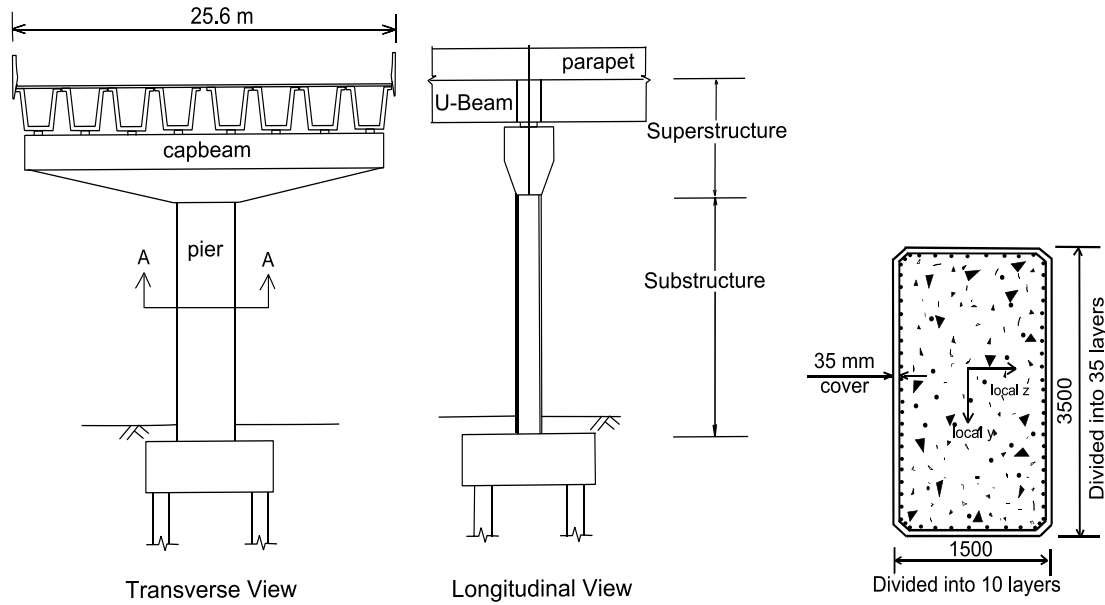
Figure 5.1   Sectional view of the Samudera Bridge: transverse view (left) and longitudinal view (right).
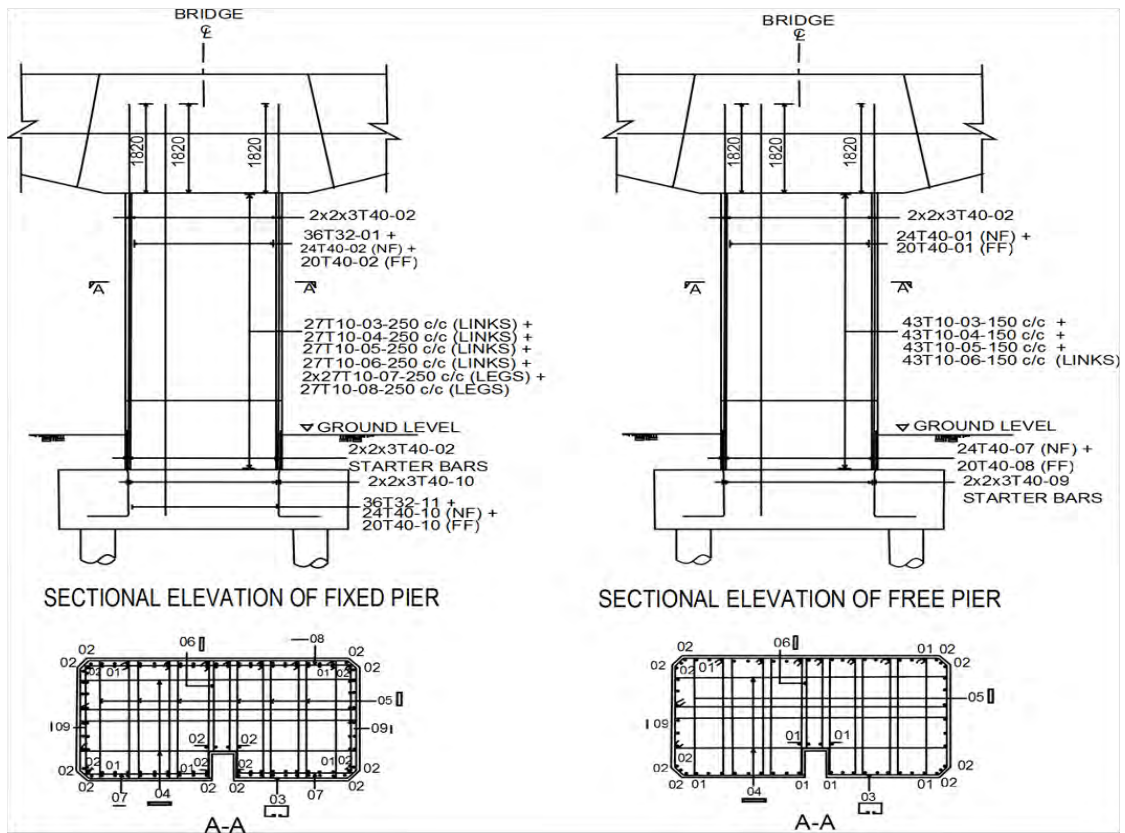
Figure 5.2   Sectional detailing of fixed (left) and free (right) piers.

5.3.1 Bridge Model

The bridge has been idealized as a multiple degree of freedom (MDOF) system, and was developed as a three-dimensional model with each nodal point having six DOFs using the OpenSees software (McKenna and Fenves, 2006). Masses were lumped at the deck and the neutral axis of the capbeam. The piers have a 28-day compressive concrete strength of 40 N/mm^2. The yield strength of both longitudinal and transverse steel reinforcements is 460 N/mm^2. Elastic moduli for grade 40 concrete (concrete strength 40 N/mm^2), and steel are 31000 N/mm^2 and 200000 N/mm^2, respectively. The capbeam elements and the vertical connection between the girder and the top of the pier have been represented by elastic elements having modulus of elasticity of 1.0×10^{10} N/mm^2. The bridge structure had been constructed on limestone area, thus, pier bases were assumed fixed. The structural damping ratio of the bridge system was assumed at two percent (2 %).

Piers were modeled as "nonlinearBeamColumn" elements, whereby plasticity is assumed to spread in the entire pier element. The pier element was discretized as concrete and steel fibers. Each fiber was modeled with appropriate stress-strain relationships representing confined concrete, unconfined concrete and reinforcing steel. Confined concrete properties have been estimated based on the constitutive model proposed by Mander *et al.* (1988). "Concrete02" was selected to model both the concrete core and cover. The pier reinforcements were modeled as "Steel02", and yielding of reinforcements would occur at a strain value of 0.0023. Figure 5.3 is an illustration of the idealized model of the bridge system.

In this study the ultimate limit state has been defined as the following: a reinforced concrete section is said to have reached the ultimate limit state as the strain in steel reaches 0.0023, while the concrete will fail when its peak compressive stress drops to a value of 80%. At the ultimate limit state, steel reinforcement would yield and crushing of concrete is expected. The displacement capacity is generally defined at the ultimate limit state and is then used to compare with the displacement demand obtained from dynamic analysis.
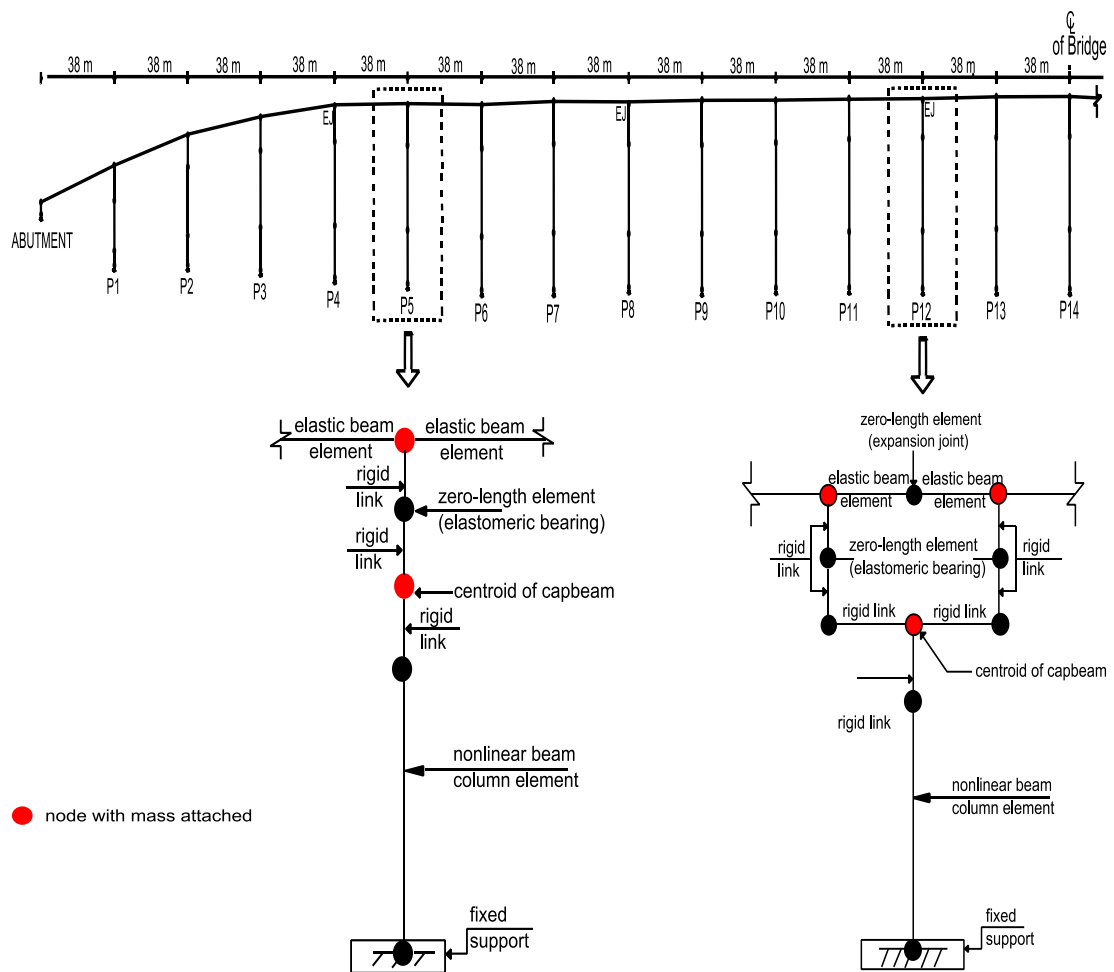
Figure 5.3 The Samudera Bridge as modeled and idealized in OpenSees.

5.4   Nonlinear Static Pushover Analysis

The nonlinear static pushover analysis, or pushover analysis for short, has been widely used as a tool to evaluate the inelastic seismic behavior of structures. One of the many objectives of pushover analysis is to determine the lateral force resisting capacity or predict the seismic demand (Mwafy *et al.*, 2007). This implies the possibility of employing the pushover analysis as a tool to determine the base shear capacity of a structure.

Essentially, the pushover analysis requires careful selection of a lateral load distribution,

estimation of target displacement and choosing the controlling node at which displacement is to be monitored during pushover analysis. Figure 5.4 represents the pushover curve considered in this study.
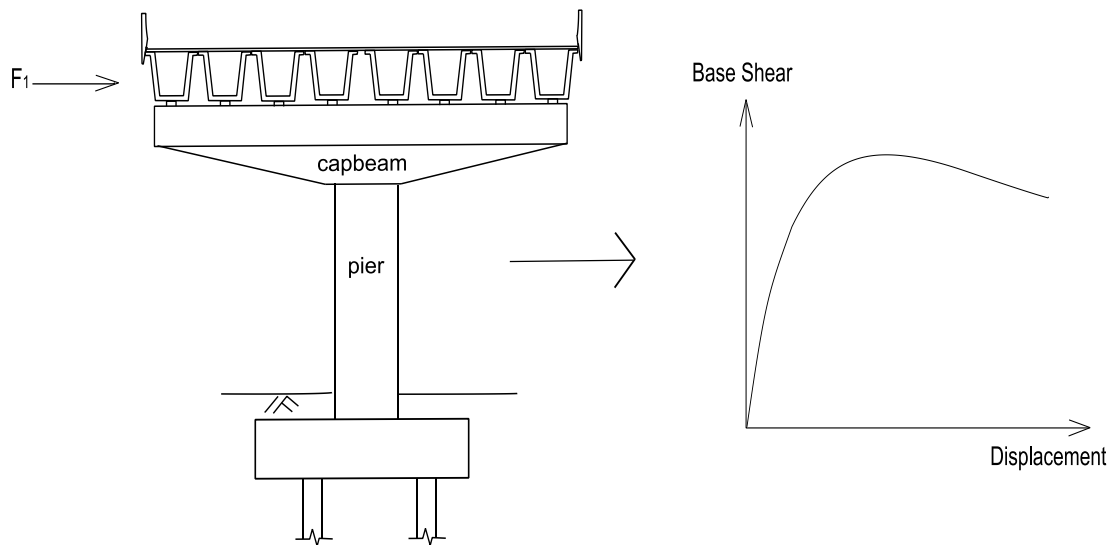
** F1 is the lateral load applied at the superstructure level

Figure 5.4   Pushover curve.

5.5   Pushover Analysis Procedures

The pushover procedures include modeling of the Samudera Bridge as idealized in Figure 5.3. In this section, input information shall be carefully identified prior to performing the pushover analysis. These include the target displacement, lateral load profile, and selection of an observation point to monitor the development of base shear capacity-displacement curve.

When dealing with nonlinear static analysis, various researchers refer to the Displacement Coefficient Method (FEMA356, 2000) or the Capacity Spectrum Method (ATC-40, 1996) for estimating the maximum displacement demand. The Capacity Spectrum Method is popular because displacement demand is represented graphically by elastic spectrum, making its application more appealing. In the Displacement Coefficient Method,

displacement demand is represented by inelastic displacement spectra, which is obtained for the elastic displacement spectra by using correction factors. However, in this study, the estimate of the displacement demand is based on the allowable 3% drift limit as recommended in the displacement-based design procedure for multi-degree-of-freedom structures (Calvi *et al.*, 1995). This is represented by equation (5.1).

$$\delta_d = 0.03 \text{ h} \tag{5.1}$$

δ_d is called the 'desired' displacement, and h refers to the height of pier or column. The overall height of piers P17 and P18 is taken as 11 m, giving a desired displacement of 330 mm. An important fact to note on the displacement demand is that its value changes with ground motion amplitude i.e. different earthquake loading gives a different displacement demand value. Thus, according to FEMA 273, it is appropriate to carry out pushover analysis to at least 150% of the calculated target displacement, so that the pushover curve will reflect the seismic capacity under extreme seismic load condition. As such, a 500 mm target displacement has been considered. The pushover analysis is stopped when the bridge reaches the predefined displacement limit of 500 mm.

In general, the lateral force profile can be accurately defined from examining the fundamental elastic first mode shape of the pier, which can be determined from the eigenvalue analysis. Since pushover analysis is performed on a one-pier system, the lateral load has been defined as a reference load. In this study, the lateral load is taken as equivalent to 5% of the gravity load, or 450 kN, and is applied to the deck level only. It should be noted that the pushover analysis accounted for application of the lateral load profile in the longitudinal and transverse directions, separately. Figure 5.4 represents the pushover curve considered in this study.

The procedure begins by loading the structure with a maximum gravity load of 18000 kN, before subjecting it to monotonically increasing displacements in small increments of 0.2 mm, to a maximum displacement value of 500 mm. The monitoring point for displacement is at the deck level of piers P17 and P18. The bridge is then subjected to a static lateral force, which reflects the inertial force distribution related to the fundamental mode of vibration.

Following the pushover analysis, the resulting seismic capacity curve (base shear versus displacement) is then used to examine the ultimate displacement at the ultimate limit state.

For design purposes, the ultimate limit state has been defined to occur when the confined compressive strength of the pier drops to 80%.

The ultimate displacement obtained from the pushover analysis is then compared to the maximum displacement response recorded, in the Samudera Bridge, from the dynamic analysis (to be conducted in Chapter 6). The extent of damage can then be evaluated with the understanding that the bridge performance is deemed satisfactory when the seismic demand is lower than the seismic capacity.

The seismic coefficient value of the piers is then calculated using the relationship as shown in equation (5.2).

$$C = \frac{V}{W} \tag{5.2}$$

where

V = base shear (from pushover curve)

W = seismic weight

5.6   Results and Discussion

Force-deformation curves from the pushover analysis are presented in Figures 5.5 through 5.8. Figures 5.5 and 5.6 illustrate the pushover curves of pier P17 subjected to lateral load in the longitudinal and transverse directions, respectively. A scrutiny of the pushover curves of free pier P17 indicates that in the longitudinal direction, the ultimate limit state occurs at a displacement capacity of 230 mm, measured at the top of the pier. At this point, the base shear capacity is 3 MN, and the ultimate curvature is expected at 0.06 (1/m). In the transverse direction, pier P17 has the capacity to deform to a maximum displacement of 76 mm before reaching its ultimate state, at a curvature of 0.016 (1/m).

Figures 5.7 and 5.8 depict the pushover curves of pier P18, subjected to lateral load in the longitudinal and transverse directions, respectively. It is observed from Figure 5.7 that fixed pier P18 has the capacity to deform to a maximum displacement of 190 mm in the longitudinal direction, before entering the ultimate limit state, at which point the curvature is predicted as 0.04 (1/m). Pushover in the transverse direction indicates that pier P18 has a

displacement capacity of 65 mm before it reaches the ultimate limit state. The corresponding curvature in the transverse direction is 0.01 (1/m).

An essential deduction from the pushover analysis is that, although the pier section is thin in the longitudinal direction it is observed that the resulting displacement capacity is large. It is also clear that in the transverse direction, the pier section is thicker, but the displacement capacity is smaller. For example, the displacement capacity of pier P17 in the longitudinal direction is 300 mm (measured at the deck level), which is 3 times larger than that in the transverse direction. In the case of fixed pier P18, the displacement capacity is slightly lower than that of pier P17 in both directions.

Essentially, the pushover analysis has provided a basis for evaluating the seismic coefficient value C for the free and fixed piers. The C values for each pier in the direction of pushover is calculated using the relationship in equation (5.2), and are as tabulated in Table 5-1.
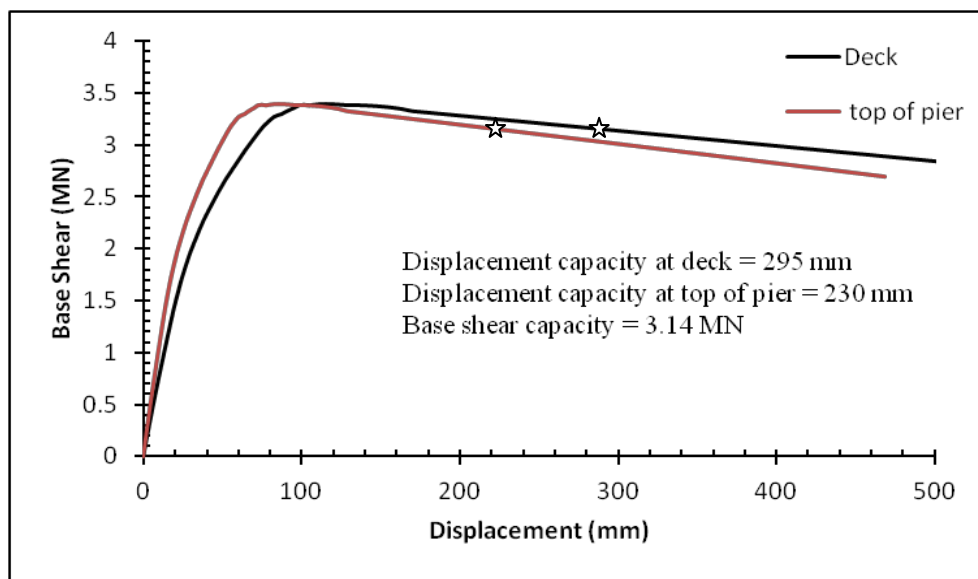
Figure 5.5   Pushover curve of P17 (base shear vs. displacement) in the longitudinal direction.
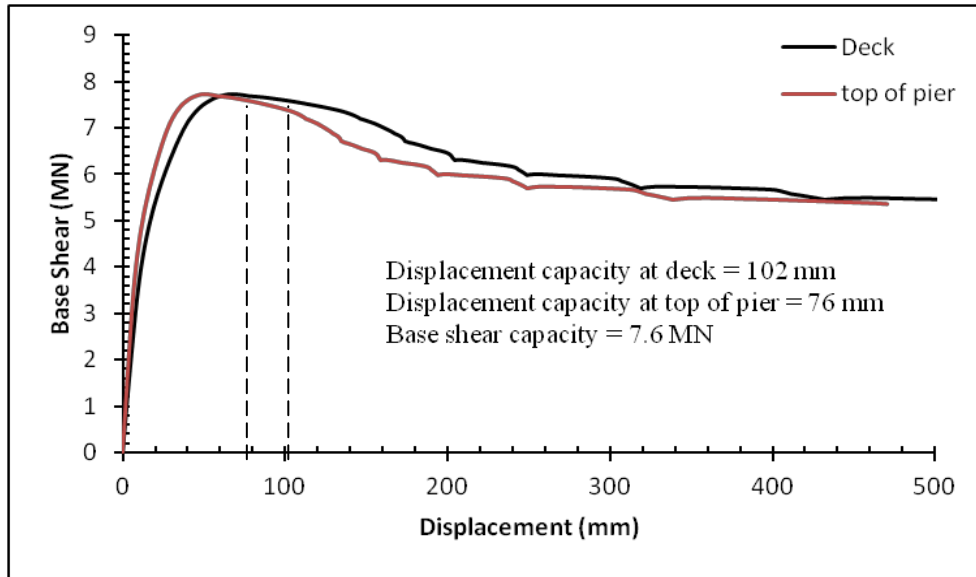
Figure 5.6   Pushover curve of P17 (base shear vs. displacement) in the transverse direction.
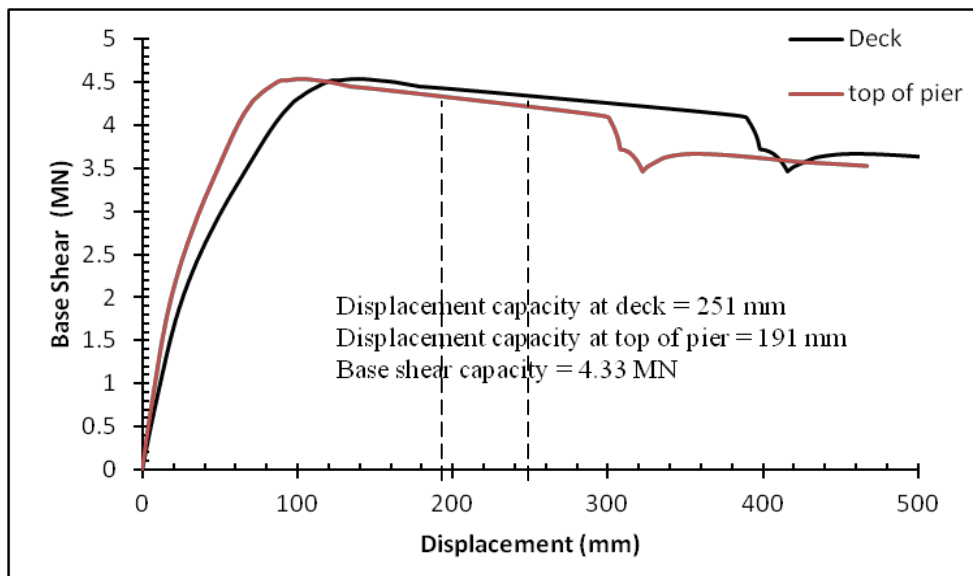
Figure 5.7   Pushover curve of P18 (base shear vs. displacement) in the longitudinal direction.
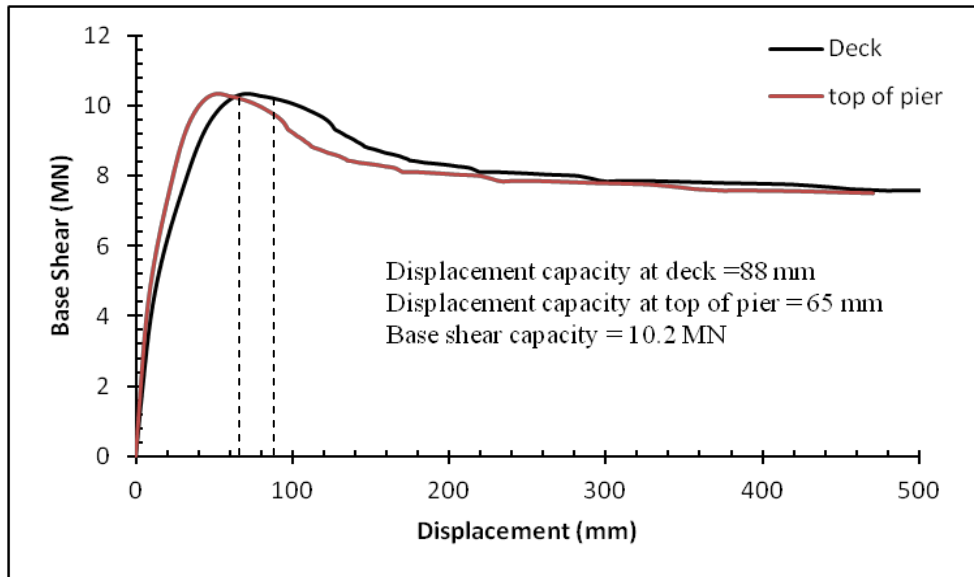
Figure 5.8   Pushover curve of P18 (base shear vs. displacement) in the transverse direction.

Table 5-1   Results of pushover curve, and estimate of seismic coefficient value C

Pier	Direction of Pushover	Base Shear Capacity (kN)	Displacement capacity (mm) (top of pier)	Total Weight of Pier (kN)	Seismic Coefficient Value C
P17	Longitudinal	3140	230	14000	0.22
	Transverse	7600	76	14000	0.54
P18	Longitudinal	4330	191	60000	0.07
	Transverse	10200	65	18000	0.57

The results in Table 5-1 shows that the seismic coefficient in the transverse direction (shorter dimension) in both types of pier is higher than that in the longitudinal direction (longer dimension).

5.7   Conclusions

Pushover analysis has been conducted on single-pier system of free pier P17 and fixed pier P18. It is significant to evaluate the seismic capacity and the ultimate displacement prior to performing the dynamic analysis because these information are fundamental in assessing the seismic performance of the Samudera Bridge. The results provided by the pushover analysis shall then be compared with the seismic demand predicted by dynamic analysis, which will be presented in Chapter 6. By comparing the seismic capacity with seismic demand, the seismic performance and the extent of damage in the Samudera Bridge, due to the excitation of a particular ground motion, may be estimated reliably.

The results, gathered from the pushover analysis, indicate an important deduction on the displacement capacity of pier sections with unequal dimensions. For this bridge structure, the pushover curve has illustrated that in the longitudinal direction, although the pier section is thin and the seismic coefficient is small, it possesses a large displacement capacity. In the transverse direction, although the pier section is thicker, and the seismic coefficient is larger, the displacement capacity in that direction is lower.

References

ATC, 1996, *Seismic Evaluation and Retrofit of Concrete Buildings, Applied Technology Council (ATC-40 Report)*, Vol. I, Redwood City, California.

Calvi, G.M. and Kingsley, G.R. 1995. Displacement-based seismic design of multi-degree-of-freedom bridge structures, *Earthquake Engineering and Structural Dynamics* 24, 1247-1266.

Federal Emergancy Management Agency (FEMA), (2000). *Pre-standard and Commentary for the Seismic Rehabilitation of Buildings*, FEMA-273, American Society of Civil Engineers, United States of America.

Federal Emergancy Management Agency (FEMA), (1997), *NEHRP Guidelines for the Seismic Rehabilitation of Buildings*, FEMA-273.

Mander, J.B., Priestley, M.J.N., Park, R. 1988. Theoretical Stress-strain Model for Confined Concrete. *Journal of the Structural Division, ASCE* 114, 1804-1826.

Mc Kenna, F. and Fenves, G.L. 2006. *The OpenSees Command Language Manual, Version 1.2*, Pacific Earthquake Engineering Research Center, University.

Mwafy, A., A. Elnashai, and W.H. Yen (2007). Implications of design assumptions on capacity estimates and demand predictions of multispan curved bridges. *Journal of Bridge Engineering*, American Society of Civil Engineering, pp 710-717.

Chapter 6

Analytical Results of Dynamic Analysis

6.1   Introduction

This chapter presents the major findings gathered from the investigation on the seismic performance of the Samudera Bridge in OpenSees (McKenna *et al.*, 2001). The investigation employed the structural model and procedures as have been detailed in chapter 4. Input ground motions used in the dynamic analysis were the 1940 El Centro, the 1995 Kobe, and the 2005 Sumatera ground motions. The seismic performance of the bridge is essentially described by the bridge response to ground motion excitations, and is conducted by performing the dynamic analysis. The dynamic analysis provides engineers with the seismic demand, which is presented as displacement response or pier hysteresis. A reliable seismic evaluation of a bridge depends heavily on the application of both the dynamic and the nonlinear static pushover analysis (NSP). NSP is useful in evaluating the seismic capacity of structures, whereby the force-deformation relationship obtained from the analysis may be used to determine the ultimate limit state at which failure occurs in the bridge. These are the fundamental information, which helps to compare the seismic capacity with the demand obtained from dynamic analysis, and thus, is significant in evaluating the extent of damage in a bridge, which is subjected to ground motions.

The investigation findings include the analytical results obtained from the static moment-curvature analysis, and from the dynamic simulations of the bridge to input ground motions. Important results discussed in this chapter are the moment-curvature relationship, stress-strain response of the concrete core and steel fibers, displacement response of piers, and the hysteresis pattern of piers recorded during dynamic analysis. The moment-curvature plot displays the force-deformation relationship anticipated in the pier cross sections. The displacement response, stress-strain response and pier hysteresis due to ground motions

would enable prediction of damage in the pier section during the simulation. Of further interest to engineers is the base shear recorded at pier bases.

In OpenSees, dynamic analysis consists of the eigenvalue and transient response analyses. The eigenvalue analysis is performed, using the "Eigen" command, to determine the eigenvalues, which correspond to the fundamental mode shapes. The transient analysis is performed using the "Transient Analysis" command, and involves using the gravity load and ground motion records to observe the dynamic response of the bridge structure under ground motion excitation.

It is also desirable, to engineers, to investigate the frequency content of a ground motion to understand the manner in which structures respond to the ground motion, and to predict the magnitude of potential damage due to a particular earthquake shaking. At this point, the response spectrum analysis is useful to display such information. For this purpose, absolute acceleration response spectrums were plotted to observe the frequency content, and the peak responses of various SDOF systems to all three input ground motions selected for study. The discussion of results focuses on the dynamic response of piers corresponding to assumptions made earlier that piers are expected to deform into the nonlinear range during large earthquake events.

6.2   Fundamental Vibration mode

Prior to performing non-linear earthquake simulation, eigenvalue analysis has been carried out in order to observe the fundamental vibration modes in the structure. Dynamic simulations were carried out for 50 seconds, using the El Centro and Kobe input motions, while the evaluation of the seismic performance to the 2005 Sumatera input motion was conducted for 115 seconds. The natural periods for the first three modes are 0.57, 0.51, and 0.45 seconds. From the analysis, it was evident that the fundamental vibration mode of the bridge system is in the transverse direction when it was subjected to the Kobe ground motion. Under the excitation of the El Centro input motion, the bridge system is observed to record a fundamental mode of vibration in the longitudinal direction.

6.3   Moment-Curvature Analysis

Moment-curvature analysis was conducted to establish the force-deformation relationship of the pier sections under increasing moment. It was also used to construct the theoretical

backbone curve, labeled as the dashed line in the hysteresis diagrams, for the hysteretic behavior of materials in pier sections. The pier sections were modeled with two nodes, having the same coordinates, and connected by a "ZeroLengthSection" element, where the pier cross section was discretized into concrete and steel fibers. The fiber discretization of the pier section has been described in detail in section 4.3.2 of chapter 4. The zero-length element geometry is as shown in Figure 6.1.

The pier section was then subjected to monotonically increasing compressive axial load, of 18000 kN, denoted as P in Figure 6.1. The axial load was applied in one hundred steps to obtain a strain profile, which reflects an equilibrium between the applied compressive axial load and the resulting internal forces. A reference moment of 1 Nmm was also applied linearly, about the stronger z-axis, to the pier section. OpenSees would further use the strain profile to calculate the corresponding curvature values at every step of gravity load application. Based on the prescribed concrete and steel properties mentioned in section 4.4.1, the resulting moment-curvature relationships for both free and fixed piers are as illustrated in Figure 6.2.

It can be observed that fixed piers have larger moment-curvature capacity compared to that of free piers. Such is because a larger amount of longitudinal reinforcements is provided in the fixed piers, thereby resulting in better strength capacity in the fixed piers. The moment-curvature relationships are used together with the concrete and steel strain limit states, defined in the material discretization, to estimate the values of yield curvature, and ultimate moment. The yield curvature corresponds to that curvature at the yielding of steel reinforcements, while the ultimate moment is defined as the value of peak moment capacity. From the moment-curvature analysis, it was observed that the yield curvature would occur at 0.00095 (1/m), when steel reinforcements are expected to yield. From Figure 6.2, the ultimate moments for the free and fixed piers are 81 MNm and 110 MNm, respectively.
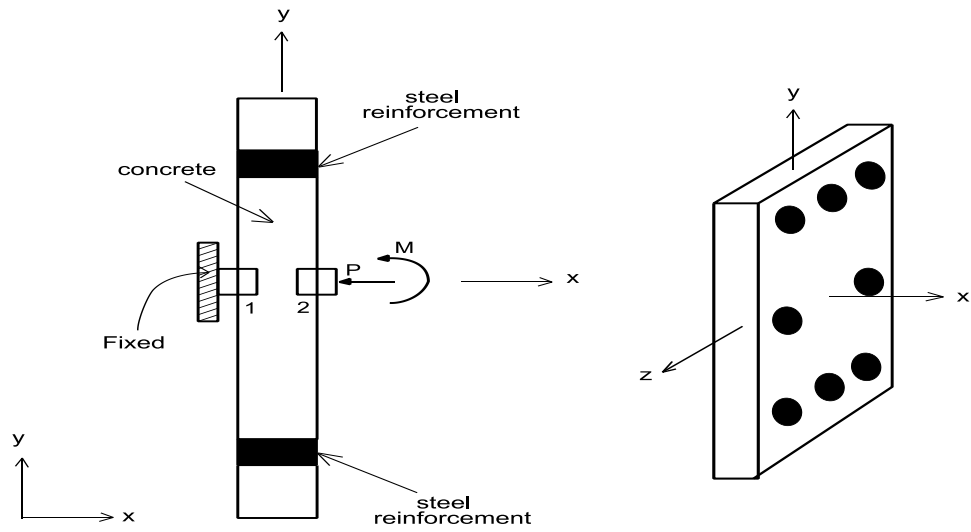
Figure 6.1   The geometry of the zero-length element used in the moment–curvature analysis in OpenSees (after Mc Kenna and Scott, 2001).
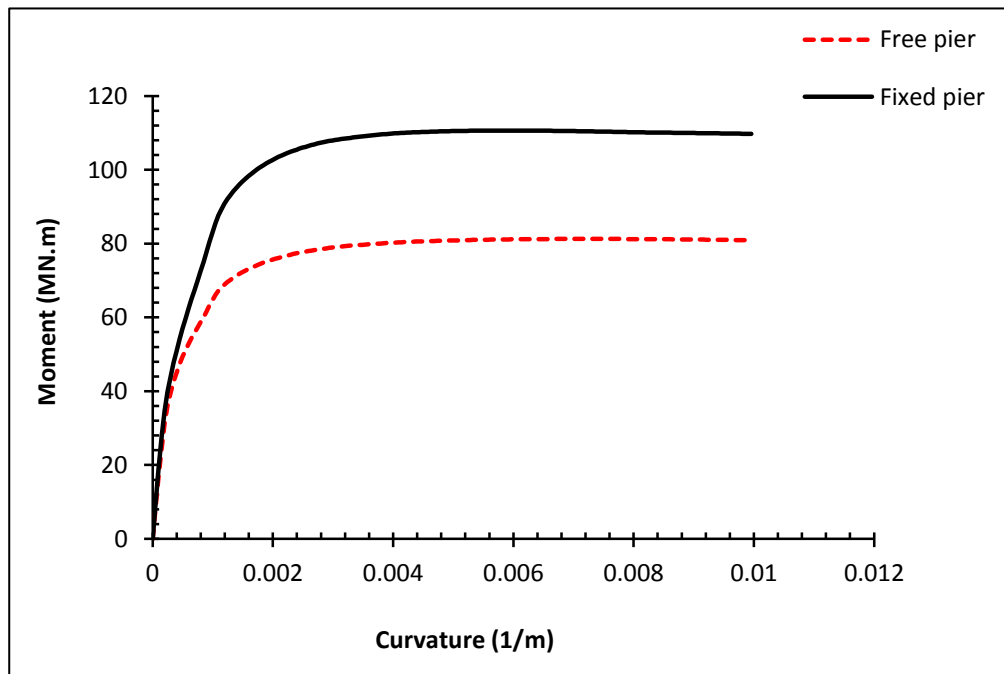
Figure 6.2   Moment-curvature relationships of the free and fixed bridge piers.

6.4   Response to the 1995 Kobe Input Motion

The Samudera bridge was excited to the Kobe input ground motion for 50 seconds. The simulation results are presented in this section to establish its seismic performance as discussed below.

6.4.1   Stress-strain Response

Plots of cyclic loading stress-strain response of concrete and steel fibers can assist an engineer on how to assess the extent of damage in pier sections following an excitation by a ground motion. The bridge structure chosen for study has 27 piers, however, for observation purposes stress-strain plots of selected piers are presented as shown in Figure 6.3.

In section 4.4.1, the criteria of failure have been defined to occur when steel reinforcement starts to yield at a strain of 0.0023. Failure of concrete core would occur at the ultimate limit state defined at 80% of the confined concrete compressive strength. In free piers, the ultimate limit state would occur at 36.8 MPa, while in fixed piers concrete is expected to crush at 35.8 MPa.

Dynamic simulation predicted that the steel reinforcement would yield in all piers between 7.28 and 8.64 seconds. Further scrutiny of the steel stress-strain response indicates that the reinforcements in fixed pier P2 yielded the earliest at 7.28 seconds into the excitation. In general, all fixed piers demonstrated steel yielding earlier than in free piers. The steel stress-strain response depicted in Figure 6.3 shows that the longitudinal reinforcements would sustain peak strains a few times higher than the yield strain of 0.0023, with free piers recording higher strains.

From the concrete core stress-strain response mapping, observed in Figure 6.3, concrete core crushing is anticipated in all piers, except in those equipped with expansion joints. Crushing of concrete is expected between 7.6 and 7.72 seconds with the shorter piers crushing earlier. It is noteworthy that crushing of concrete may occur if transverse reinforcements are insufficient. Insufficient transverse reinforcements may lead to low confinement, which in turn may lead to shear failure in piers and collapse of piers. The summary of damage in the piers is tabulated in Table 6-1.

Table 6-1 Observation of damage in piers, due to excitation under the Kobe ground motion, in terms of yielding of reinforcement steel and crushing of concrete core in piers

Pier	Time (sec)	
	Steel Yielding	Concrete Crushing
P1	7.52	7.62
P2	7.28	7.6
P3	7.58	7.64
P4	8.64	no damage
P5	7.6	7.68
P6	7.32	7.64
P7	7.62	7.68
P8	7.94	no damage
P9	7.62	7.68
P10	7.32	7.64
P11	7.62	7.68
P12	7.94	no damage
P13	7.62	7.7
P14	7.32	7.66
P15	7.62	7.68
P16	7.94	no damage
P17	7.62	7.68
P18	7.32	7.64
P19	7.62	7.68
P20	8.62	no damage
P21	7.62	7.68
P22	7.32	7.64
P23	7.64	7.72
P24	8.6	no damage
P25	7.58	7.64
P26	7.86	7.62
P27	7.54	7.62
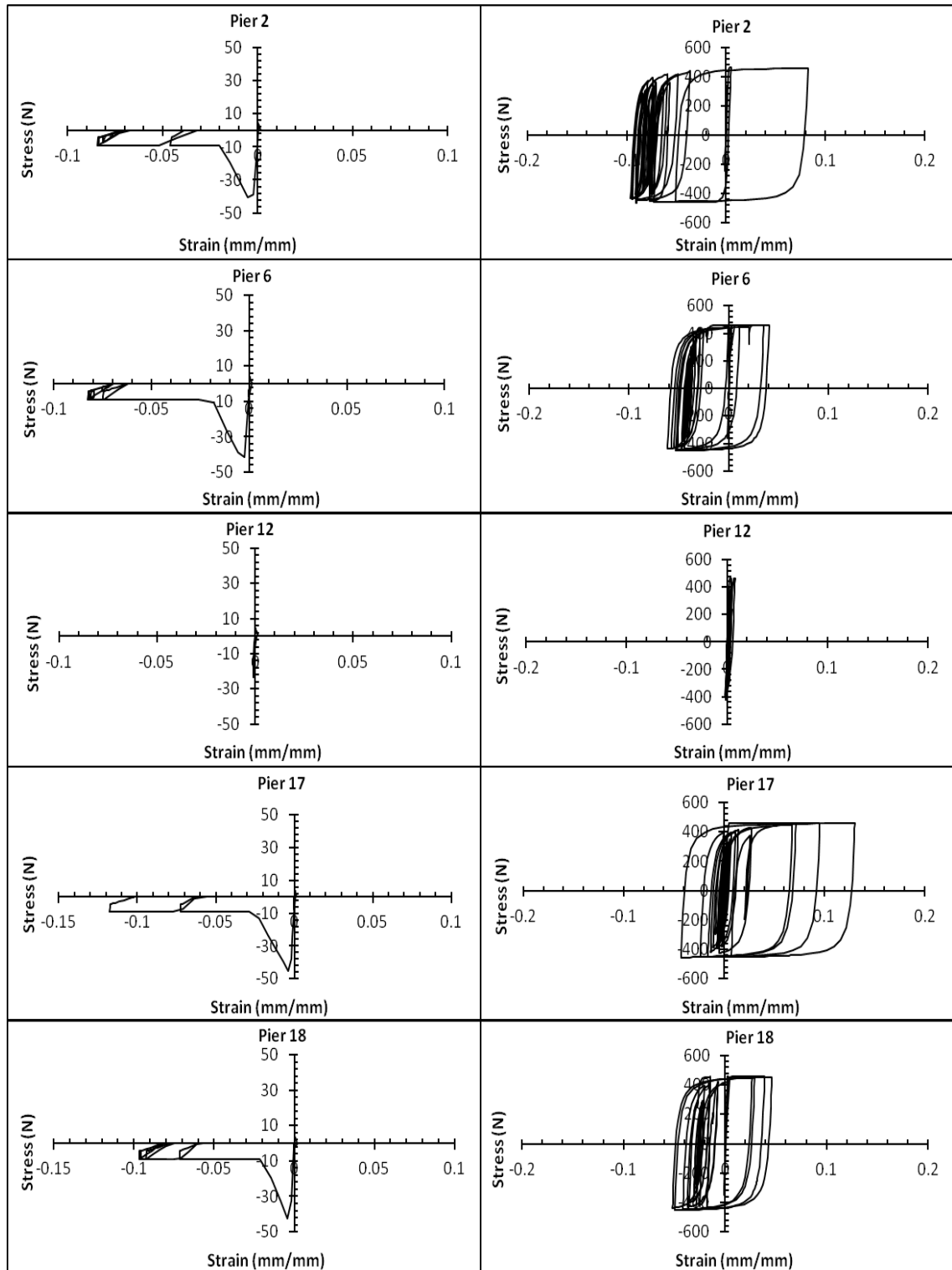
Figure 6.3 Selected stress-strain response relationships of concrete core (left) and steel reinforcement (right), as a result of excitation under the 1995 Kobe time histories.

117

6.4.2 Displacement Response

Deformation or damage in a bridge during an earthquake is associated with how much the structure is displaced under an earthquake excitation. Hence, it is of interest to engineers and designers to observe the displacement response recorded in a bridge in order to estimate the extent of deformation following an exposure to ground motions.

Table 6-2 summarizes the displacement responses of the bridge structure in the transverse and longitudinal directions. These displacements are maximum values observed in each pier throughout the simulation period. From the simulation, it is evident that displacement responses are more dominant in the transverse direction, both at the top of the piers and at the superstructure level.

The largest displacement observed in the longitudinal direction, at the top of the pier, was 230 mm, corresponding to the deformation at fixed pier P14. In the transverse direction free pier P17 recorded the largest displacement response of 255 mm.

Similar behavior was observed at the deck level, whereby the maximum response was recorded as 354 mm, at pier P8. The deck recorded consistent displacements in the piers belonging to the same block. A block refers to all piers making up the structure, separated by expansion joints. It is clear that, piers P1 to P4, of block 1, demonstrated displacement response of 114 mm; piers P5 to P8, of block 2, recorded a consistent displacement response o f 217 mm; and so on. Such observation demonstrates an elastic response behavior at the superstructure level. The largest displacement response recorded at the deck level, in the longitudinal direction, was 232 mm in pier P16. Meanwhile, the deck recorded a larger displacement response of 354 mm in the transverse direction

Figures 6.4 and 6.5 illustrate selected plots of the displacement response time histories at the top of the piers and their corresponding deck level, respectively. These plots are representative of the displacement response in other piers.

The pushover analysis performed on single-pier P17 indicates that the displacement capacity in the longitudinal direction, at the top of the pier, is 230 mm. This value is almost equal to the seismic demand recorded through dynamic analysis. This gives an indication that the bridge almost reaches the ultimate limit state in that direction. In the transverse direction, the maximum seismic demand is 255 mm, three times the value obtained by pushover analysis. Thus, it is clear that the bridge is anticipated to sustain severe damage when subjected to the Kobe input motion.

Table 6-2　Summary of the estimated displacement response recorded in the transverse and longitudinal directions, using the 1995 Kobe acceleration time history.

Pier	Height (m)	Maximum Displacement (mm)			
		Top of Pier		Deck Level	
		Longitudinal	Transverse	Longitudinal	Transverse
P1	4.5	33	53	114	73
P2	6.5	114	90	114	115
P3	7.7	207	146	114	174
P4	8.5	65	22	113	233
P5	8.5	124	134	217	157
P6	8.5	217	159	217	191
P7	8.7	211	227	217	265
P8	8.7	67	23	217	354
P9	8.7	177	184	228	215
P10	8.8	228	180	228	214
P11	8.8	174	250	228	291
P12	8.9	83	25	228	353
P13	9.0	161	171	231	199
P14	9.0	230	175	230	208
P15	8.9	207	172	231	200
P16	8.8	64	23	232	192
P17	8.7	157	255	222	297
P18	8.7	225	185	225	221
P19	8.7	227	178	228	207
P20	8.8	77	23	229	216
P21	8.7	158	218	221	254
P22	8.7	221	168	221	201
P23	10.4	172	143	221	164
P24	8.4	63	22	221	127
P25	8.0	166	160	140	189
P26	7.4	140	99	140	123
P27	4.4	21	53	140	72
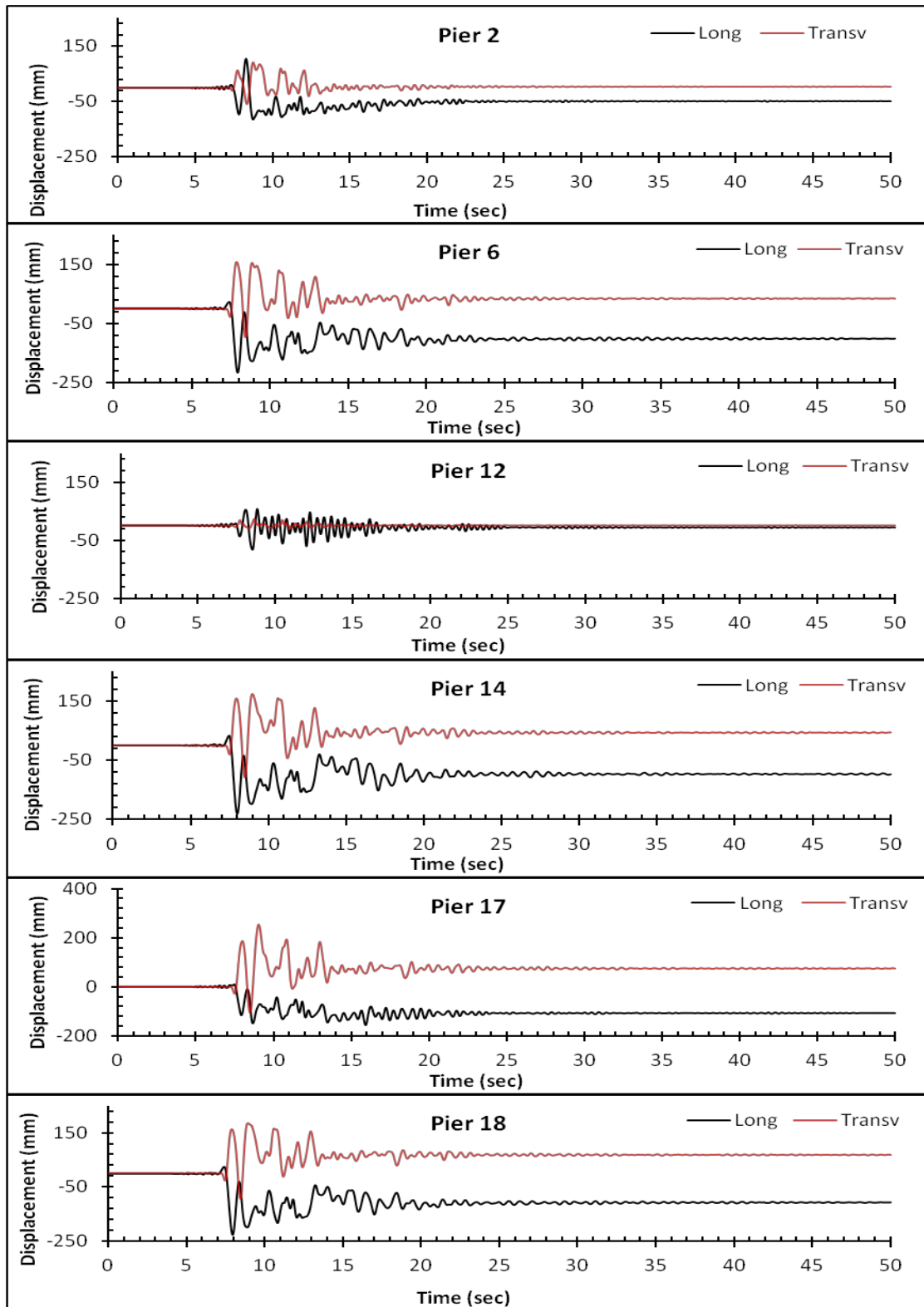
Figure 6.4 Displacement responses observed at the top of selected piers, as a result of excitation to the 1995 Kobe ground motion.
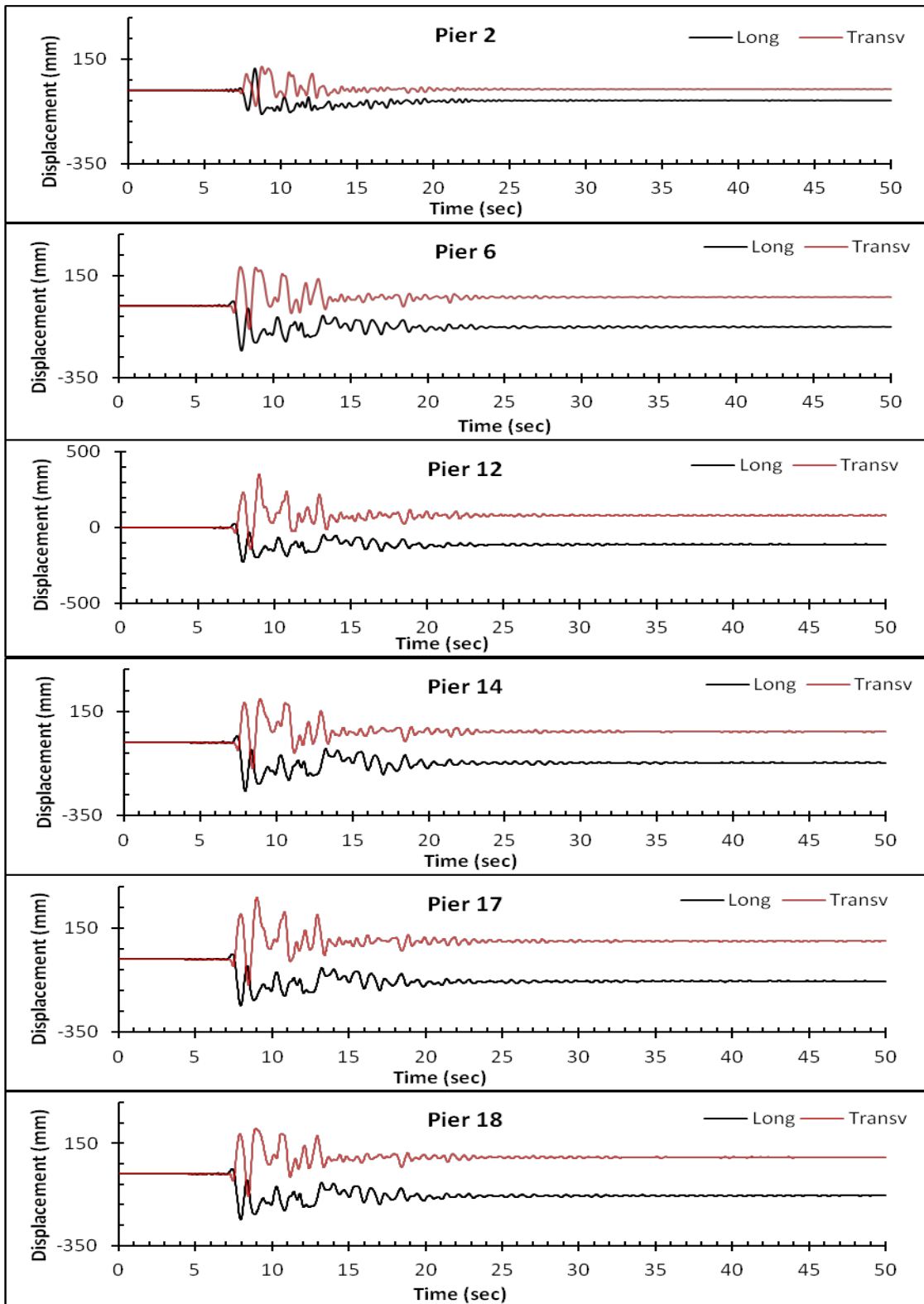
Figure 6.5   Displacement response observed at the superstructure level supported by selected piers, as a result of excitation to the 1995 Kobe ground motion.

6.4.3 Hysteresis Loop

Typical in any earthquake simulation, it is of great interest to ascertain the nonlinear behavior of piers subjected to ground motion excitations. This nonlinear behavior is commonly presented as hysteresis loops, as a result of cyclic deformation due to inelastic behavior. In this study, hysteresis of piers is presented in the form of cyclic moment-curvature response. Hysteresis plots of selected piers are as illustrated in Figure 6.6. The theoretical backbone curve, shown as dashed line, has been included to observe whether the cyclic dynamic response is within the envelope of the monotonic response, which was derived using the moment-curvature analysis.

In general, the dynamic simulation results display hysteresis loops, which are within the envelope of the backbone curve i.e. the simulation results are in good agreement with that predicted by static analysis. The simulation results further indicate that under large earthquake excitations such as that generated during the 1995 Kobe earthquake, all the piers, except those equipped with expansion joints, would deform inelastically through losses in stiffness and strength. In general, hysteresis loops are observed about the local y and z-axes, whereby hysteresis is more dominant about the y-axis. In all piers, except those with expansion joints, the hysteresis indicates that these piers are heavily damaged. The piers failed in the longitudinal direction first due to loss of stiffness. The curvature observed in the longitudinal direction exceeded the curvature capacity at the ultimate limit state.

Figure 6.6 also illustrates that the fixed piers are anticipated to sustain larger deformation, in the longitudinal direction, under the Kobe earthquake excitation. This is supported by the large deformation observed in both the local y and z-axes.

Taking into consideration the displacement and stress-strain response relationships from Figures 6.3 through 6.5; and hysteresis diagrams shown in Figure 6.6, it can be deduced that the damages are significant and collapse of the bridge structure is likely if transverse reinforcements present in the piers are insufficient to prevent shear failure in the bridge piers.
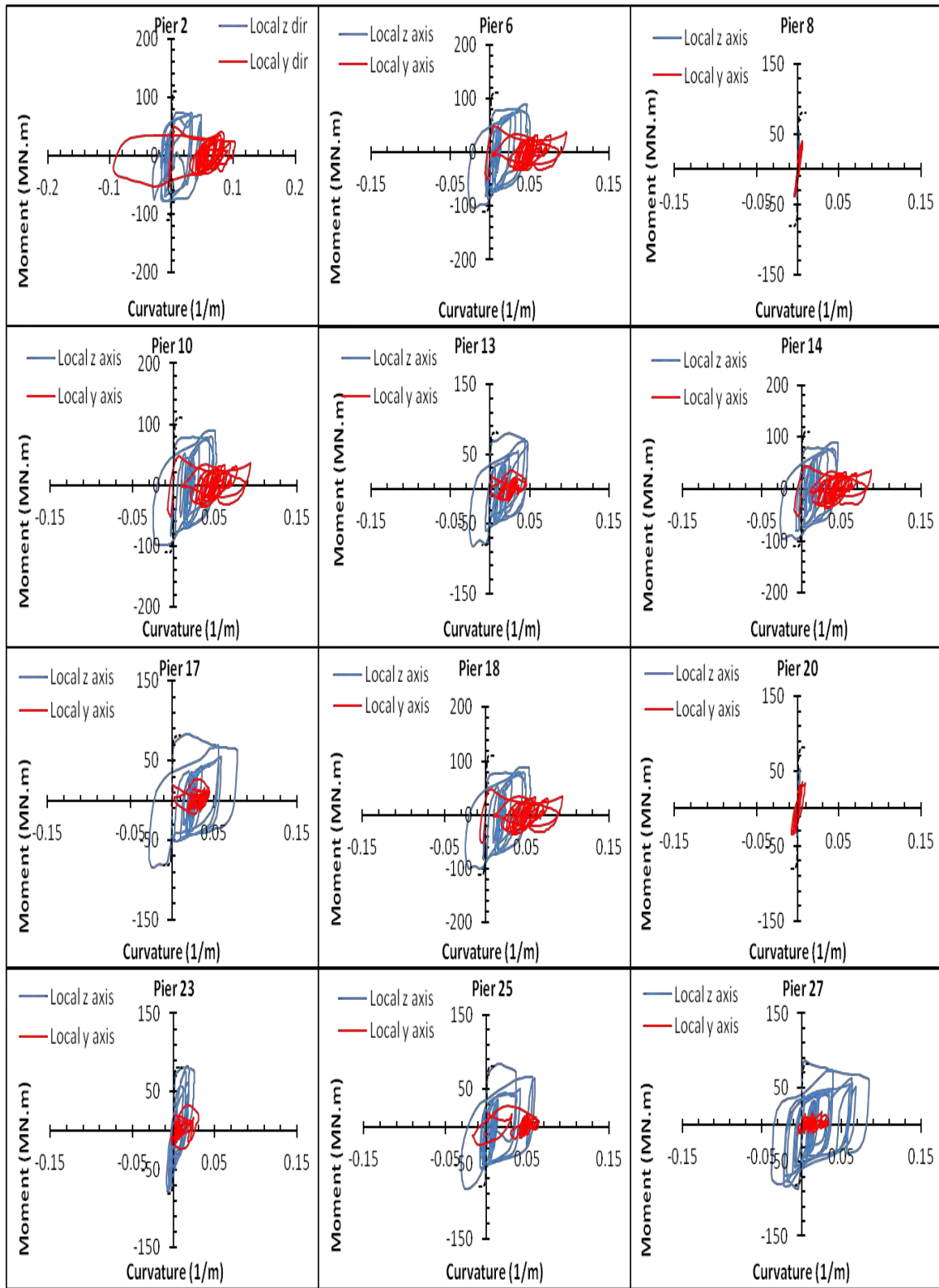
Figure 6.6   Hysteresis diagrams of selected piers demonstrating nonlinear behavior in pier sections when the bridge is subjected to the 1995 Kobe ground motion.

123

6.5 Response to the 1940 El Centro Input Motion

The following section discusses the response of the Samudera Bridge structure to the 1940 El Centro acceleration time histories. The emphasis of discussion makes reference to the dynamic simulation results in the longitudinal direction, in correspondence to the bridge fundamental mode of vibration.

6.5.1 Stress-strain Response

The stress-strain response of the concrete and steel fibers, of selected piers, to the El Centro time histories are presented in Figure 6.7. The seismic performance of the bridge is dictated by the allowable strain limits as defined in section 4.4.1. The dynamic simulation predicted that all piers, except short piers P1 and P27; and those equipped with expansion joints i.e. P4, P8, P12, P16, P20 and P24 would sustain yielding of steel reinforcement. Steel yielding is anticipated at a period as early as 1.54 seconds in fixed pier P22. Steel yielding is expected following tension strain response in the steel fibers, which is larger than the allowable strain limit of 0.0023. Simulation also shows that all fixed piers would suffer concrete crushing. Within the free pier group, piers P7, P11, P13, P15, P17, and P21 are anticipated to sustain concrete crushing. This is because the recorded compression strain response in the concrete fibers illustrated higher values than the allowable strain limit defined for concrete crushing. The summary of the damage in the piers are as tabulated in Table 6-3.

6.5.2 Displacement Response

A summary of the displacement response corresponding to the excitation to the El Centro ground motion is as tabulated in Table 6-4. It is evident from Table 6-4 that the displacement response is dominant in the longitudinal direction at the top of the piers and the superstructure level. It can be observed that the response in the longitudinal direction of the fixed piers tend to be equivalent to that recorded at the deck level. Observation of response at the top of the piers shows that the maximum displacement in the longitudinal direction was 84 mm, recorded at the tallest pier P23. The response at the top of the piers, in the transverse direction was 63 mm in pier P11.

Comparison of the maximum displacement response obtained by dynamic analysis with the seismic capacity value obtained from pushover analysis in the longitudinal direction

shows that the demand is 80 mm versus the displacement capacity of 230 mm. This suggests that the demand is lower than the capacity, indicating that small damage is expected in the longitudinal direction. Similarly, in the transverse direction, the demand is 63 mm, which is lower than the estimated capacity of 76 mm. Thus, it is safe to deduce that the piers would experience damage, but will survive the El Centro ground motion. However, the bridge piers would sustain moderate damages in the transverse direction or face. In piers with expansion joints, displacement response recorded are relatively smaller i.e. approximately 30 mm.

In the case of fixed piers, the maximum displacement recorded in the longitudinal direction was 70 mm in comparison to the estimated displacement capacity by pushover analysis of 191 mm. The demand in the transverse direction was observed as 53 mm, which is lower than the value predicted by pushover analysis of 65 mm. Thus, the bridge is expected to satisfactorily withstand the seismic forces generated by the El Centro input motion.

A similar trend was observed at the superstructure where displacement response is dominant in the longitudinal direction. The largest displacement response recorded in the longitudinal direction is 71 mm in pier P13, which smaller than the displacement capacity of 295 mm. The deck behaved elastically, as demonstrated by the consistent displacement response in all piers within the pier blocks, each block separated by expansion joints. Figures 6.8 and 6.9 depict the displacement response at the top of selected piers and at the superstructure level, respectively. These are representative of the displacement responses in all piers recorded during the dynamic simulation.
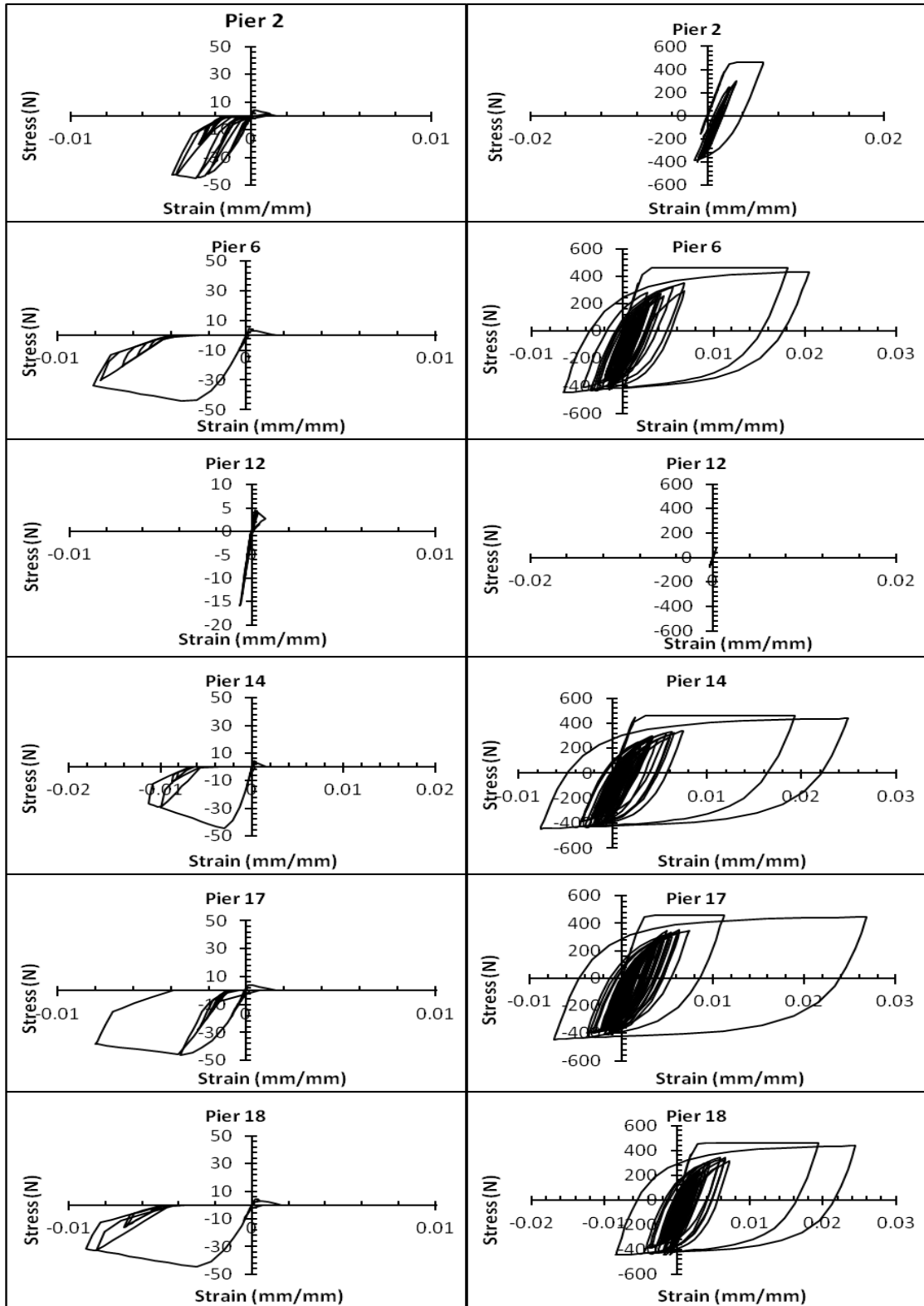
Figure 6.7 Stress-strain response relationships of the concrete core (left) and steel reinforcement (right) of selected piers, as a result of excitation to the 1940 El Centro acceleration time histories.

Table 6-3 Observation of damage in piers, due to excitation to the El Centro ground motion, in terms of yielding of reinforcement steel and crushing of concrete core in piers

Pier	Time (sec)	
	Concrete Crushing	Steel Yielding
P1	No Damage	No Damage
P2	4.62	4.56
P3	No Damage	4.68
P4	No Damage	No Damage
P5	No Damage	2.04
P6	1.94	2
P7	2.2	2.04
P8	No Damage	No Damage
P9	No Damage	2.04
P10	1.92	2
P11	2.22	2.06
P12	No Damage	No Damage
P13	2.24	2.06
P14	1.94	1.58
P15	2.24	2.06
P16	No Damage	No Damage
P17	2.22	2.04
P18	1.94	2
P19	No Damage	2.04
P20	No Damage	No Damage
P21	2.24	2.06
P22	1.92	1.54
P23	No Damage	2.12
P24	No Damage	No Damage
P25	No Damage	2.02
P26	4.7	2
P27	No Damage	No Damage

Table 6-4 Summary of the displacement response recorded in the transverse and longitudinal directions as a result of excitation by the 1940 El Centro ground motion

Pier	Height (m)	Maximum Displacement (mm)			
		Top of Pier		Deck Level	
		Longitudinal	Transverse	Longitudinal	Transverse
P1	4.5	3	5	20	7
P2	6.5	20	9	20	12
P3	7.7	23	16	20	21
P4	8.5	21	5	68	31
P5	8.5	37	30	68	37
P6	8.5	68	39	68	48
P7	8.7	54	50	68	61
P8	8.7	18	5	64	43
P9	8.7	56	44	64	53
P10	8.8	64	53	64	64
P11	8.8	51	63	64	75
P12	8.9	23	5	71	56
P13	9.0	56	51	71	61
P14	9.0	70	53	70	64
P15	8.9	57	53	70	63
P16	8.8	25	5	69	60
P17	8.7	52	59	64	71
P18	8.7	64	51	64	61
P19	8.7	59	45	64	55
P20	8.8	19	5	64	48
P21	8.7	59	53	63	64
P22	8.7	63	47	63	57
P23	10.4	84	46	63	54
P24	8.4	28	5	63	53
P25	8.0	33	23	42	28
P26	7.4	42	13	42	17
P27	4.4	2	4	42	6
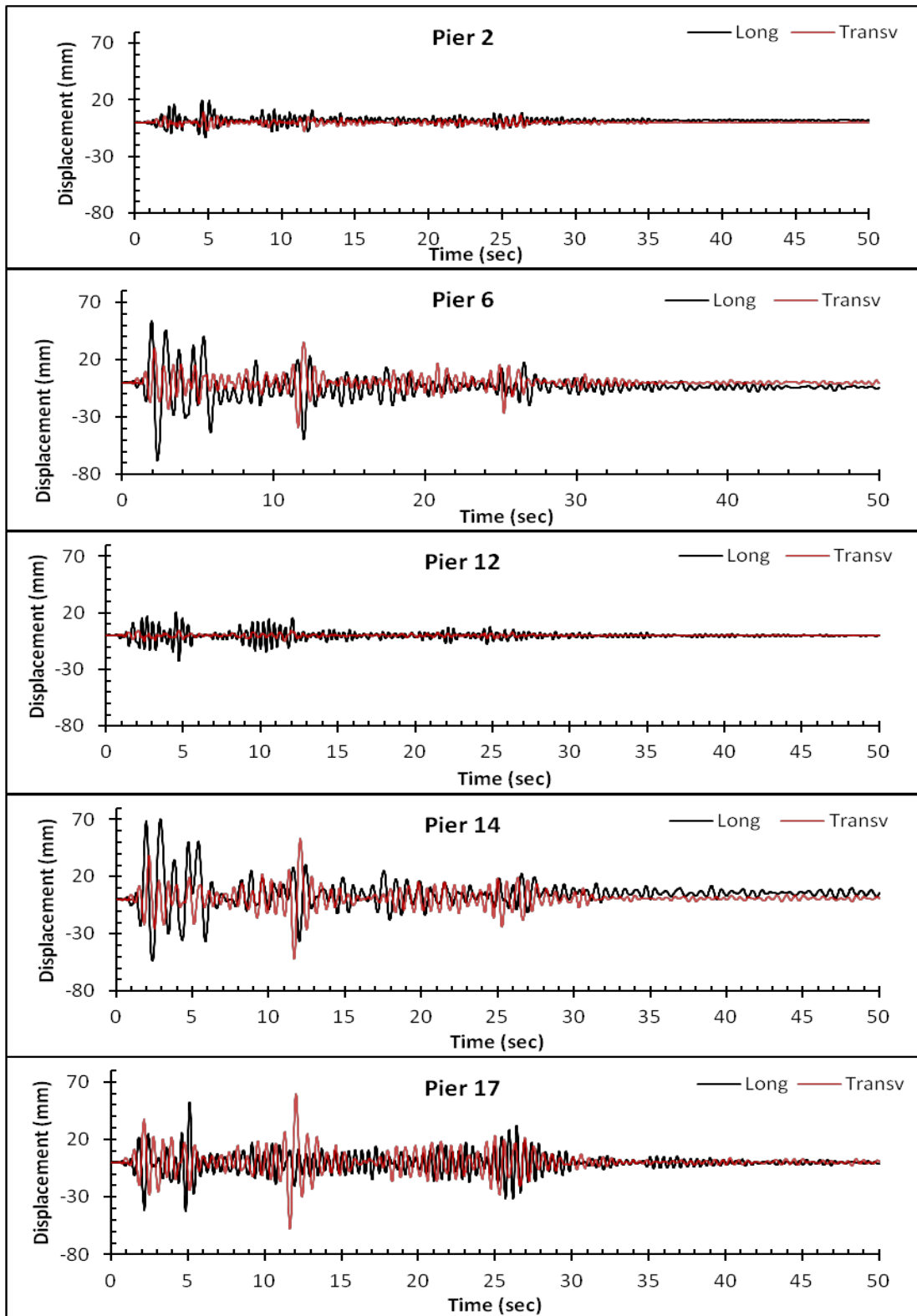
Figure 6.8 Displacement responses at the top of selected piers, as a result of excitation to the 1940 El Centro ground motion.
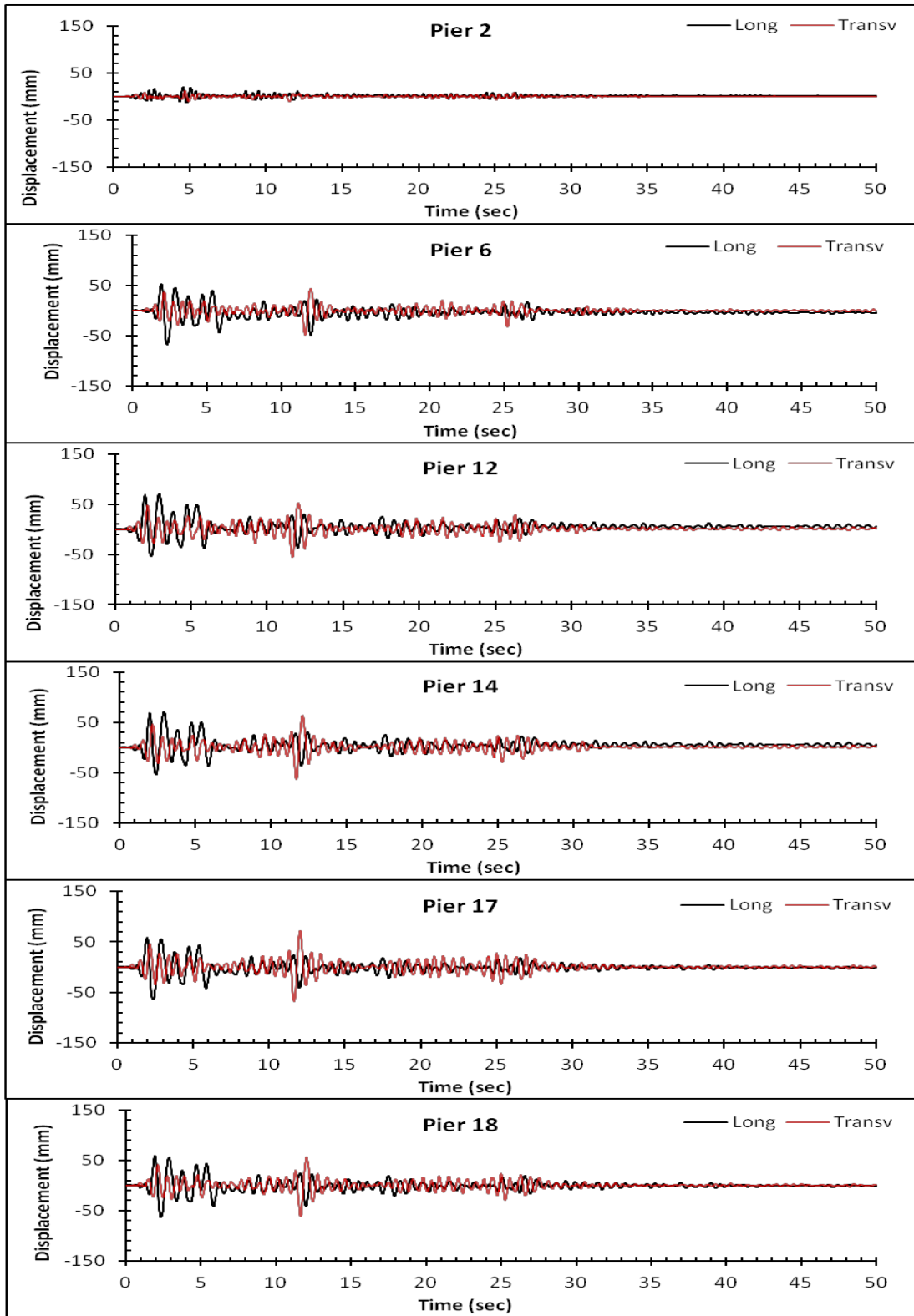
Figure 6.9 Displacement responses at the deck level supported by selected piers, as a result of excitation to the 1940 El Centro ground motion.

6.5.3 Hysteresis Loops

In this section, the response of the Samudera Bridge to the El Centro input motion is displayed as the cyclic moment-curvature hysteresis as shown in Figure 6.10. Hysteresis of selected piers in Figure 6.10 is representative of the hysteresis in entire bridge structure. It can be observed that nonlinear response is expected in all piers.

In general, Figure 6.10 suggests that the stiffnesses of the pier sections are higher in the transverse direction (about the major axis) than they are in the longitudinal direction. This justifies the fundamental mode of vibration in the longitudinal direction, and that the pier sections are stiffer in the transverse direction. It can be observed that nonlinear response is anticipated in all fixed piers with the pier sections expected to sustain a curvature of 0.022 (1/m) and 0.004 (1/m) about the weak axis (local y-axis) and z-axis, respectively. These values are well above the curvature capacity, and as such fixed piers are expected to fail due to crushing in the longitudinal direction first.

Nonlinear behavior can also be observed in piers P7, P9, P11, P13, P15, P17, P19, P21 and P23, which have been identified earlier on, in section 6.5.1 as sustaining concrete crushing.

It can be deduced from the hysteresis plots, in addition to the stress-strain response relationships, that the bridge system is expected to satisfactorily withstand the El Centro ground motion, without facing the danger of collapse.
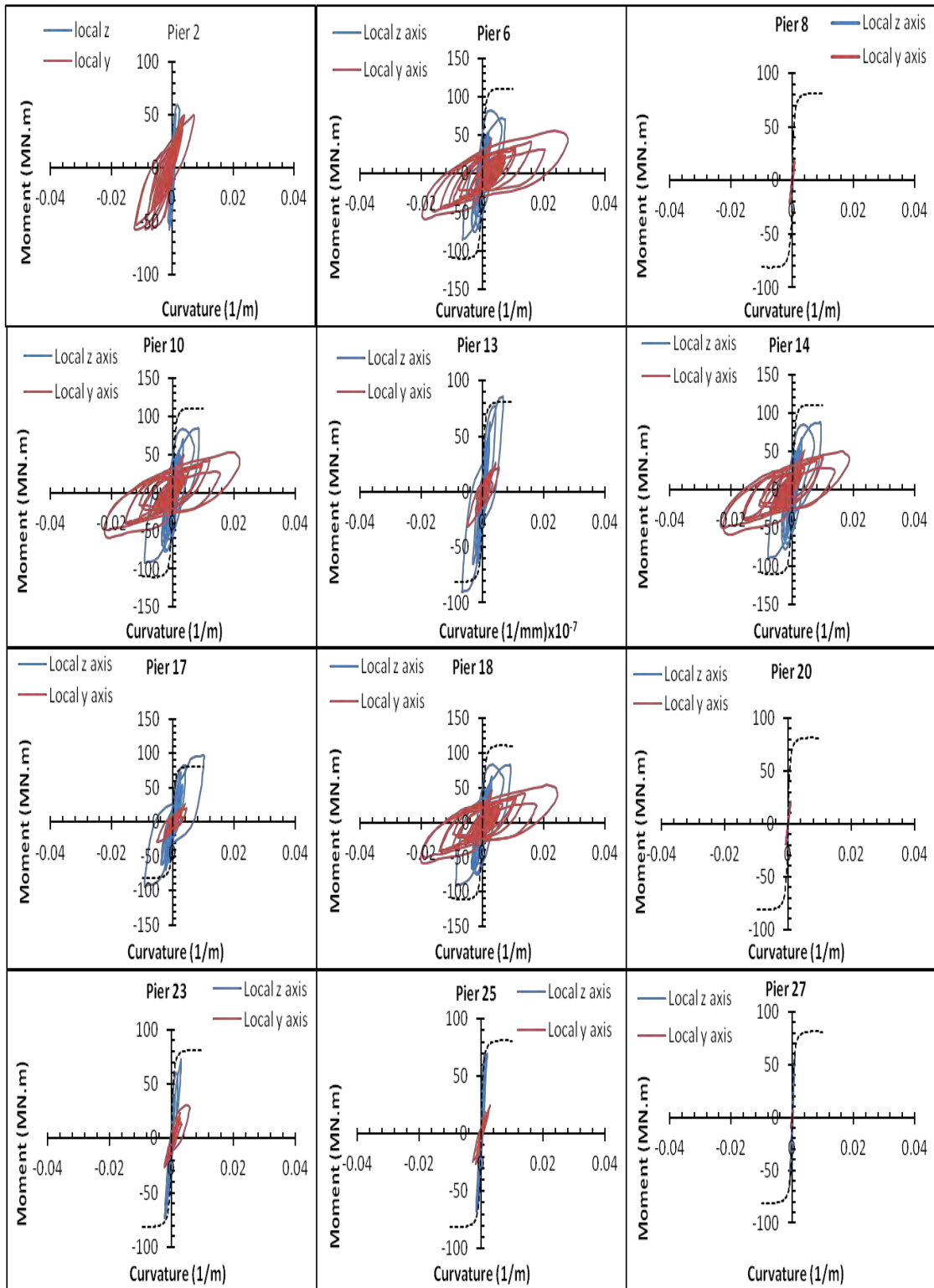
Figure 6.10 Hysteresis diagrams of selected piers demonstrating nonlinear behavior in pier section when the bridge is subjected to the 1940 El Centro ground motion.

6.6   Response to the 2005 Sumatera Input Motion

Apart from conducting investigations to study the seismic performance of the bridge structure to large and medium scale ground motions, such as that generated by the 1995 Kobe and the 1940 El Centro events, it is also essential to observe the response of the bridge to small, locally recorded earthquakes. For this reason, the Samudera Bridge was dynamically simulated to the, 0.02 g, 2005 Sumatera earthquake. The simulation results are discussed in this section.

6.6.1   Stress-strain Response

The Samudera Bridge was excited to the 2005 Sumatera input ground motion for 115 seconds. Figure 6.11 depicts the stress-strain response plots of the concrete and steel fibers of selected bridge piers. It is very clear that when the bridge was excited to the small intensity 2005 Sumatera input motion, the bridge piers exhibited a linear response in both the steel and concrete fibers. This is shown by the linear relationship between stress and strain as observed in Figure 6.11. Dynamic simulation predicts that in all the piers, damage is unlikely to occur as evidence indicates that the tension strain response recorded in steel, and the compression strain response in concrete fibers were well below the limiting strain values defined, in section 4.4.1. It is anticipated that the concrete core would remain intact, while steel reinforcements would not yield throughout the excitation. Hence, the bridge would be able to withstand the excitation satisfactorily without apparent damage. Table 6-5 summarizes the damage anticipated in the bridge as a result of excitation under the 2005 Sumatera ground motion.

6.6.2   Displacement Response

Figures 6.12 and 6.13 illustrate the displacement response time histories at the top of the piers and superstructure level of selected piers. These are representative plots of the deformation in the entire bridge structure. It is apparent from Figures 6.12 and 6.13 that the bridge responded fundamentally in the transverse direction.

A summary of peak displacements in response to the 2005 Sumatera input motion is as tabulated in Table 6-6. These are displacements recorded in the transverse and longitudinal directions. The maximum displacement response recorded in the transverse direction, at the top of the pier, was as a mere 0.6 mm at pier P23. At the deck level, the largest

displacement response in the transverse direction was observed as 1.0 mm, corresponding to the deformation at pier P14. The bridge response in the longitudinal direction is anticipated to be insignificant in most piers with the largest displacement recorded, at the top of the pier, as 1.0 mm. In general, deformation is anticipated to be very small to observe by the naked eyes, and as such, it can be concluded that the Samudera Bridge would experience insignificant response to the 2005 Sumatera ground motion. The superstructure remained elastic, as illustrated by very small and similar displacement response in all piers. It is anticipated that the Samudera Bridge would successfully withstand the local ground motion of 0.02 g.

Table 6-5 Observation of damage in piers, due to excitation to the 2005 Sumatera ground motion

Pier	Time (sec)	
	Steel Yielding	Concrete Crushing
P1	No Damage	No Damage
P2	No Damage	No Damage
P3	No Damage	No Damage
P4	No Damage	No Damage
P5	No Damage	No Damage
P6	No Damage	No Damage
P7	No Damage	No Damage
P8	No Damage	No Damage
P9	No Damage	No Damage
P10	No Damage	No Damage
P11	No Damage	No Damage
P12	No Damage	No Damage
P13	No Damage	No Damage
P14	No Damage	No Damage
P15	No Damage	No Damage
P16	No Damage	No Damage
P17	No Damage	No Damage
P18	No Damage	No Damage
P19	No Damage	No Damage
P20	No Damage	No Damage
P21	No Damage	No Damage
P22	No Damage	No Damage

P23	No Damage	No Damage
P24	No Damage	No Damage
P25	No Damage	No Damage
P26	No Damage	No Damage
P27	No Damage	No Damage
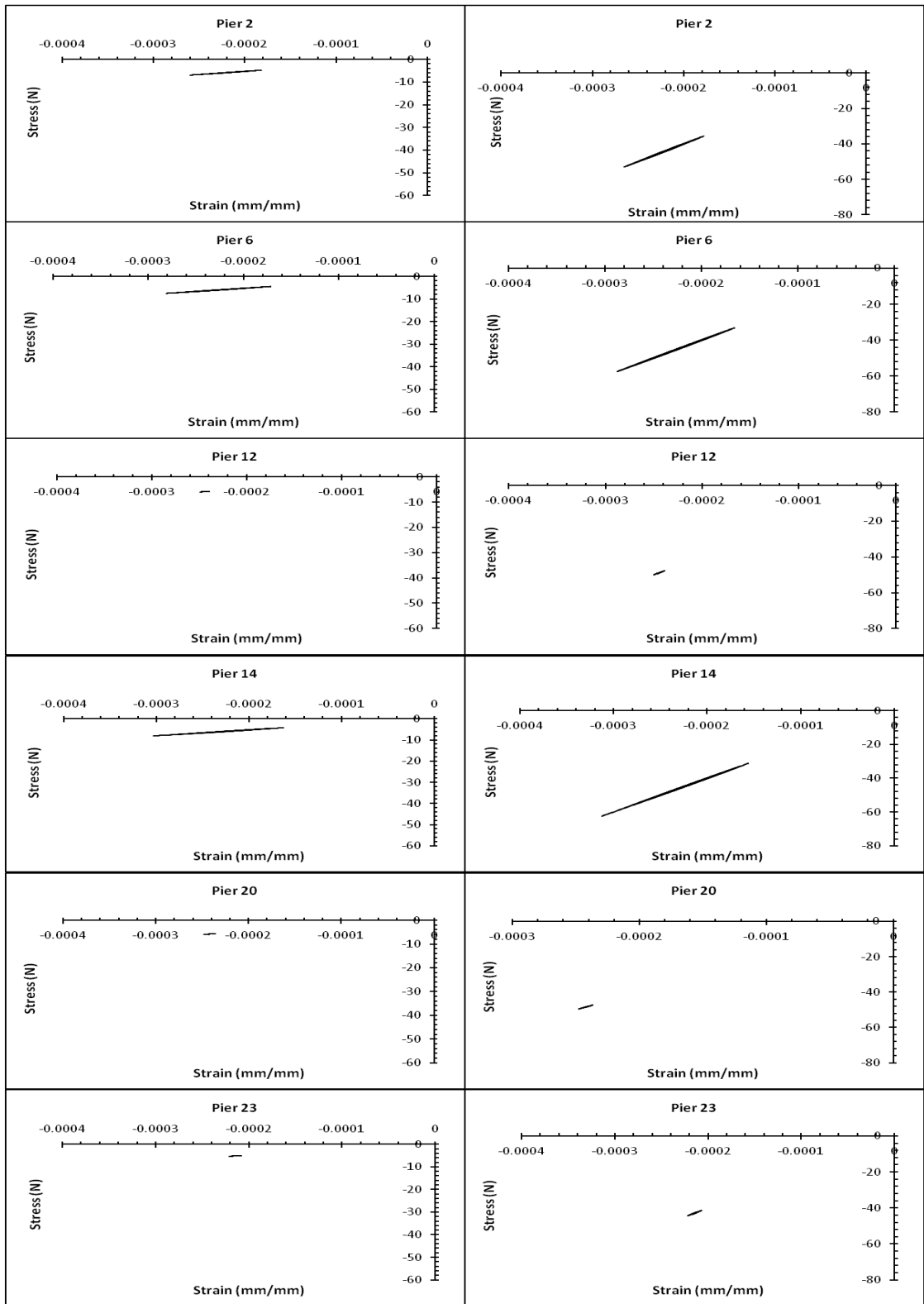
Figure 6.11 Linear stress-strain response of concrete core (left), and steel reinforcement (right) indicating damage is unlikely if the bridge were to be subjected to the 2005 Sumatra input motion.

136

6.6.3 Hysteresis Loop

In order to observe the likely performance of piers under the excitation of the 2005 Sumatera input motion, hysteresis diagram of selected piers have been plotted as shown in Figure 6.14. These hysteresis plots are typical cyclic deformation responses observed in the entire bridge system, and are representative of the response in the entire bridge. The simulation results indicate linear response with very small curvature sustained in all piers. This is a reflection of very small displacement responses as observed in figures 6.12 and 6.13. This linear response further confirmed the claims made in section 6.5.1 that the bridge piers are unlikely to experience any damage. As such, the bridge is expected to withstand small intensity excitation, such as the 2005 Sumatera ground motion, satisfactorily without having to enter the nonlinear range.

Table 6-6   Summary of peak displacement responses in the longitudinal and transverse directions recorded under the 2005 Sumatera acceleration time-history.

Pier	Height (m)	Displacement (mm)			
		Top of the pier		Deck level	
		Longitudinal	Transverse	Longitudinal	Transverse
1	4.5	0.03	0.10	0.27	0.44
2	6.5	0.25	0.27	0.30	0.77
3	7.7	0.06	0.42	0.31	0.93
4	8.5	0.06	0.50	0.31	1.01
5	8.5	0.06	0.49	0.65	1.01
6	8.5	0.65	0.48	0.65	1.00
7	8.7	0.07	0.51	0.65	1.04
8	8.7	0.06	0.51	0.65	1.04
9	8.7	0.06	0.52	0.87	1.05
10	8.8	0.87	0.52	0.87	1.06
11	8.8	0.07	0.53	0.87	1.07
12	8.9	0.07	0.54	0.87	1.08
13	9.0	0.07	0.55	1.06	1.09
14	9.0	1.06	0.55	1.06	1.10
15	8.9	0.07	0.54	1.06	1.08
16	8.8	0.07	0.53	1.06	1.07
17	8.7	0.08	0.52	0.80	1.06
18	8.7	0.80	0.52	0.80	1.06
19	8.7	0.07	0.53	0.80	1.07
20	8.8	0.06	0.53	0.80	1.08
21	8.7	0.06	0.52	0.90	1.07
22	8.7	0.87	0.53	0.90	1.08
23	10.4	0.12	0.59	0.90	1.08
24	8.4	0.06	0.52	0.90	1.06
25	8.0	0.05	0.47	0.46	1.01
26	7.4	0.43	0.35	0.45	0.88
27	4.4	0.03	0.07	0.43	0.34

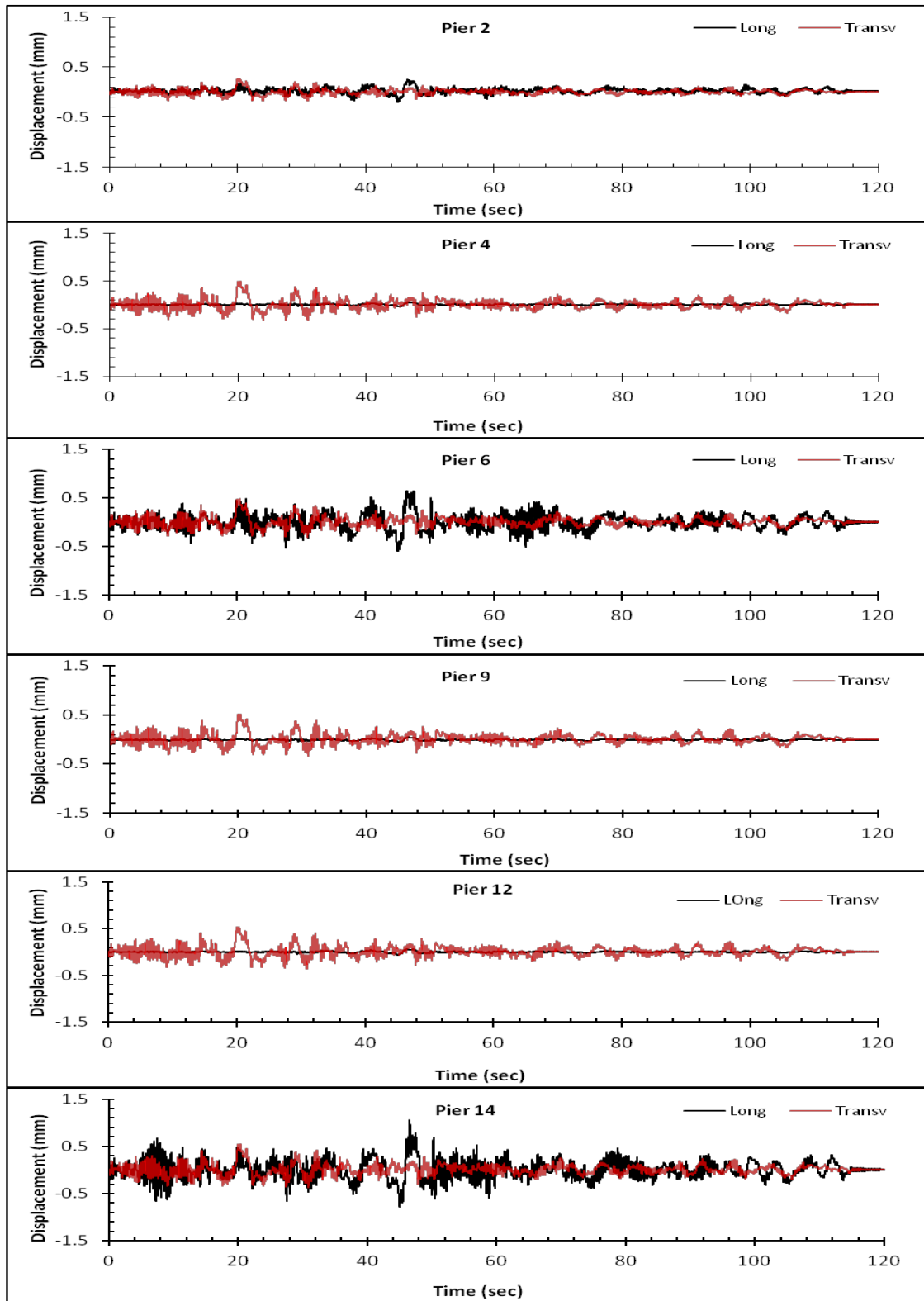Figure 6.12 Displacement response at the top of selected piers, as a result of excitation to the 2005 Sumatera ground motion.
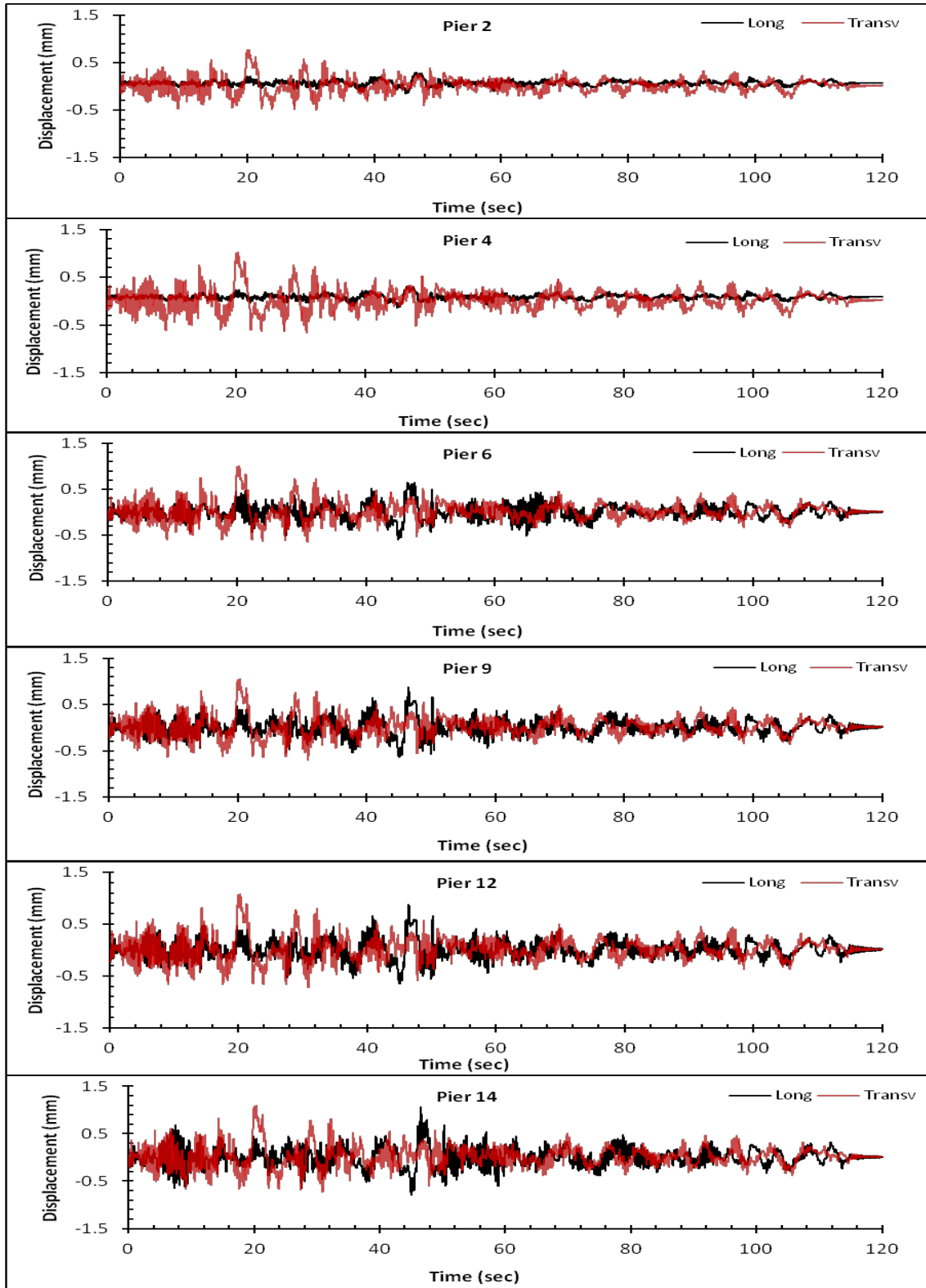
Figure 6.13 Displacement response at the deck level supported by selected piers, as a result of excitation to the 2005 Sumatera ground motion.
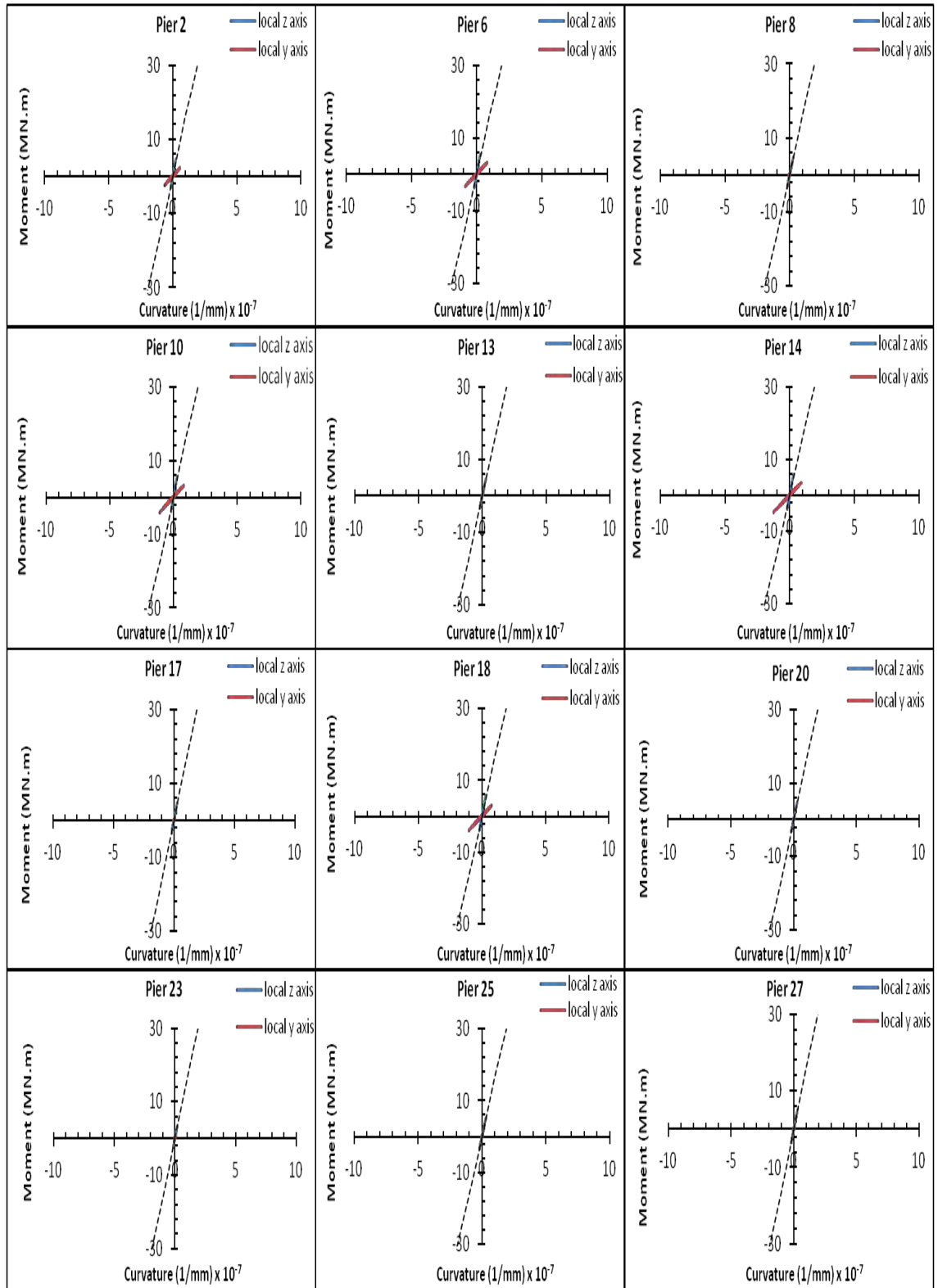
Figure 6.14 Hysteresis loops of selected piers illustrating linear behavior in the bridge system when excited by the 2005 Sumatera ground motion.

6.7   Response Spectrum

A response spectrum may be used to describe the frequency content of a recorded ground motion. The frequency content of a ground acceleration record has become an essential tool in explaining the behavior of a structure under an earthquake excitation.

In this section, evaluation of the absolute acceleration response spectrums for all three selected ground input motions were carried out to study the differences between their frequency contents. A series of elastic single degree of freedom (SDOF) systems have been subjected to all the acceleration time histories chosen for study, and the absolute acceleration response spectrums in the transverse direction have been plotted considering a 5 percent damping ratio. Figures 6.15, 6.16 and 6.17 depict the response spectrum plots of the 1995 Kobe, the 1940 El Centro and the 2005 Sumatera input motions, respectively. The response spectrums for the Kobe and El Centro earthquakes illustrate high frequency content region between 0.2 and 0.6 seconds. In contrast, the 2005 Sumatera ground motion demonstrates high frequency content region between 1.5 and 3.0 seconds.

As have been shown in previous sections, dynamic simulation using the Kobe and El Centro input motions predict that the bridge piers deformed into the nonlinear range. Simulation also indicates that when the structure was excited using the 2005 Sumatera ground motion, small deformation was observed and all piers remained elastic. However, before concluding that small, locally recorded ground accelerations are incapable of causing damage to structures in Malaysia, it is essential to illustrate where the bridge structure is located on the response spectrum.

It is evident from Figure 6.15 that the fundamental period of the structure is within the region of high frequency content, and this explains the reason for the damage experienced by the bridge through steel yielding, spalling and cracking of concrete in most piers when the bridge is excited to the Kobe input motion. From Figure 6.16 it can be observed that the fundamental period of the bridge is located within the high frequency range of the El Centro response spectrum. However, since the acceleration response is a half of that recorded by the Kobe earthquake, the damage extent in the bridge is anticipated to be lower than when it is excited under the Kobe input motion. This justifies the smaller damage in bridge piers when excited to the El Centro time-histories. On the other hand, Figure 6.17 shows that the natural period of the structure is located where the frequency content is low; hence, very small deformation would be expected if the bridge were to be simulated under the 2005 Sumatera input motion. The response spectrum also suggests that slightly larger

deformation would be expected in a structure with fundamental periods between 1.5 and 3 seconds. Thus, the derivation of response spectrum has shown us that locally recorded acceleration time history can affect structures with lower natural frequency.
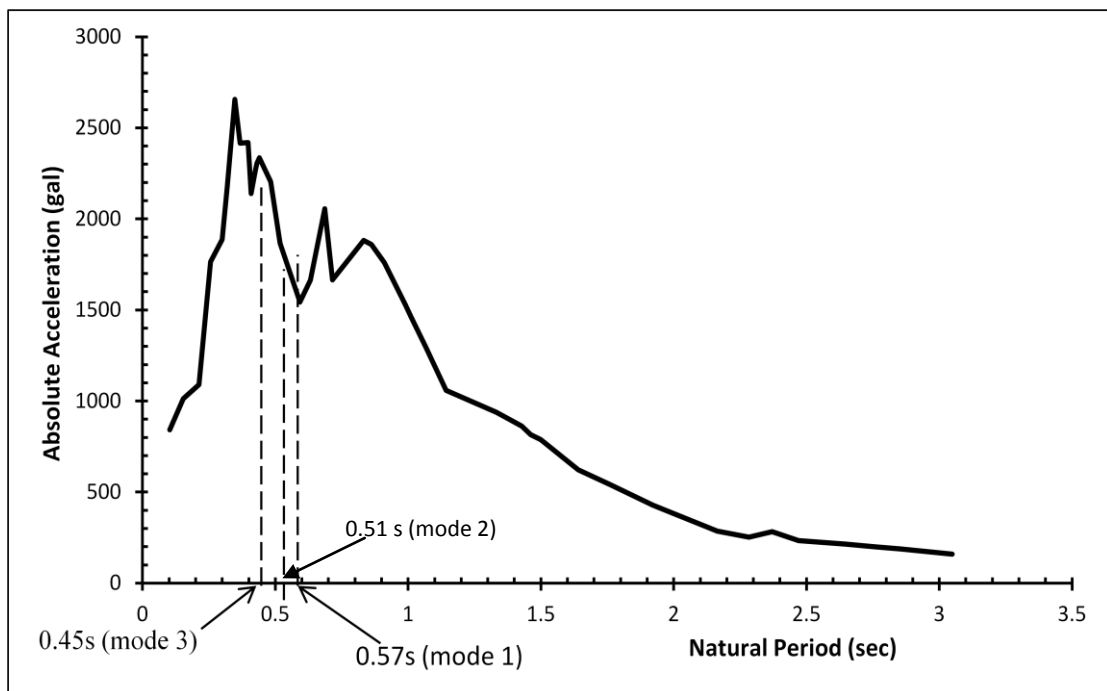

Figure 6.15   Absolute acceleration response spectrum of the1995 Kobe ground motion, damping ratio = 5 percent.
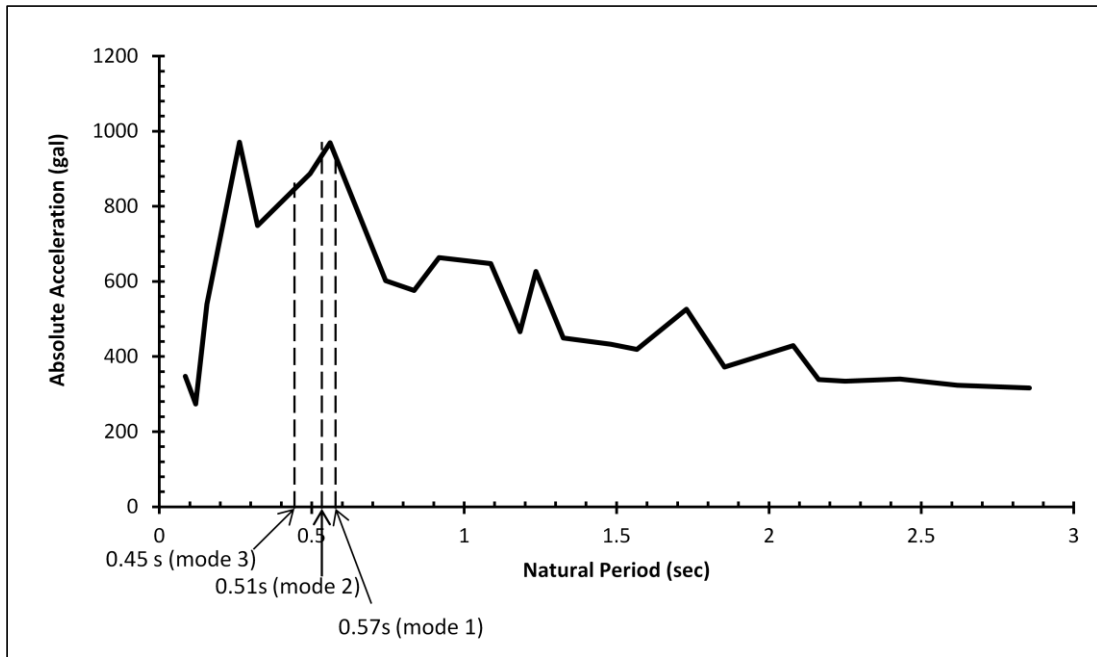
Figure 6.16   Absolute acceleration response spectrum of the 1940 El Centro ground motion, damping ratio = 5 percent
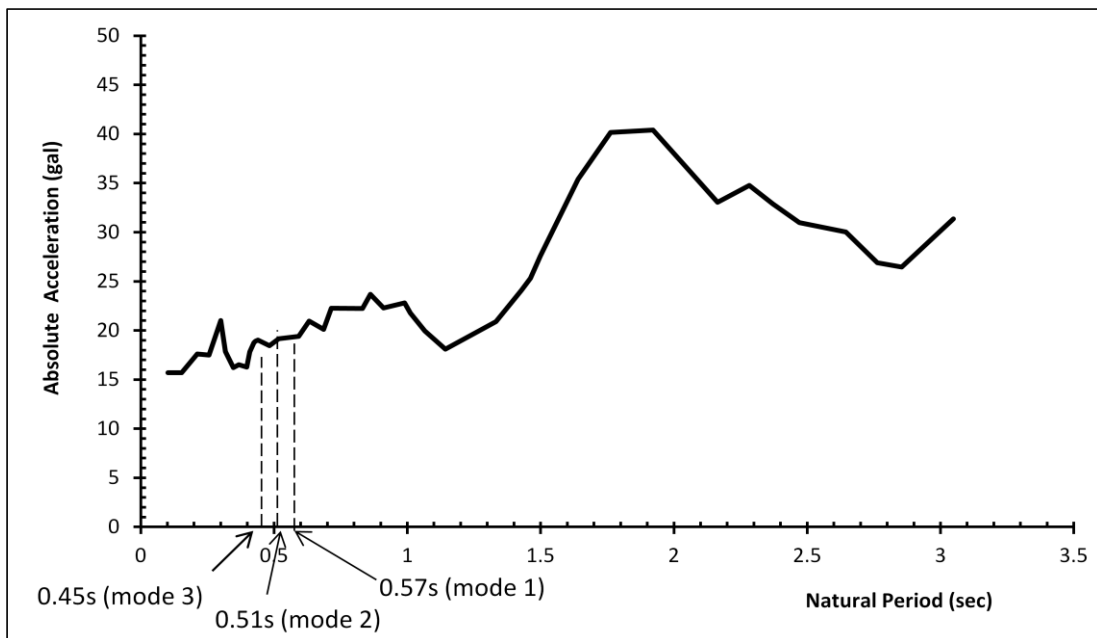

Figure 6.17   Absolute acceleration response spectrum of the 2005 Sumatera ground motion recorded in Malaysia, damping ratio = 5 percent.

6.8   Conclusions

Malaysia's capital city, Kuala Lumpur, stands third in the list of states, which have recorded felt earthquakes in Malaysia (MMD, www.met.gov.my). Kuala Lumpur has observed maximum intensity of VI, on the MMI scale within an observation period of approximately 110 years. This information confirms the existence of seismic hazard in the capital city. Combined with the fact that existing bridges in Malaysia were designed to the existing design codes, which exclude the effects of seismic forces, it is of great interest to observe the behavior of bridges in or near the proximity of Kuala Lumpur.

Evaluation of the seismic performance of bridges has become a popular task among researchers in the low seismicity regions. This chapter has also been dedicated to evaluating the seismic performance of the Samudera Bridge, mainly to accomplish two main objectives. The first objective is to investigate the likely performance of the bridge to possible maximum magnitude earthquake of 6.5, and the second objective is to derive an acceptable seismic coefficient value for bridge design in Malaysia. The decision to select the most appropriate seismic coefficient value for Malaysia will have to incorporate the pushover analysis results and the seismic response from dynamic analysis.

The Samudera Bridge has been selected for investigation of its seismic performance against three ground motions: the 1995 Kobe, the 1940 El Centro and the 2005 Sumatera ground motions. Dynamic simulations performed suggest that the bridge under study is likely to face the danger of sustaining severe damages or even suffer collapse when subjected to large earthquakes, such as that generated during the 1995 Kobe earthquake. This is mainly supported by simulation results featuring nonlinear hysteresis loops observed in all the piers. In addition, the seismic demand recorded by the bridge under the excitation of the Kobe input motion exceeded the displacement capacity determined using the pushover analysis. The curvature capacity is also greatly exceeded, and thus it is believed that the bridge would be heavily damaged in the event of large earthquakes. If the longitudinal bars are confined by sufficient transverse reinforcements, the displacement demand would be significantly reduced, and collapse may be avoided.

Excitation of the bridge to the 1940 El Centro ground motion predicts that the Samudera Bridge is capable of withstanding the seismic forces without experiencing collapse. However, cracks or damage caused by concrete crushing are expected in fixed piers and the piers in the middle portion of the structure. Damage is also anticipated through yielding of

longitudinal reinforcement in all piers except in those at locations of expansion joint after only 1.58 seconds into the excitation.

In the event that the bridge structure is subjected to the largest earthquake motion recorded locally, the structure is capable to withstand the 0.02 g input motion and only experience minute damages unseen by the naked eyes. This has been deduced based on the linear hysteresis pattern in all piers indicating linear behavior in piers when excited by the 2005 Sumatera earthquake. However, it is important to note that the response spectrum analysis has aided us to understand that other structures having natural periods between 1.5 and 3.0 seconds are likely to experience larger deformation if they were to be subjected to such acceleration time histories.

The investigation of the seismic performance functions to study the anticipated seismic demand and level of damage of the Samudera Bridge. Analysis results are based on the expected behavior by which the structure was modeled i.e. damage is expected in piers but not the superstructures. It is aimed that the modeling would assist in estimating the seismic coefficient value for the design of new bridges, as well as for assessing the seismic performance of existing bridges in low seismicity areas. Another objective of the seismic performance investigation is to gather information on the seismic demand to compare with the seismic capacity of the Samudera Bridge. Thus, the extent of damage under different levels of ground motion can be predicted. Table 6-7 summarizes the seismic demand information derived from subjecting the Samudera Bridge to three ground motions.

From pushover analysis, it has been observed that the seismic coefficients of the free pier P17 and fixed pier P18, in the longitudinal direction, are low i.e. 0.22 and 0.07, respectively, and the displacement capacities for both piers in that direction are quite high, at 295 mm and 250 mm, respectively. In the transverse direction, the seismic coefficients of the free and fixed piers are relatively similar at 0.54 and 0.57, respectively, but their displacement capacities are low i.e. 100 mm and 90 mm, respectively. Observation of the damage during dynamic analysis, for instance under the Kobe excitation, indicates that the piers are heavily damaged in both the transverse and longitudinal directions. An important observation is that although the seismic coefficient value is higher in the transverse direction, the pier is heavily damaged in that direction. Similarly, the pier is heavily damaged in the longitudinal direction where the seismic coefficient is lower. Thus, it can be deduced that seismic coefficient is not an important factor, which dictates the survival of the bridge structure under a large excitation. Rather, displacement capacity plays an important role to ensure the survival of the bridge during a large ground motion.

146

Table 6-7   Summary of the seismic demand resulting from excitation to the 1995 Kobe, 1940 El Centro, and 2005 Sumatera ground motions

Ground motion	Maximum displacement (mm)			
	Top of pier		Superstructure Level	
	Longitudinal	Transverse	Longitudinal	Transverse
1995 Kobe	230	255	232	354
1940 El Centro	84	59	71	75
2005 Sumatera	< 1	< 1	< 1	1

References

Mc Kenna, F. and Fenves, G.L. (2001) *The OpenSees Command Language Manual, Version 1.2*, Pacific Earthquake Engineering Research Center, University of California at Berkeley, California (http://opensees.berkeley.edu/).

Chapter 7

The Impact of Introducing Seismic Resistant Design to the Malaysian Economy

7.1   Introduction

As much as the structural engineering community in Malaysia would like to welcome the introduction of seismic design guidelines, many stakeholders perceive that the inclusion of seismic design requirements for the design of bridges would lead to an excessive increase in the construction cost. Such perception may hamper the implementation of seismic resistant design, and may further heighten the anxiety of the public on the level of safety of structures in Malaysia.

This chapter explores the impact of introducing seismic resistant design on the cost of bridge constructions to be implemented by the government of Malaysia. The methodology used involved examining the level of ductility in the fixed pier section by employing the nonlinear pushover analysis. The pushover analysis shall be used to determine the pushover curve (base shear versus displacement), from which the ductility factor may be estimated. The procedure is presented in the following section.

7.2   Proposed Method for Estimating Cost of Aseismic Design

Aseismic design minimizes damage in bridges and loss of life in the event of an earthquake by accounting seismic forces, in addition to dead and live loads, during analysis. In performance-based design concept, designers aim to design structures to achieve a satisfactory deformation state under a design-level earthquake. Consequently, aseismic design emphasizes on enhancing ductility to ensure that a bridge structure has the ability to deform into the inelastic range with acceptable stiffness reduction. Such behavior is

149

favorable because it enhances the seismic performance of a bridge structure, even though damages are allowed to occur.

Ductility of concrete can be improved by increasing its confinement by using transverse steel reinforcement (Elnashai and Di Sarno, 2008). By increasing the transverse reinforcement, the confinement of concrete core can be enhanced, thus, boosting its seismic performance. It is largely known that improved confinement helps reduce the displacement demand under an earthquake excitation.

With this concept in mind, it is proposed that the investigation on economy would account for displacement ductility focusing on enhancing the transverse reinforcement while retaining the amount of longitudinal reinforcements.

In this study, the fixed pier is chosen as the subject for investigation because it has smaller amount of transverse reinforcement in comparison to the free pier. The as-built drawings on pier detailing show that the fixed piers are confined with 10 mm diameter transverse bars at 250 mm spacing. The free piers, on the other hand, have been provided with a richer amount of transverse reinforcement (T10 bars at 150 mm spacing), almost double the amount in fixed piers.

Bearing in mind that recent seismic design has been incorporating the 'flexible' design concept, this study will employ the use of the original pier section and a modified section, which is flexible, but is ductile enough to survive seismic forces. Furthermore, to illustrate how seismic resistant design may not necessarily end up with skyrocketing construction cost, this study has chosen to educate readers that the use of flexible piers in a bridge may help in keeping the construction cost at a reasonable level.

A detailed description of the procedure used in this study is as discussed below:

a. Choice of pier: Pier P18, also known as the 'original' section, is selected for study mainly because it has lower transverse reinforcement than the free pier. The pushover curve of Pier P18 has been previously established and studied in Chapter 5. Thus, focus shall be given to performing the pushover analysis on the modified section.

The modeling of pier is explained in detailed in chapter 4.

b. Modified section: Only one section shall be investigated. A flexible pier can be achieved by making the original section smaller. The limit of section reduction considers the provision in BS5400: Part 4(1990). This guideline was used because

the Samudera Bridge was designed to this design standard. Thus, consider the slenderness limit of

$$l_o = 100b^2/h \le 60b \qquad\qquad (7.1)$$

where l_o, h and b are column clear height, the larger dimension of a column, and the smaller dimension of the column, respectively. This limit suggests a modified section of size 2800 x 1500 mm.

The revised pier reinforcement ratio in the modified section is based on the provision stated in BS 5400:Part 4 i.e. the minimum percentage of longitudinal reinforcement is 0.4%, but longitudinal reinforcement should not exceed 6%. The total longitudinal reinforcement provided in the modified section is 48T40 + 56T32.

c. **Calculate the confined concrete properties for modified section**: The confined concrete compressive strength and its ultimate strain are calculated based on the model proposed by Mander *et al.* (1988). These values are obtained from equations (4.1) to (4.11) in chapter 4. This model suggests that the modified section has a confined concrete strength of 48 N/mm^2, and crushes at an ultimate limit state of 0.025.

d. **Conduct pushover analysis on the modified section**: Perform pushover analysis on the modified section in the longitudinal and transverse directions, separately. Apply gravity loading, followed by a lateral load equivalent to 5% the superstructure weight. The pushover analysis shall be conducted to a maximum displacement of 500 mm with monitoring node at the deck level. Establish the force-deformation relationship of the pier. Observe and identify the displacement at the ultimate limit state. The ultimate limit state shall be defined at 80% its peak compressive strength. Yielding of steel reinforcement shall be taken to occur when the strain reaches 0.0023.

e. **Estimate the ductility**: The ductility of the original and modified sections shall be estimated in order to evaluate the 'flexibility' of the modified section. Flexible section should be able to deform larger than the original section. The relationship is as shown in Figure 7.1.
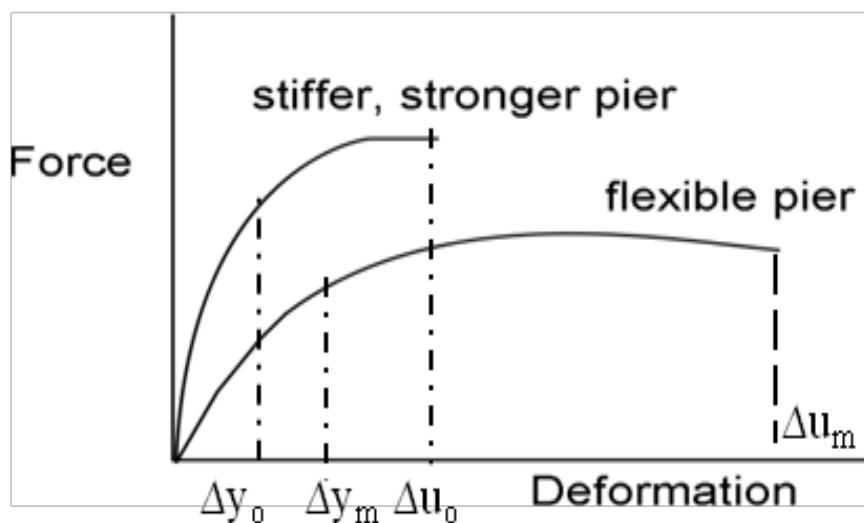
Figure 7.1　Force-deformation relationship, obtained from pushover analysis, used to estimate ductility

The estimate of displacement ductility factor is as given below

$$\mu_\Delta = \frac{\Delta_u}{\Delta_y}$$ (7.2)

where

Δ_{yo} = yield displacement of the original section (mm)

Δ_{ym} = yield displacement of the modified section (mm)

Δ_{uo} = ultimate displacement of the original section (mm)

Δ_{um} = ultimate displacement of the modified section (mm)

f. Run dynamic analysis to determine displacement response: Compare the displacement response of the original and modified sections recorded by the dynamic analysis. If the responses are approximately equal, then the modified

152

section can be assumed to have similar ability to resist seismic forces, as that by the original section. Thus, economically, the modified section may be used as an alternative section to the larger, stiffer original section.

g. **Calculate the amount of saving or additional spending**: The impact on the economy can be determined as a percentage of the total cost of the bridge structure. The prices of building materials such as steel reinforcement in piers and concrete shall refer to the contract document of the project "Menaiktaraf Jalan Serta Pembinaan Bertingkat di Persimpangan Jalan Taman Samudera dan Perusahaan kecil di Batu Caves" (PWD, 2003).

7.3   Results of Pushover Analysis

Pushover analysis has been performed on the original section (from Chapter 5), and the modified section. Figure 7.2 represents the ductility of the original and modified sections, respectively. From Figure 7.2, it can be observed that the modified section is more ductile, as shown by the larger displacement capacity. The ductility factor of the original section is 2.86, while the modified section 2.57. This supports the fact that the modified section is more ductile than the original section.
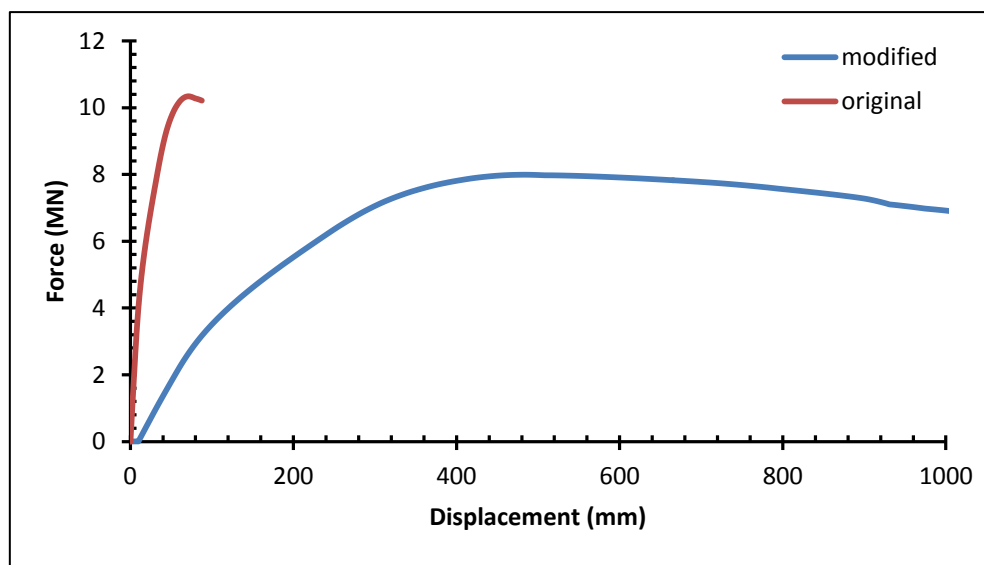

Figure 7.2   Comparison of ductility factor between the modified and original sections.

7.4   Results of Dynamic Analysis

Dynamic analysis is performed on the entire bridge system using the Kobe input motion. The modified section recorded a maximum displacement response of 205 mm, while the original section recorded 250 mm. The displacements recorded using dynamic analysis did not differ too much, and thus the modified section can be used as an economical alternative pier section in the bridge system.

7.5   How Expensive is Seismic Resistant Design?

Most people perceive seismic resistant design as an expensive solution to mitigate seismic risk. This is true a few decades ago when construction of seismic resistant structures generally used bulky and stiffer structural elements. However, in recent years, the engineering community has understood the role of flexible elements in seismic resistant structures. Flexible elements have gained popularity due to their ability to withstand seismic forces with smaller sections, which are ductile and more economical.

This study has attempted to use the flexible pier element as a strategy to illustrate how smaller sections can survive an earthquake excitation, and offer an economical solution to the construction industry.

The contract document prepared for the Samudera Bridge project is used as a reference for the cost of material. The main materials involved in the calculation of savings or spending, due to the implementation of the seismic resistant design are concrete and reinforcements. The currency used in the calculation of addition or savings in the construction cost is the Malaysian Ringgit or MYR.

The cost reference for concrete and reinforcements are MYR 230 per cubic metre of concrete and MYR 1.80 per kg of steel reinforcements. The total reduction of concrete volume from 27 piers due to downsizing of pier size is 233 cubic metre. This is translated as a saving of MYR 54,000. With smaller pier sections, less longitudinal reinforcements are used and as a result, there is a reduction of 19679 kg of T40 bars and 6816 kg of T32 longitudinal bars. As such, there is a further savings of MYR 48,000. In fixed piers, transverse reinforcements have been added to enhance their seismic performance, and due to that, an additional 920 kg T10 bars have been used, which marks a spending of MYR 1655. It can be demonstrated that by using flexible pier sections in the construction of the bridge, a savings of MYR 100,000 is possible.

Apart from these savings, smaller pier sections require the use of smaller foundations and pile size. Thus, flexible sections would result in further savings. However, one must realize that due to a reduction in pier size, displacement response may increase, and thus fail-safe mechanism may be required. Fail-safe mechanism secures bridges from unexpected large earthquakes. It is important to consider the installation of fail-safe mechanism in bridges and an allocation for it should be made in the construction of bridges. This budget can be taken from the savings on material cost, calculated earlier, and can be added when necessary.

Since there has been no reference, in Malaysia, of the cost of fail-safe mechanism to protect a bridge from the damaging effects of seismic forces, this study will consider the cost of elastomeric bearings to estimate this cost. Noting that fail-safe mechanisms shall be provided at locations of expansion joints, they will be installed at piers P4, P8, P12, P16, P20 and P24. Based on the highest price of a piece of 600 (W) x600 (L) x200 (H) mm elastomeric bearing, which is MYR 1500, a pier requires a cost of MYR 24,000 for fail-safe mechanism. Thus, the total cost to protect the bridge from unexpected large earthquakes, which may result in large displacement response, is approximately MYR 200,000. This cost is calculated based on the material cost of the year 2003 and may vary due to price change in the market.

Assuming the calculation above, the cost of seismic resistant design for the Samudera Bridge is 0.4%. However, this is only the price of material alone, and after an addition of the installation cost, the total cost of fail-safe mechanism may be estimated at a minimum of 0.5%, but not to exceed one percent.

7.6   Fail-safe Mechanism

Historical earthquakes have given us invaluable insights of the possible types of damage in a bridge structure excited by ground motions. Thus, researchers are able to understand the nature of damage and improve bridge design in order to minimize seismic risk. Some of the common damages observed at superstructure level are span failures due to unseating at movement or expansion joints following pounding between adjacent elements or structures (Priestley *et al.*, 1996).

Excessive movement has been linked to bridge collapse during several earthquakes in high seismicity countries such as the United States and Japan. Reconnaissance reports from the 1995 Kobe earthquake confirm that pounding effects contributed to the collapse of

155

bridge decks (Otsuka *et al.*, 1996). In the United States, bridge failures due to separation at expansion joints in bridge decks were devastating during the 1994 Northridge earthquake. Bridge deck collapse from supports and joints observed during the 1971 San Fernando earthquake events were some examples of how "failures may have been prevented with the application of ties or restrainers across expansion joint" (Roberts, 2005).

Recent seismic design requires that superstructure should be designed as elastic and nonlinear response is expected in columns during large earthquakes. Thus, damage is anticipated in columns rather than at superstructure. As such, superstructure collapse due to unseating or separation at expansion joints is undesirable and must be avoided. During a large earthquake, adjacent beams or structures separated by a gap can vibrate out-of-phase because these beams are not connected together and are free to move independently. Consequently, there is a relative displacement between them and if the relative displacement exceeds the initial gap width provided, the deck may give way and collapse.

Evidently, superstructure collapse can be avoided by considering fail-safe mechanisms in bridges. The California Department of Transportation (CALTRANS), in a seismic retrofitting program of bridges across California, has explored some structural control techniques to improve the seismic performance of existing bridges. An example of protection technique considered were the hinge restrainer cables to allow for elastic movement. In many designs, restrainers have been provided across the movement joint to prevent excessive movement, which can lead to collapse of span. Restrainers work to prevent separation of adjacent structures and unseating during an earthquake. They gain popularity following the collapse of several bridges during the 1971 San Fernando earthquake (DesRoches *et al.*, 2002).

Although the use of fail-safe mechanism in bridges is widely emphasized in high-seismicity regions, it is a good practice to investigate its application in low seismicity regions for preparedness against unexpected larger magnitude earthquakes.

It is noteworthy that although the use of flexible piers in bridges may seem appealing, one should realize that flexible piers may experience larger displacement response under an earthquake excitation. Thus, flexible piers should be considered together with the application of fail-safe mechanism. In fact, fail-safe mechanism must be compulsory in all seismic regions, be it of high, moderate or low seismicity. This is because earthquakes cannot be predicted, thus, preparation for the worst is necessary.

7.7   Conclusions

Essentially, seismic resistant design does not necessarily mean allocating a large budget in construction. Rather, a reliable and smart resistant design may keep the construction cost at an acceptable level. Of course, important structures may need extra strengthening but, basically an additional cost involved in seismic resistant design is due to providing and installing fail-safe mechanisms.

Based on the illustration of savings in material cost and an additional budget for fail-safe mechanism, calculated in section 7.5, it is observed that the cost, which will be incurred to implement seismic resistant design, is less than one percent of the bridge structure cost. It is important to note that for a low seismicity region, flexible sections may be used to achieve ductility; however, designers must be aware that flexible sections may result in larger displacement response during an earthquake. Thus, fail-safe mechanisms must be provided. It is only natural to use the savings resulted from using flexible sections as an allocation for fail-safe mechanism.

References

DesRoches, R. and Delemont, M. (2002). Seismic retrofit of simply supported bridges using shape memory alloys. *Engineering Structures* 24: 325-332.

Kawashima, K., Kosa, K., Takahashi, Y., Akiyama, M., Nishioka, T.,Watanabe, G., Koga, H. and Matsuzaki, H. (2011). *Damage of bridges during 2011 Great East Japan Earthquake.*

Muthukumar, S. and DesRoches, R. (2006). A Hertz model with non-linear damping for pounding simulation. *Earthquake Engineering and Structural Dynamics* 35: 811-828.

Otsuka, H., Unjoh, S., Terayama, T., Hoshikuma, J., and Kosa, K. *Damage to highway bridges by the 1995 Hyogoken Nanbu earthquake and the retrofit of highway bridges in Japan.* 3rd US-Japan Workshop on Seismic Retrofit of Bridges, Osaka, Japan, 10-11 December 1996.

Priestley, M.J.N., F. Seible and G.M. Calvi (1996). *Seismic Design and Retrofit of Bridges*, J. Wiley & Sons, New York.

Public Works Department Malaysia (2003). *Contract Document: Menaiktaraf Jalan Serta Pembinaan Persimpangan Bertingkat di Persimpangan Jalan Taman Samudera dan Perusahaan Kecil di Batu Caves (JL TII Fasa 2)*, Public Works Department of Malaysia, Kuala Lumpur.

Roberts, J.E (2005). Caltrans structural control for bridges in high seismic zones. *Earthquake Engineering and Structural Dynamics* 34: 449-470.

Chapter 8

Conclusions

8.1   Introduction

Despite being geographically located on the stable Sunda shelf and categorized in the low hazard region, evaluation of seismic design motion is indispensible in Malaysia. Such is attributable to evidence of seismic hazard from distant, active seismic sources of Sumatera; and ground motions recorded within the country. Felt earthquakes have psychologically affected the public and the question as to whether bridges in Malaysia are able to perform satisfactorily in the event of an earthquake has become a subject of concern to stakeholders in the construction industry. Although bridge designers are aware of seismic hazard in Malaysia, bridges are continuously designed according to the traditional design guidelines, which ignore seismic requirements. Such practice exposes bridges to the destructive effects posed by earthquakes, and consequently public safety is at risk.

Based on this scenario, the government of Malaysia has shown a great interest on mitigation of seismic risk and the destructive effects of earthquakes. A recognized approach to achieve this is through implementation and enforcement of seismic resistant design. This research was conducted as an attempt to evaluate a seismic design motion for the design of bridges in Malaysia. A summary of findings is presented below.

8.2   Suitable Attenuation Model for Malaysia

For countries belonging to the low seismicity region, attenuation models may be applied to estimate the seismic hazard or seismic design motion pertaining to each country. For this reason, comparisons of observed peak ground acceleration (PGA) and peak ground velocity (PGV) at seismic stations with those values predicted by attenuation models were carried out. Four attenuation models have been considered in this research: the Atkinson and Boore

(1995), Toro *et al.* (1997), Dahle *et al.* (1990), and Si and Midorikawa (1999). Their selections were based on the types of tectonic environment they represent i.e. for shallow crustal earthquakes and subduction zone; and source-to-site distance. It was deduced that attenuation relationships established by Dahle *et al.* (1990) and that by Atkinson and Boore (1995) may appropriately reflect the seismic conditions in Malaysia.

In addition, maximum magnitude earthquake for Peninsular Malaysia has been predicted as magnitude 6.5, based on historical data of Malaysia. Peak ground velocity is estimated at 60 cm/s, while peak ground displacement is estimated as 150 mm. For this reason the Kobe ground motion has been selected for dynamic analysis. It is also of interest to adopt the peak ground displacement of 150 mm as the maximum displacement allowed in bridges, in the event of moderate to large earthquakes.

8.3   Evaluation of Seismic Performance of the Samudera Bridge

The most fundamental step prior to the evaluation of the Samudera Bridge is modeling of the bridge system to capture acceptable behavior and responses during earthquake excitation by incorporating the performance-based design framework. After careful modeling, the bridge was subjected to the 1995 Kobe earthquake, 1940 El Centro and 2005 Sumatera earthquake time-histories.

Simulation results demonstrate nonlinear behavior of piers and the bridge is anticipated to sustain severe damages under the Kobe earthquake. Excitation of the bridge to El Centro and 2005 Sumatera earthquakes shows small damages in the bridge. In general, the bridge performs satisfactorily, without collapse, under the El Centro and 2005 Sumatera ground motions.

Prior to performing dynamic analysis, pushover analysis has been carried out to determine the displacement capacity at ultimate limit state. Pushover analysis was also used to estimate the seismic coefficient of free and fixed piers. After conducting dynamic analysis using the Kobe ground motion, it was observed that the piers with higher seismic coefficient but low displacement capacity were heavily damaged, whereas the piers with low seismic coefficient, but having high displacement capacity survived. This shows that seismic coefficient is not an important parameter to survive an earthquake. Rather, displacement capacity is most important. It is noteworthy that displacement capacity can be enhanced by enriching the transverse reinforcement in piers.

8.4 Prediction of Seismic Coefficient Value using the Nonlinear Static Pushover Analysis

The attempt to develop suitable and reliable seismic design motions for low seismicity regions has remain one of the many challenges in earthquake engineering discipline since a few decades ago. This is due to insufficient ground motion data for establishing a design response spectrum. Therefore, for a country such as Malaysia, it is difficult or quite impossible to estimate a design motion by employing procedures, which were developed for regions with abundant ground motion records. Rather, an alternative approach to evaluate a design motion is by deriving seismic coefficient values, as have been widely employed in seismic design codes for buildings. To achieve this goal, the nonlinear static pushover analysis has been employed. With the help of dynamic analysis, it has been confirmed that for a low seismicity country such as Malaysia, seismic coefficient is not significant in ensuring seismic resistance. Rather, displacement capacity must be set a priority in seismic design of bridges. Displacement capacity can be enhanced by introducing proper confinement in bridge piers.

8.5 The Impact of Seismic Resistant Design on Economy

Many people perceive that seismic resistant design is an expensive 'solution' to mitigating the destructive effects of earthquakes. A supporting study was carried out to examine the impact of implementing seismic resistant design on the construction cost. This is a study to observe the effect of reducing displacement response on construction cost. The price difference was based on the contractual price of the steel reinforcement and concrete materials listed in the bill of quantities for the Samudera Bridge project. The increase in construction cost due to the implementation of seismic resistant design has been predicted not to exceed one percent of the bridge structure cost only.